

Partnership for the Assessment of Risks from Chemicals

Deliverable D6.2

First Report on innovative methods based on PBK models

WP 6 – T6.2



Co-funded by
the European Union

This partnership has received funding from the European Union's Horizon Europe research and innovation programme under Grant Agreement No 101057014.

Technical reference	
Work package	WP 6 - Innovation in regulatory risk assessment
Task	T 6.2 - Integrative exposure and risk assessment
Dissemination level ¹	PU
Lead Beneficiary/ Responsible AE	AUTH, INERIS
Contributing Participants	ANSES, IISPV, RIVM, SLU, IVL, TNO, VITO, NIPH, IFRMN, WR, ISSeP, ONIRIS, CSIC, OVAM, KWR, WSFR, CSIC-IDAEA, IUSS, MU (RECETOX)
Responsible author(s)	Spyros Karakitsios (AUTH) spyros.karakitsios@gmail.com Achilleas Karakoltzidis (AUTH) karakoltzidis.achilleas@gmail.com Aude Ratier (INERIS) aude.ratier@ineris.fr
Co-authors (Alphabetical order)	Pierre-André Billat (INERIS) pierre-andre.billat@ineris.fr Jos Bessems (VITO) jos.bessems@vito.be Rayane Boufalaas (INERIS) rayane.boufalaas@ineris.fr Cleo Bodin (INERIS) cleo.bodin@ineris.fr Deepika Deepika (IISPV) deepika@iispv.cat Jasper Engel (WR) jasper.engel@wur.nl Thomas Gastellu (ONIRIS) thomas.gastellu@oniris-nantes.fr Joan O. Grimalt (IDAEA-CSIC) joan.grimalt@idaea.csic.es Johannes Kruisselbrink (WR) johannes.kruisselbrink@wur.nl Vikas Kumar (IISPV) vikas.kumar@urv.cat Klára Komprdová (MU) klara.komprdova@recetox.muni.cz Sanah Majid (KWR) Sanah-Majid.Shaikh@kwrwater.nl Simone Stefano (MN) simone.stefano@marionegri.it Arno Van Der Beke (VITO) arno.vanderbeke@vito.be Joost Westerhout (RIVM) joost.westerhout@rivm.nl Anne Zwartsen (RIVM) anne.zwartsen@rivm.nl Monika Witala (IVL) Monika.Witala@ivl.se Carolina Vogs (SLU) carolina.vogs@slu.se Florence Zeman (INERIS) florence.zeman@ineris.fr

Internal Reviewers	Amélie Crépet / ANSES / amelie.crepet@anses.fr Jacob van Klaveren / RIVM / jacob.van.klaveren@rivm.nl Katleen de Brouwere / VITO / katleen.debrouwere@vito.be
External Reviewers	Claudia Heppner / EFSA / Claudia.HEPPNER@efsa.europa.eu Sylvia Escher / Fraunhofer Gesellschaft e.V. / sylvia.escher@item.fraunhofer.de
Due date of deliverable	30 April 2025
Actual submission date	19 June 2025

¹ PU = Public

PP = Restricted to other programme participants (including the Commission Services)

RE = Restricted to a group specified by the consortium (including the Commission Services)

CO = Confidential, only for members of the consortium (including the Commission Services)

Document history

Version	Date	Reviewer name/Institutions	Short description of changes
1	30/04/2025	Responsible authors and internal reviewers	1 st version
2	03/06/2025	Responsible authors and internal reviewers	Updates from the external reviewing

“Funded by the European Union. Views and opinions expressed are, however, those of the author(s) only and do not necessarily reflect those of the European Union or the Health and Digital Executive Agency. Neither the European Union nor the granting authority can be held responsible for them.”

Abstract

Physiologically Based kinetic (PBK) models are essential tools in toxicology and next-generation risk assessment (NGRA), providing insights into chemical kinetics and exposure-related health risks. PBK models simulate chemical reactions in the human body, helping us understand potential health risks. While they provide valuable insights, regulators use them as just one piece of evidence, along with other pieces of information, to set safe exposure levels (like points of departure). These models support decision-making but are not the solitary basis for regulations. Their ability to account for inter-individual variability enhances their relevance across exposure scenarios. Key contributions that will be addressed herein include methodological advancements in PBK modeling, particularly for aggregating routes of exposure and tracing internal dose back to external sources.

This deliverable advances PBK modeling by addressing key challenges for risk assessment including probabilistic modeling and FAIR PBK with the aim to enhance their regulatory applicability. It presents case studies refining PBK approaches for contaminants such as methylmercury (CH₃Hg), inorganic mercury (iHg), inorganic arsenic (iAs), lead (Pb), and per- and polyfluoroalkyl substances (PFAS). Key improvements include age-specific physiological modeling, dietary risk assessment, and lifetime exposure analysis. A pregnancy-specific PBK (p-PBK) model simulates fetal neurotoxicant exposure, while blood-brain barrier integration in adults, for now, enhances neurotoxic chemical distribution assessment. Additionally, a PBK ontology promotes FAIR (Findable, Accessible, Interoperable, Reusable) data practices in the PARC consortium and the scientific community, ensuring greater transparency, reusability, and regulatory integration. Implementing uncertainty analysis, particularly for PFAS, strengthens model reliability and confidence in predictions. These advancements support PBK integration into regulatory frameworks, improving chemical risk assessment and public health protection. This deliverable underscores the increasing importance of PBK models in next-generation risk assessment.

Key Words

PBK models, Exposure modeling, BBB (Blood-Brain Barrier), PBKO (PBK Ontology), FAIR PBK, PFAS, lifetime exposure

List of abbreviations

ADME	Absorption, distribution, metabolism and excretion
As	Arsenic
ASL	Airway Surface Liquid
AVSF	Alveolar Subphase Fluid
BBB	Blood-brain barrier
BLL	Blood lead level
Cd	Cadmium
CH₃Hg	Methylmercury
CI	Credibility interval
CPF	Chlorpyrifos
EDI	Estimated daily intake
EPR	Epithelial Lining Fluid-to-plasma Ratio
GFR	Glomerular filtration rate
GI	gastrointestinal
HBM	Human Biomonitoring
Hg	Mercury
iHg	Inorganic Mercury
IPRLu	Isolated perfused respiring rat lung
IVIVE	<i>In vitro</i> to <i>in vivo</i> extrapolations
J_{max}	Maximum flux
k_p	Permeation coefficient
LC-MS	Liquid Chromatography Mass Spectrometry
LLF	Lung-lining fluid
MC	Monte Carlo
MCMC	Markov Chain Monte Carlo
MER	Macrophages – Epithelial lining fluid Ratio
NGRA	Next-generation risk assessment
p-PBK model	Pregnancy Physiologically based kinetic model
PBK model	Physiologically based kinetic model
Pb	Lead
PFAS	Per- and polyfluoroalkyl substances
PS	Permeability surface
qAOP	Quantitative Adverse Outcome Pathways
QSAR	Quantitative Structure Activity Relationship
RA	Risk Assessment
RT	Respiratory tract
SC	Stratum corneum
WP	Work Package

Table of contents

Technical reference	2
Document history	4
Abstract	5
Key Words	5
List of abbreviations	6
Table of contents	7
1. Introduction	9
2. PBK model developments and refinements	11
2.1. Library of lifetime physiological equations for PBK models	11
2.2. PBK model for mercury (Hg)	13
2.2.1. Structure of the model	13
2.2.2. Model parametrisation	14
2.2.3. Main Results	16
2.2.4. Conclusion and perspectives	16
2.3. PBK model for Arsenic (As)	17
2.3.1. Model parametrisation	17
2.3.2. Model validation	19
2.3.3. Reverse dosimetry	21
2.4. Pregnancy PBK model for Pb	23
2.4.1. Structure of the p-PBK model	23
2.4.2. Model parametrisation	24
2.4.3. Model calibration	24
2.4.4. Main Results	25
2.4.5. Conclusions and perspectives	26
2.5. PFAS PBK modeling refinement	27
2.5.1. PFAS PBK models developed during the first years of PARC	27
2.5.2. PFAS PBK model working group	27
2.5.3. OECD evaluation template GD 331 and PFAS PBK models	27
2.5.4. PFAS PBK modeling and uncertainty analysis	28
2.6. PBK models to aggregate exposure routes	29
2.6.1. Oral Exposure	30
2.6.2. Inhalation Exposure	33
2.6.3. Dermal Exposure	35
2.6.4. QSAR models	37
2.6.5. Limitations and Outlook	37
2.7. Blood-Brain Barrier in inventoried PARC PBK models	41
2.7.1. Overview of the blood-brain barrier	41
2.7.2. BBB implementation in the inventoried PBK models in PARC	41
2.7.3. In vitro data in support of the implementation of BBB in PBK models, link with WP5	43
2.7.4. QSAR models in support of the implementation of BBB in PBK models	45

2.7.5. Summary and perspectives	45
2.8. FAIR PBK model standard and ontology	47
2.8.1. PBK Ontology (PBKO)	47
2.8.2. FAIR PBK model	48
2.8.3. Combining FAIR PBK and PBK ontology	49
2.8.4. Next steps	49
3. Perspectives and Conclusions	50
4. Appendices	51
Annex 1 - Library of lifetime physiological equations for PBK models	51
Annex 2 - Development of a pregnancy PBK model for Pb (Daoud et al. (2023) article)	51
Annex 3 – List of Publications	51
Annex 4 – List of congress (oral communications and posters)	51
Annex 5 – QSAR models for exposure routes	53
Annex 6 – Overview of brain compartment(s) in PBK models inventoried in the first year of PARC	58
Annex 7 – Parameterization for implementing the BBB in PBK models	62
5. References	64

1. Introduction

PBK models are widely employed in human safety assessment to assess the risks associated with chemical exposures and have emerged as important tools for next-generation risk assessment (NGRA) (Desalegn et al., 2019; Painsi et al., 2019). These models can simulate the kinetics of environmental contaminants in human populations, providing insights into potential health risks and informing risk assessment strategies across life stages. The fundamental objective of PBK modeling is to create a detailed representation of the human body, which is divided into compartments that correspond to various organs and tissues (Kuepfer et al., 2016). This compartmentalization allows for the simulation of chemicals distribution across different tissues and the prediction of concentration-time profiles in plasma and other biological fluids. The integration of these physiological parameters enables PBK models to account for inter-individual variability, including differences in age, sex, body weight, etc. (Johnson et al., 2022; Wang et al., 2021).

This deliverable aims to further develop the state of PBK modeling, addressing current challenges such as e.g., the gap in FAIR PBK modeling for a unified modeling and identifying areas for improvement. Furthermore, the need for PBK models is amplified by the increasing scientific and regulatory interest in aggregating multiple routes of exposure and linking external and internal exposure as well as interactions of chemicals in mixtures (Reale et al., 2024). This work supports the broader objective of enhancing their position in the field of regulatory science and decision-making processes by focusing on significant aspects of PBK modeling, supported by case studies. Aggregate exposure refers to the total exposure an individual experiences from all relevant sources and routes (e.g., ingestion, inhalation, dermal contact) of a single chemical or contaminant over a defined period (Pelletier et al., 2017).

Regulatory agencies across the European Union have emphasized the need for more efficient, transparent, and integrated approaches to chemical risk assessment. Two key initiatives driving this evolution are the "One Substance, One Assessment" (OSOA) principle and the ExpoAdvance Roadmap commissioned by EFSA (Lamon et al., 2024). These frameworks aim to streamline hazard and exposure assessments, reduce duplication of efforts, and enhance the use of innovative methodologies including PBK modeling to support evidence-based decision-making. The OSOA initiative, proposed by the European Commission, aims to promote a more harmonized approach for chemical evaluations. In theory, this could reduce duplication by allowing assessments to be shared across regulatory domains. However, full implementation would require alignment of sector-specific legislation, posing practical challenges. Similarly, EFSA's strategic roadmap ExpoAdvance outlines a strategic vision for advancing exposure science, explicitly advocating for the adoption of PBK models to improve the prediction of internal dosimetry and reduce reliance on default assumptions. In response to these regulatory ambitions, this deliverable demonstrates how PBK modeling can provide a robust, mechanistic framework to address key challenges in chemical safety assessment. Through this work, we contribute to the broader adoption of PBK modeling in regulatory science contexts, supporting the vision set forth by OSOA and EFSA's strategic roadmap ExpoAdvance for a more efficient and accurate risk assessment paradigm.

In response to these visions, the present deliverable aims address some key challenges related to OSOA and the ExpoAdvance Roadmap through the implementation of insightful use cases. One case study focuses on developing improved PBK models that consider age-specific physiological alterations throughout a lifetime to enhance the dietary risk assessment of food contaminants. To precisely simulate Hg exposure in a variety of the general population, the study integrates nonlinear organ growth equations for 24 organs into the PBK models for methylmercury (CH_3Hg) and iHg inorganic mercury (iHg). The study compares simulated hair Hg- concentrations to HBM data from the French study, ESTEBAN (Oleko et al., 2024), and evaluates body burden through

developing lifetime food exposure trajectories and simulating the accumulation of CH₃Hg in the body. Applying the lifetime-based methodology, improved risk characterization across life-stages was conducted to address the risks associated with iHg and CH₃Hg exposure via food consumption. Similarly, a PBK model for arsenic has been developed. In another case study, a pregnancy-specific PBK (p-PBK) model was developed that imitates lead (Pb) exposure in fetuses, particularly during crucial neurodevelopmental stages. The model uses Bayesian inference to estimate placental transfer rates and maternal bone remodeling, adapting an existing Pb PBK framework for pregnant women and fetuses.

Through advanced modeling methods, another case study aims to improve the knowledge of human exposure to per- and poly-fluoroalkyl substances (PFAS), mainly the PFOA and PFOS. It included modeling exposure in vulnerable populations, such as children and mother-child pairs, establishing risk assessments through a range of life stages, and integrating systems toxicology and biokinetic modeling to link PFAS exposure to potential health impacts.

Moreover, a case study highlights the importance of the blood barrier to regulate the distribution of chemicals from the blood to the brain and how it could be incorporated into PBK models to enhance the understanding of the kinetics of neurotoxic chemicals, including pesticides.

To promote reusability and data sharing, a framework for FAIR (Findable, Accessible, Interoperable, and Reusable) PBK modeling is being developed in close collaboration with PARC WP7 and T8.3. It incorporates a PBK ontology and harmonized standards for implementation of PBK models to support FAIRification of PBK models. Relating to this, a methodology was developed to improve the FAIRness of PBK models. Finally, an uncertainty analysis for PBK models related to PFAS exposure is implemented. The delivery also highlights the physiology of chemical absorption through different exposure routes and how inventoried PBK models translated this into compartmental structures.

2. PBK model developments and refinements

2.1. Library of lifetime physiological equations for PBK models

People are continuously exposed to various chemicals in food throughout their lives, potentially triggering the risk of developing adverse health issues. Risk assessment procedures compare dietary exposure levels with hazard characteristics to assess the likelihood of developing an adverse health effect in exposed populations. Estimating dietary exposure is usually conducted via real-life intakes based on data on food consumption and chemical levels in food or/and quantifying exposure levels in sampled human matrixes (e.g., blood, urine, hair, breastmilk, etc.). Both exposure strategies are, however, time-consuming, costly, partly invasive, and restricted to a time snapshot. Moreover, the development of new approaches, such as quantitative Adverse Outcome Pathway (qAOP), needs information on chronic exposure to human organs (e.g., target organs, storage organs, eliminating organs, etc.), which is currently limited (Deepika & Kumar, 2023).

An increasingly common approach is to estimate human internal exposure by PBK models. This mathematical approach combines ADME processes of chemicals, with measured dietary intake and/or human exposure levels. Many different PBK models were developed in the past with a focus on estimating human internal exposure for a specific age range. In contrast, chronic exposure over a lifetime has been considered just by a few PBK models as this requires an empirical understanding on organ volume changes implemented in the PBK model. Additionally, lifetime exposure scenario needs the integration of a coherent dietary exposure evolution over life (Pruvost-Couvreur et al., 2020).

In the PARC project on the refinement and development of PBK models for human risk assessment (project 6.2.2.a), Gastellu et al. (2025a) established a comprehensive library of lifetime equations based on 12 lifetime PBK models (Beaudouin et al., 2010; Deepika et al., 2021; Haddad et al., 2001; Haddad et al., 2006; Mallick et al., 2020; Pendse et al., 2020; Price et al., 2003; Ring et al., 2017; Sarigiannis et al., 2020; Smith et al., 2014; Verner et al., 2008; Wu et al., 2015). Hereby, Gastellu et al. (2025a) surveyed empirical equations used in the 12 lifetime PBK models (consisting of 5 to 22 compartments) to estimate volume growths for 24 organs for both sexes (Figure 1). The refinement and the application of the library is provided in the next section (Section 2.2). This library of lifetime physiological equations was applied for risk assessment for a lifetime exposure to a mixture of trace elements (Cd, iHg, CH₃Hg, iAs and Pb) (Gastellu et al., 2025a; Gastellu et al., 2025b).

Organs such as liver, intestine, kidney, skin and muscle were often implemented in the inventoried lifetime PBK models, while organ growths of thyroid, breast, pancreas, and diaphragm were rarely considered (Figure 1). The empirical equations for modeling organ growth varied because they were calibrated to different population data and used different body parameters (e.g., age, body weight, height) as input. Sex differences in volume growth were considered in 9 of the 12 PBK models. Figure 2 illustrates variabilities of organ volume growths for 5 representative organs in both sexes considering the physiological equations extracted from the 12 PBK models for both sexes. The detailed equations available for each organ and sex was provided in supplementary materials of Gastellu et al. (2025a).

Gastellu et al. (2025a) provided a comprehensive library of all extracted equations in an excel spreadsheet that can be used as a user-friendly and efficient application to calculate volume

growths for the inventoried organs over a lifetime. Additionally, an R code was created that can be easily implemented in future PBK models. Both applications can be found on [GitHub](#) and [Zenodo](#). Overall, the comprehensive library of physiological equations aims to facilitate the estimation of chronic dietary exposure for risk assessment purposes, as outlined in the mercury case study (section 2.2).

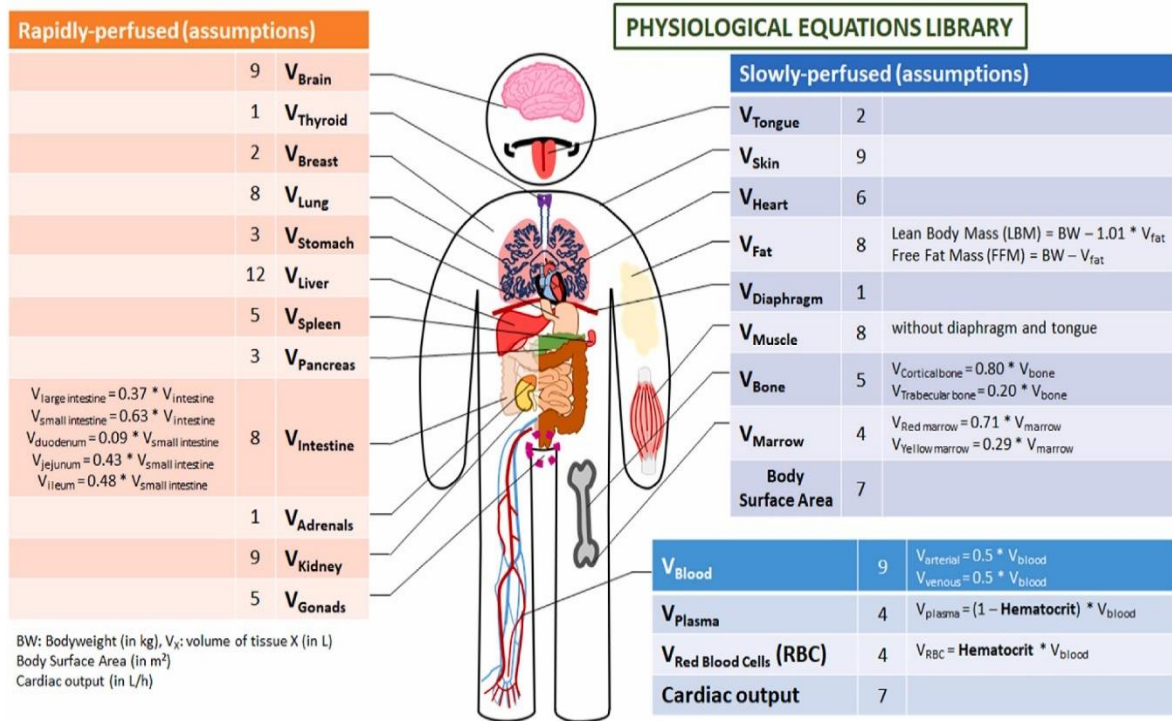


Figure 1. Overview of the number of physiological equations for each organ based on the 12 inventoried lifetime PBK models. The collected equations are summarized in a comprehensive library and can be found in an Excel spreadsheet in Gastellu et al. (2025a). The figure was adapted from Gastellu et al. (2025a).

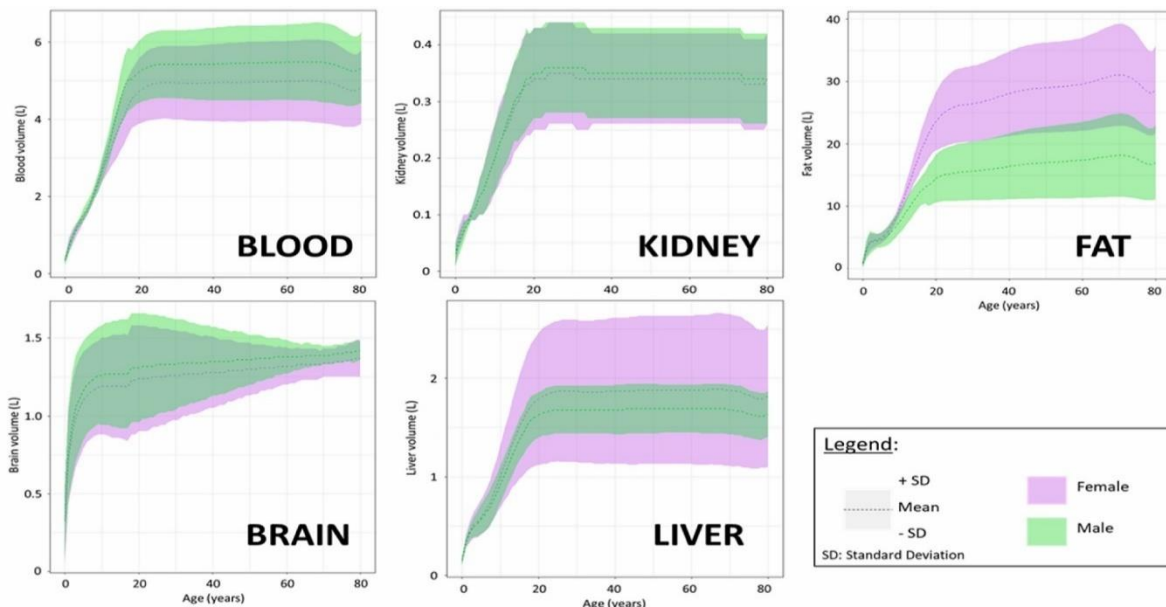


Figure 2. Graphical representation of the volume growth variability for major organs (e.g., blood, kidney, fat, brain, and liver, in L) over time (years) depending on the different lifetime physiological equations. The dashed curves represent the average volume growth based on all physiological equations. The colored areas represent the standard deviation values. The variability is indicated for both sexes. The growth curves of other organs are depicted in the Excel file (Supplementary materials of Gastellu et al. (2025a)). The figure was adapted from Gastellu et al. (2025a).

2.2. PBK model for mercury (Hg)

Mercury is a trace element ubiquitous in the environment, not essential to life but triggering adverse effects such as neurodevelopmental by CH_3Hg or renal effects by iHg (ATSDR, 2022). (ATSDR, 2022) Diet is the mainly source of CH_3Hg through the consumption of seafood (Sirot et al., 2008) but also a source of iHg (ANSES, 2011). Internal exposure to mercury can be assessed by measuring concentrations of total mercury in hair and urine which are good biomarkers of exposure for CH_3Hg and iHg , respectively (Branco et al., 2017). Nonetheless, internal exposure to iHg may come from the exposure to this metal and from the metabolism of CH_3Hg (Farris et al., 1993). To better explain the biomarker levels of mercury exposure, a lifetime model for total mercury was developed.

2.2.1. Structure of the model

Previously, Abass et al. (2018) developed a PBK model for mercury by merging PBK models for each speciation of mercury, including the model of Carrier et al. (2001) for CH_3Hg and the model from Farris et al. (2008) for iHg . New models were developed to simulate the fate of CH_3Hg in the human body refining internal exposure estimations (Ou et al., 2018; Pope & Rand, 2021). The model developed in our study was based on the approach of Abass et al. (2018) by updating and linking the PBK models for each speciation of mercury. The PBK model for CH_3Hg was developed on the models of Ou et al. (2018) and Pope and Rand (2021) as detailed in a previous study assessing lifetime exposure to CH_3Hg (Gastellu et al. (2024)). The PBK model for CH_3Hg was built on 11 compartments: plasma, red blood cells, brain, liver, fat, gut, gut lumen, kidney, rapidly perfused tissues, slowly perfused tissues and hair (Figure 3). For iHg , the model of Carrier et al. (2001) was selected because its structure is based on several organ-compartments (blood, brain, liver, kidney, hair, urine and feces) and it is the last specific model developed for this chemical. PBK model for iHg (Figure 1). CH_3Hg and iHg exposure were absorbed in gut lumen and blood compartments, respectively as proposed by Abass et al. (2018).

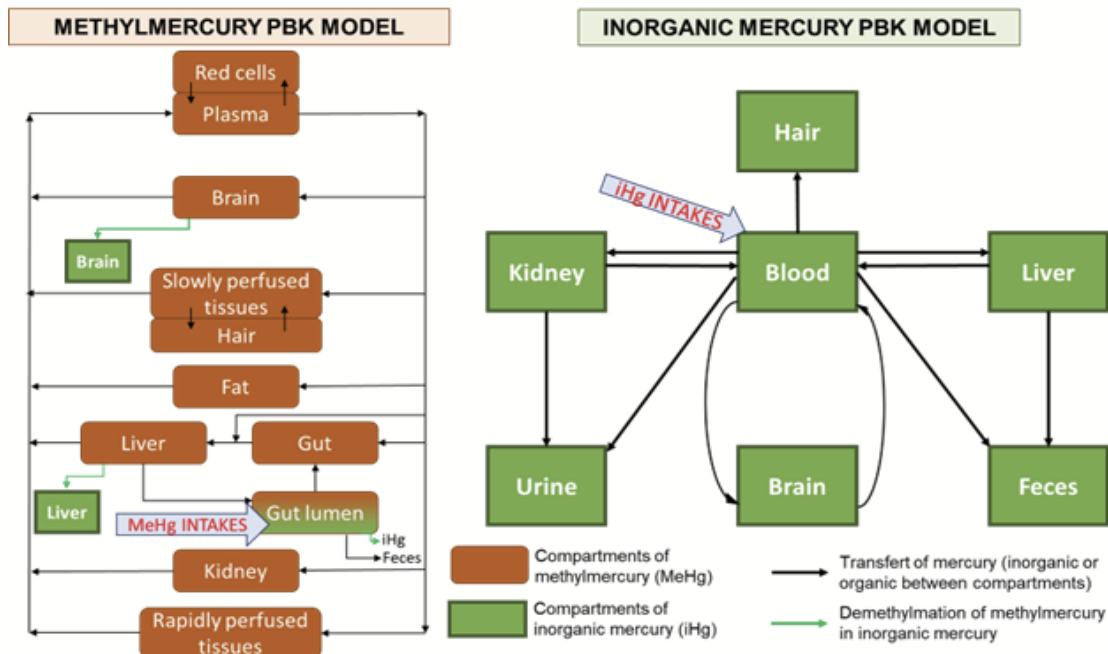


Figure 3. Representation of PBK models for all mercury species. The boxes in orange represent the compartments for methylmercury and the boxes in green represent the compartments for inorganic mercury (Gastellu et al., 2024).

2.2.2. Model parametrisation

To estimate the evolution of internal exposure over life, the physiological parameters were adapted to integrate lifetime growth of the body using the library of lifetime physiological equations developed in PARC (see section 2.2.1). First, the evolution of the bodyweight and the height was scaled on the French population. For each compartment of the PBK model, a single parameter or multiple input parameters (e.g., bodyweight, height, age) were used. Several combinations of growth equations were tested considering a realistic dietary exposure to mercury throughout lifetime to estimate the evolution of organ concentrations of mercury (Gastellu et al., 2024). The dietary exposure was performed using the approach of the lifetime trajectories. Lifetime trajectories were created for a fictive population and a realistic dietary exposure from the French Total Diet Studies was imputed for each day of life in each lifetime trajectory. More details and references are explained in the article on the lifetime trajectory approach (Gastellu et al., 2024). The combination of physiological equations was selected based on Beaudouin et al. (2010); Deepika et al. (2021); Mallick et al. (2020); Ring et al. (2017) that led to the best fits compared to concentrations of mercury measured in different organs (brain, liver, kidney and hair) of autopsied individuals (Bellouard et al., 2022). The physiological equations selected for the lifetime PBK model for mercury were implemented from Beaudouin et al. (2010) and complemented with the equations from Deepika et al. (2021) for adipose tissues, from Ring et al. (2017) for bone tissues, and from Mallick et al. (2020) for haematocrit. Finally, this combination of selected physiological equations was validated with other HBM data of the general French population based on autopsied individuals (for brain, kidney and liver) (Goullé et al., 2010) and the National French Health and Nutrition study performed from 2014 to 2016, ESTEBAN, which realized a human biomonitoring study of total mercury into hair and urine (Oleko et al., 2024). Beaudouin et al. (2010); Deepika et al. (2021); Mallick et al. (2020); Ring et al. (2017)

Kinetic parameters for CH₃Hg and iHg were those from the previous PBK models selected for each speciation. The kinetic parameters are detailed in table 1 for methylmercury PBK model and in table 2 for inorganic mercury PBK model. Inorganic mercury kinetic parameters were those from Carrier et al. (2001). For the kinetic parameters for methylmercury, Ou et al. (2018), Pope and Rand (2021) selected the same parametrization. In addition, Pope and Rand (2021) refined faecal excretion for each gender and different stages of life. The integration of lifetime growth allowed scaling kinetic parameters on bodyweight. Kinetic parameters are detailed in supplementary materials of Gastellu et al. (2025a).

Table 1. Kinetic parameters of methylmercury PBK model. This data sourced from Gastellu et al. (2025a).

Parameters	Value
Brain / Plasma partition coefficient	3.0
Fat / Plasma partition coefficient	0.15
Gut / Plasma partition coefficient	1.0
Hair / Plasma partition coefficient	248.7
Kidney / Plasma partition coefficient	4.0
Liver / Plasma partition coefficient	5.0
Rapidly perfused tissues / Plasma partition coefficient	1.0

Slowly perfused tissues / Plasma partition coefficient	2.0	
Demethylation rate in brain (in L/day)	$1.2e^{-5} * 24 * BW^{\frac{3}{4}}$	
Biliary clearance (in L/day)	$1.0e^{-4} * 24 * BW^{\frac{3}{4}}$	
Demethylation rate in gut (in L/day)	$1.0e^{-4} * 24 * BW^{\frac{3}{4}}$	
Reabsorption rate in gut (in L/day)	$0.005 * 24 * BW^{\frac{3}{4}}$	
Red blood cells to plasma diffusion (in L/day)	0.3 * 24	
Plasma to Red blood cells diffusion (in L/day)	3.0 * 24	
Absorption rate in gut (in L/day)	0.3 * 24	
Excretion rate from gut tissue to gut lumen (in L/day)	0.10 * 24	
Excretion into hair (in L/day)	$kha = 7.0e^{-6} * 24 * BW^{\frac{3}{4}}$	
Fecal excretion (in L/day)	If age < 7 years	$2.08e^{-3} * 24 * BW^{\frac{3}{4}}$
	If age > 7 years and male	$6.25e^{-3} * 24 * BW^{\frac{3}{4}}$
	If age > 7 years and female	$5.0e^{-3} * 24 * BW^{\frac{3}{4}}$

Table 2. Kinetic parameters of inorganic mercury PBK model. This data sourced from Gastellu et al. (2025a).

Parameters	Value (day ⁻¹)
Blood to liver transfert coefficient combined with liver metabolism rate constant of organic mercury	0.1750
Liver to blood transfer coefficient	0.8940
Blood to liver transfer coefficient	0
Blood to kidney transfer coefficient	17.1234
Kidney to blood transfer coefficient	0.0010
Kidney to urine transfer coefficient	0.006949
Blood to hair transfer coefficient	0.1400
Blood to urine transfer coefficient	0.06994
Blood to feces transfer coefficient	3.9917
Liver to feces transfer coefficient	1.5476
Blood to brain transfer coefficient	0.0028
Brain to blood transfer coefficient	0.0520

2.2.3. Main Results

The estimated biomarkers of exposure were compared to Hg concentrations measured in the French HBM study, ESTEBAN, across life stages (Oleko et al., 2024). Estimated Hg levels in hair followed the trend of HBM measurements but were generally underestimated, except during childhood, where they aligned well (figure 4 B). This discrepancy may stem from challenges in estimating seafood consumption due to its variety and irregular intake (Gastellu et al., 2024). Urinary mercury concentrations were underestimated by a factor of 2 to 3, likely due to unaccounted exposures from iHg via ingestion, inhalation, or dental amalgams (Oleko et al., 2024) (figure 4 A). The uncertainty may be induced by the parametrization of the model which was extrapolated from adulthood for lifetime.

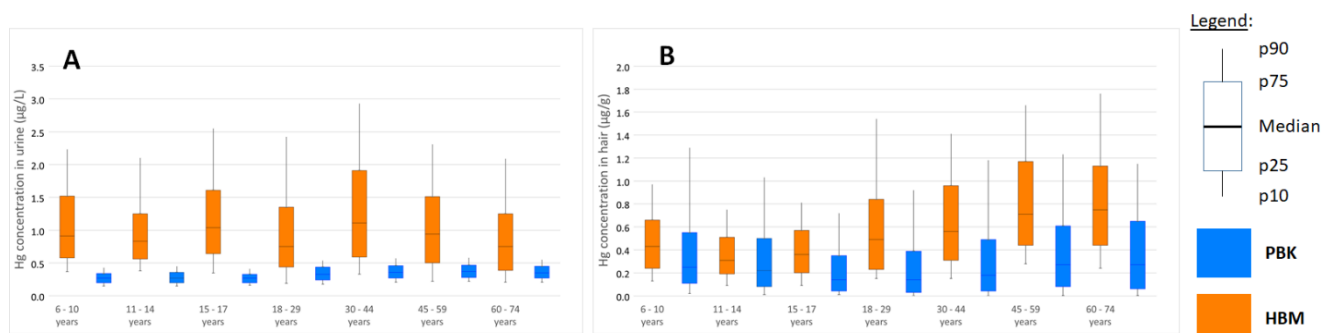


Figure 4. Comparison of simulated concentration of total mercury in (A) urine and (B) hair using the selected lifetime PBK model of mercury with HBM data from ESTEBAN study (Oleko et al., 2024) (extracted from Gastellu et al. (2025a))

The PBK model for total mercury refined risk assessment by establishing correlations between exposure biomarkers and target organs. Mercury concentrations in hair and urine correlated strongly with those in the brain and kidney, confirming their reliability as biomarkers for neurodevelopmental and renal risks. Scenarios based on European regulations in accordance with European Commission Regulation (EU) 2023/915B and seafood consumption patterns assessed mercury levels in hair and urine throughout life. The maximal levels of contamination defined by European regulation are 0.3, 0.5 and 1.0 mg/kg for specified seafood items. A simulation was realized for each value of the European regulation considering a common contamination of methylmercury in all seafood items. While the risk of renal effects from oral exposure alone can be excluded under current regulations, neurodevelopmental risks remain for high Hg contamination in seafood. Diversifying seafood intake and limiting highly contaminated items are essential to reduce Hg exposure, particularly during childhood, see for instance Capodiferro et al (2022).

2.2.4. Conclusion and perspectives

This model was an application of the library of physiological equations developed in the framework of PARC. We succeeded in estimating the contribution of dietary exposure in exposure to Hg. This work showed the interest and the concept of lifetime PBK modelling and how to adapt an age-specific PBK model to lifetime PBK model. The next steps could be to include pregnancy in this PBK model to estimate the *in-utero* exposure to mercury. Moreover, other sources of exposure can be aggregated to the exposure scenarios such as inhalation to better predict the concentrations of biomarkers of exposure compared to those measured in the population. At

present, this approach can help regulators to define maximum levels of contamination in food, based on consumption and the body growth over life, and thus define levels of protection throughout life.

2.3. PBK model for Arsenic (As)

Inorganic arsenic (iAs), a naturally occurring metalloid in water, soil, air, and food, poses significant health risks. Chronic exposure via drinking water is associated with cancers (skin, bladder, lung) and cardiovascular/peripheral vascular diseases (Navas-Acien et al., 2005; Yoshida et al., 2004), leading to public health crises in regions like India and Bangladesh (Alam et al., 2002; Khan et al., 2003; Mukherjee et al., 2005). This prompted regulatory actions, including the U.S. lowering its drinking water standard to 10 ppb (US EPA, 2001), aligning with WHO guidelines (IPCS, 2001). In water, iAs exists as arsenate (AsV) or arsenite (AsIII). Metabolism involves AS3MT-mediated reduction and methylation (Thomas et al., 2007; Waters et al., 2004a; Waters et al., 2004b), with GST omega aiding reduction (Chowdhury et al., 2006; Zakharyan & Aposhian, 1999). Non-enzymatic cycling occurs (Thomas et al., 2004). Most importantly, methylation is now recognized as activation, producing highly toxic trivalent metabolites (MMA(III): Monomethylarsonous Acid, DMA(III): Dimethylarsinous Acid) that are more cytotoxic, genotoxic, and enzyme-inhibitory than pentavalent forms (Schwerdtle et al., 2003), with DMA(III) implicated in rat bladder carcinogenesis (Cohen et al., 2006). Urinary metabolite profiles are used for study but may not reflect tissue-specific accumulation, complicating risk assessment (Kenyon et al., 2005a; Kenyon et al., 2005b). To address uncertainties, a human PBK model predicts target tissue dosimetry of arsenic and its metabolites, incorporating updated metabolism data and distinguishing predictions of trivalent arsenical formation/excretion (El-Masri & Kenyon, 2008; Mann et al., 1996a, 1996b; Yu, 1999a, 1999b).

2.3.1. Model parametrisation

The physiological parameterization of the model has been extensively detailed in the work of Sarigiannis et al. (2020). The model's partition coefficients are presented in Table 3, while the chemical-specific parameters are summarized in Table 4 (El-Masri & Kenyon, 2008). Model structure is presented in Figure 5. Metabolism of arsenic species is presented in Figure 6.

Table 3. Partition coefficients of the inorganic As PBTK model and its metabolites. This data sourced from (El-Masri & Kenyon, 2008).

	<i>AS^V</i>	<i>AS^{III}</i>	<i>MMA</i>	<i>DMA</i>
<i>GI</i>	2.7	8.3	2.2	2.1
<i>SKIN</i>	7.9	7.4	2.61	2.4
<i>BRAIN</i>	2.4	2.4	2.2	3.3
<i>HEART</i>	7.9	7.4	2.61	2.4
<i>KIDNEY</i>	8.3	11.7	4.4	3.8
<i>LIVER</i>	15.8	16.5	3.3	3.3
<i>MUSCLE/OTHER</i>	2.1	6.7	1.3	1.3
<i>LUNG</i>	7.9	7.4	2.61	2.4

Table 4. Chemical-specific parameters of the PBTK model of inorganic As and its metabolites (El-Masri & Kenyon, 2008).

PARAMETER	DESCRIPTION	VALUE	UNITS
<i>DMA</i>			
K_a	Oral absorption	0.007	min ⁻¹
K_{red}	Reduction of DMA	0.004	min ⁻¹
K_{ox}	Oxidation of DMA III	0.65	unitless

$K_{urine/DMA}$	Urine Excretion Const	0.13	min^{-1}
MMA			
K_a	Oral Absorption	0.007	min^{-1}
K_{red}	Reduction of MMA	0.008	min^{-1}
K_{ox}	Oxidation of MMA III	0.63	unitless
$V_{max} (MMA_{III} \rightarrow DMA)$	Methylation of MMA III	$6.6 \times 10^{-7} \text{ } 10^{-7}$	mole/min
$K_m (MMA_{III} \rightarrow DMA)$		3×10^{-6}	M
K_{inh}	Noncompetitive Const inhibition	4×10^{-5}	M
$K_{urine/MMA}$	Urine Excretion Const	0.3	min^{-1}
INORGANIC As			
$K_a (AsV)$	Oral absorption	0.003	min^{-1}
$K_a (AsIII)$		0.004	min^{-1}
K_{red}	Reduction of AsV	0.003	min^{-1}
K_{ox}	Oxidation of As III	0.25	unitless
$V_{max} (AsIII \rightarrow MMA)$	Methylation of As	$5.3 \times 10^{-7} \text{ } 10^{-7}$	mole/min
$K_m (AsIII \rightarrow MMA)$		3×10^{-6}	M
$V_{max} (AsIII \rightarrow DMA)$		2×10^{-6}	mole/min
$K_m (AsIII \rightarrow DMA)$		3×10^{-6}	M
K_{inh}	Noncompetitive inhibition const	4×10^{-5}	M
$K_{urine/As}$	Urine Excretion Const	0.07	min^{-1}

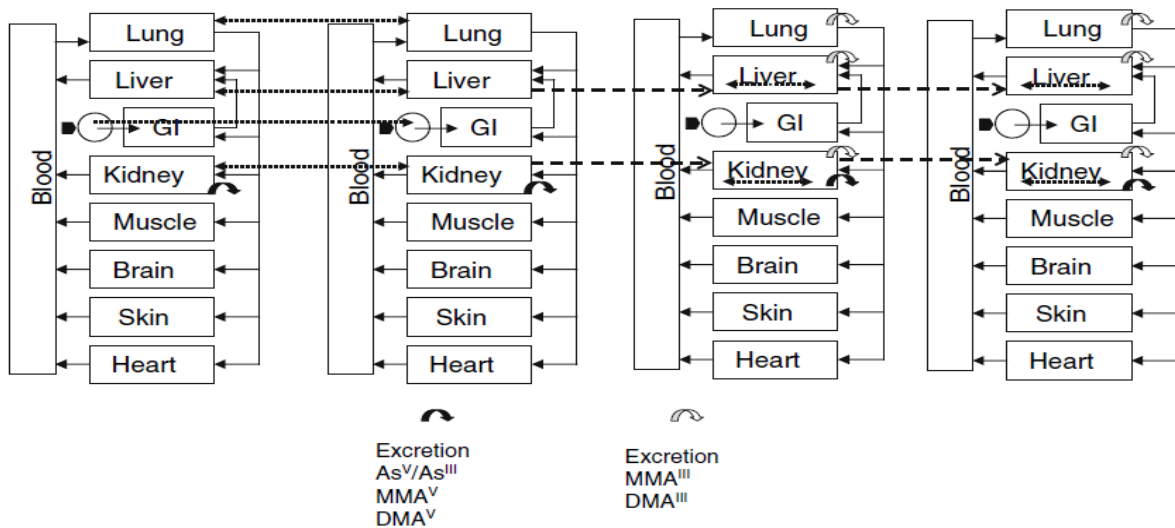


Figure 5. Structure of the PBK model adapted to INTEGRA framework. Sourced from El-Masri and Kenyon (2008). The model consists of 6 compounds namely AS(V), As(III), MMA(V), MMA(III), DMA(V), and DMA(III). Metabolism occurs in kidneys and liver while oxidation and reduction has been assumed to occur only in Liver, Kidneys, and Lungs. The model includes all the main human organs including lungs, liver, GI tract, kidneys, muscle, brain, skin, and heart. As an excretion route only, urine has been considered.

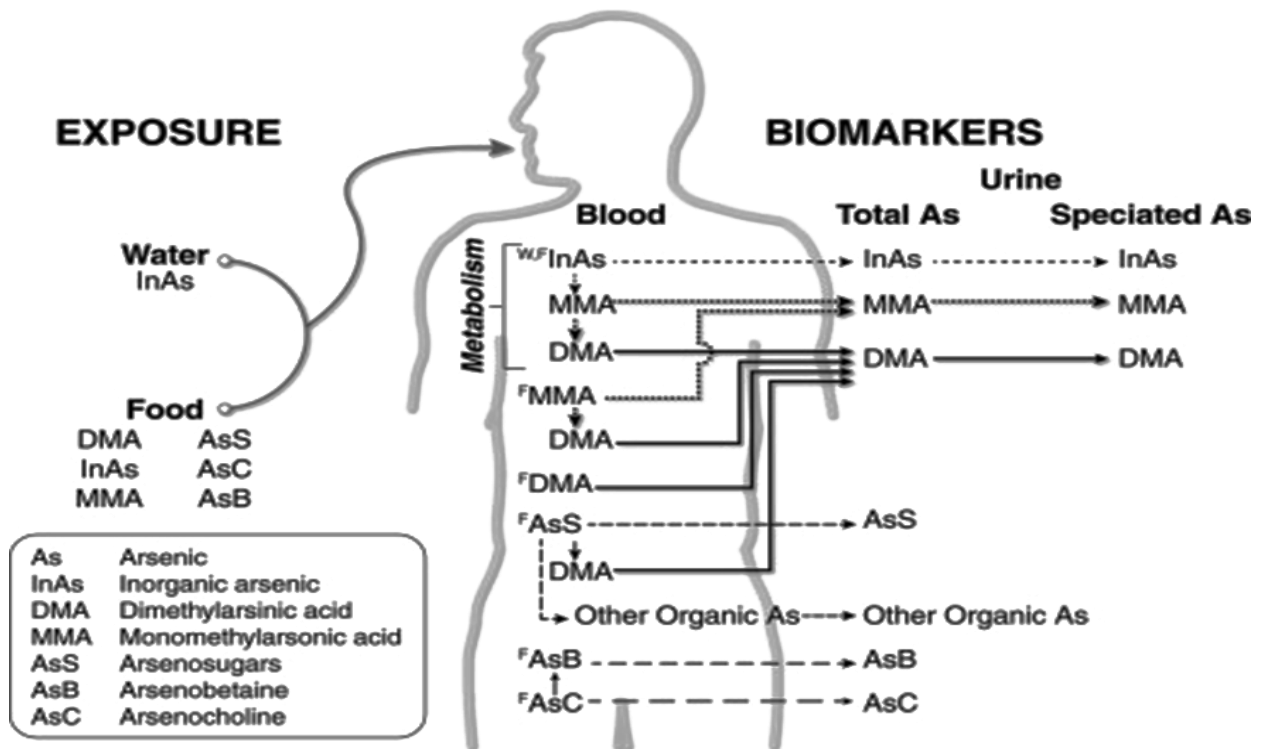


Figure 6. Source – to – internal – dose continuum used. Model design graphical illustration (Tsuji et al., 2021). Schematic representation of arsenic exposure, metabolism, and biomarker distribution in the human body. Arsenic exposure occurs through ingestion of contaminated water and food, introducing various arsenic species, including inorganic arsenic, monomethylarsonic acid (MMA), dimethylarsinic acid (DMA), arsenosugars (AsS), arsenobetaine (AsB), and arsenocholine (AsC). Following ingestion, inorganic arsenic undergoes methylation in the liver to MMA and DMA. These species, along with organic arsenicals, circulate in the blood and are excreted in urine as biomarkers, both as total arsenic and speciated forms (InAs, MMA, DMA, and organic As). The figure illustrates the pathway from exposure to biomarker detection, highlighting internal metabolism and urinary excretion profiles.

2.3.2. Model validation

The model was validated against the data published by Buchet et al. (1981). In this study, 3 participants digested 500 µg As^{III} in the form of NaAsO₂, 4 participants digested 500 µg CH₃AsO₃Na₂, and 4 participants digested 500 µg (CH₃)₂AsO₃Na. Model performance is illustrated in Figure 7 for DMA, in Figure 8 for MMA, and in Figure 9 for iAs exposure. Detailed fitting process and evaluation procedure are about to be published by the end of 2025.

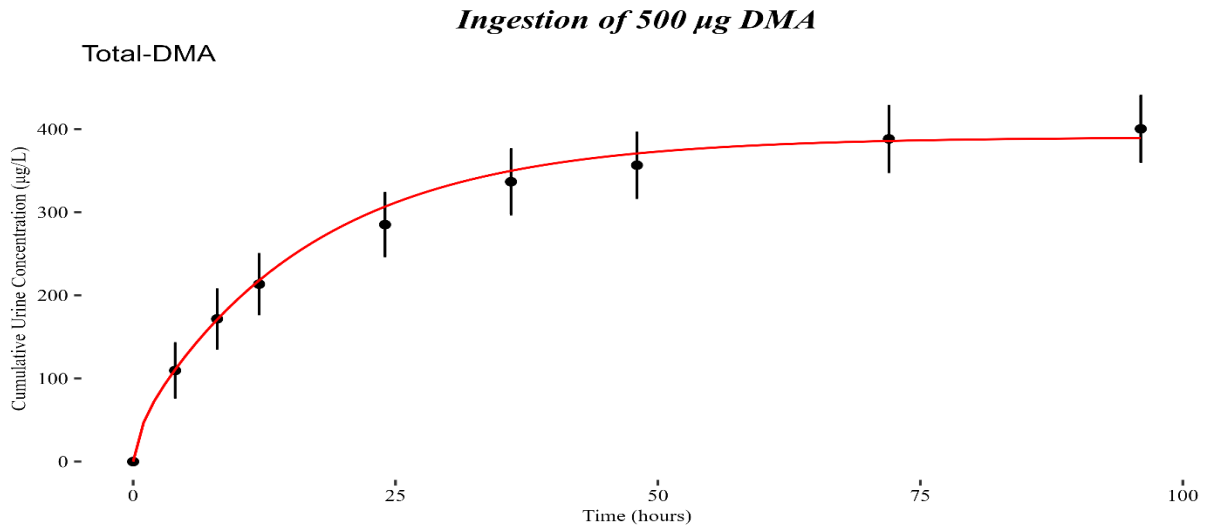


Figure 7. Ingestion of 500 µg $(CH_3)_2AsO_3Na$. The model performance is given in red while experimental data is provided in black dots with the corresponding error bars. Black dots represent observed biomonitoring data with standard deviation error bars, while the red line indicates the predicted urinary excretion profile simulated by the PBPK model. The model shows a good fit to the data, capturing the rapid initial rise and plateauing of urinary DMA concentrations over 96 hours.

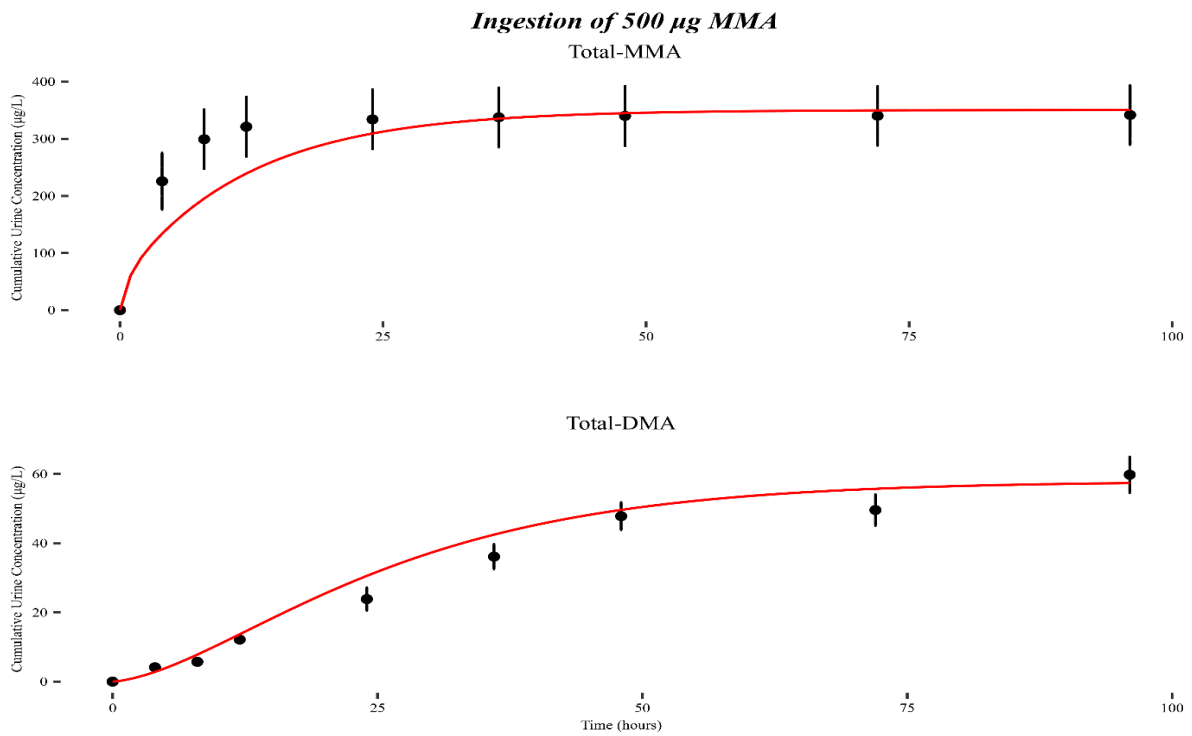


Figure 8. Ingestion of 500 µg $CH_3AsO_3Na_2$. Cumulative urinary concentrations of monomethylarsonic acid (MMA, top) and dimethylarsinic acid (DMA, bottom) over time following ingestion of 500 µg MMA. Black dots represent observed biomonitoring data with standard deviation error bars, while red lines show the PBPK model predictions. The model accurately captures both the rapid urinary excretion of MMA and the delayed formation and excretion of DMA, reflecting metabolic conversion and clearance dynamics.

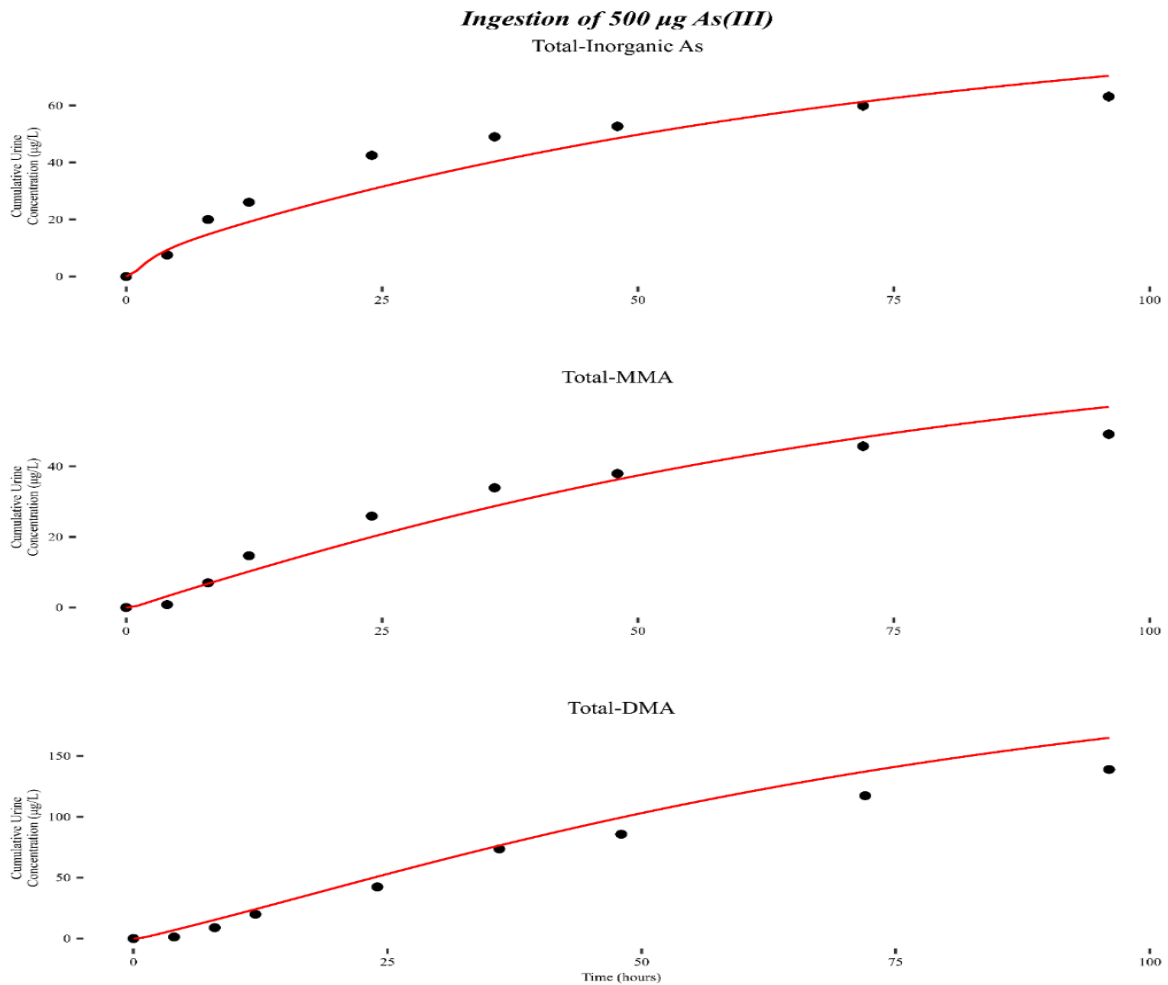


Figure 9. Ingestion of 500 μg NaAsO_2 . The model performance is given in red while experimental data is provided in black dots with the corresponding error bars. Black dots represent observed biomonitoring data with standard deviation error bars, while red lines show the PBPK model predictions. The model accurately captures both the rapid urinary excretion of iAs, MMA and the delayed formation and excretion of DMA, reflecting metabolic conversion and clearance dynamics.

2.3.3. Reverse dosimetry

Exposure reconstruction plays an important role in risk assessment by enabling the estimation of past or unmeasured exposures. This is achieved by integrating biomonitoring data, environmental concentration measurements, and physiological modeling approaches. This process improves the accuracy of dose-response evaluations, allowing for better-informed regulatory science decisions and recommending risk mitigation strategies. The process followed to reconstruct exposure is based on the work of Georgopoulos et al. (2009) and has been previously presented in the study of Sarigiannis et al. (2019). The human biomonitoring data was obtained from the HBM4EU dashboard, which reports total arsenic species in urine samples collected over a 24-hour period. Data from the dashboard is presented in Figure 10. Reconstructed exposures are presented in Figure 11. Detailed analysis of the results presented here will be presented in a dedicated manuscript which is currently in preparation and expected to be published by the end of 2025.

24h-Urine of Total Arsenic Species: HBM4EU dashboard

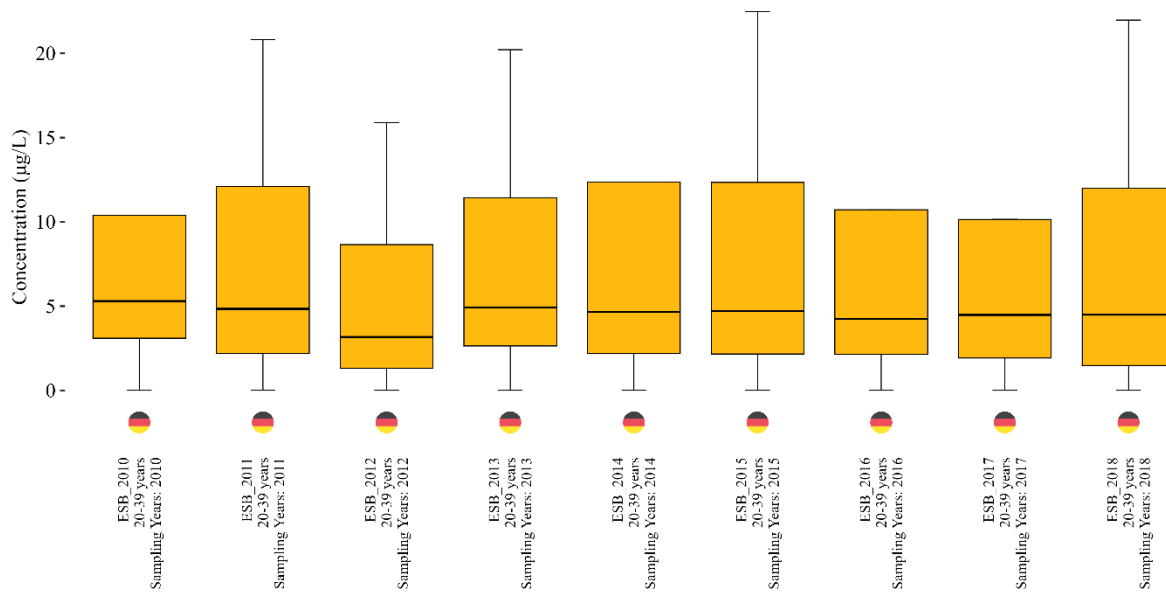


Figure 10. 24-hour urine concentrations of total Arsenic species as sourced from the HBM4EU dashboard. Each box represents a different sampling year, showing the median (horizontal line), interquartile range (IQR, the box), and range of the data (whiskers), with potential outliers indicated by individual points. It is important to highlight the stable levels of total arsenic species over the years.

Reconstructed iAs Exposures from HBM4EU dashboard

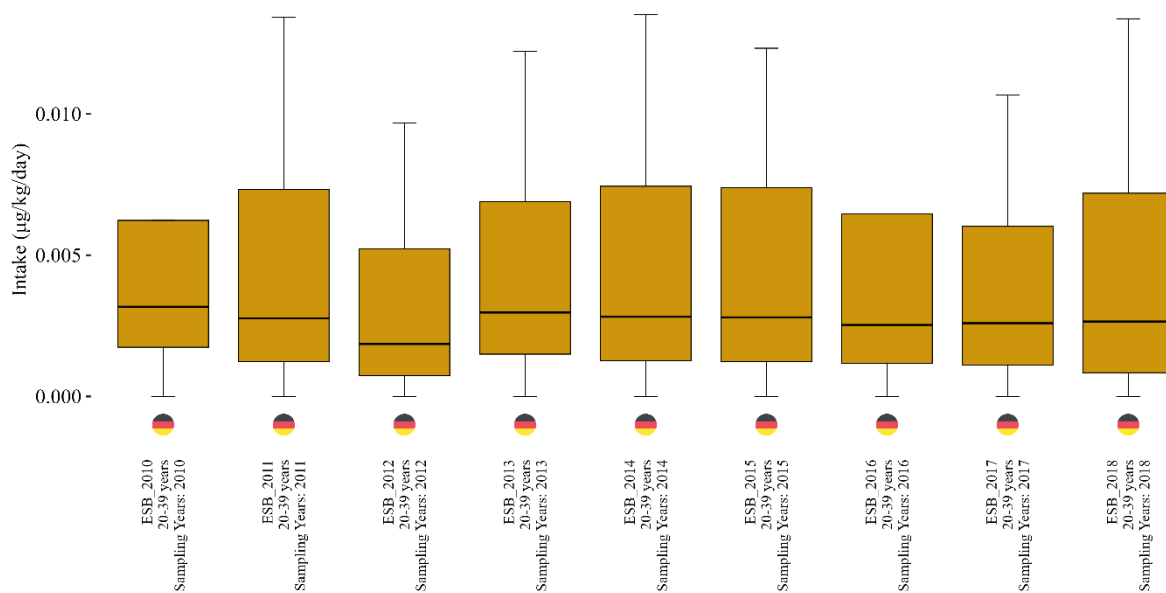


Figure 11. Reconstructed daily intake of inorganic arsenic (iAs) exposures in $\mu\text{g}/\text{kg}/\text{day}$ from 2010 to 2018, derived from the HBM4EU dashboard. Each box plot summarizes the distribution of iAs intake for a given sampling year, indicating the median, interquartile range, and overall spread of the data, potentially from a German population. Unfortunately, only information for Germany does exist in HBM4EU dashboard. While there is year-to-year variability in the distributions, the median iAs intake appears to remain relatively stable across the sampling years, generally falling around $0.0025\text{--}0.005\mu\text{g}/\text{kg}/\text{day}$. The interquartile ranges (the boxes) also show consistent spread. There are some noticeable differences in the upper whiskers and maximum values, particularly in years like 2011 and 2014, suggesting occasional higher exposures or a wider range of values in those specific years. Overall, the data points to a generally consistent exposure level to inorganic arsenic over the period shown, with some fluctuations in the higher exposure percentiles. This consistency could imply stable environmental exposure sources or effective regulatory measures, if any, maintaining exposure within a certain range.

2.4. Pregnancy PBK model for Pb

An existing PBK model developed to describe Pb disposition from birth to adulthood was extended to pregnancy and prenatal life by INERIS during the first years of PARC. The resulting p-PBK model was published (Daoud et al., 2023) as 'Development of a physiologically based toxicokinetic model for lead in pregnant women: the role of bone tissue in the maternal and fetal internal exposure'. The associated model code (GNU MCSim, v6.2.0) is available at [Zenodo](#)¹. The aim was to extend the PBK model for Pb developed by O'Flaherty to pregnant women and their foetuses. The anatomical and physiological changes during pregnancy were integrated. In particular, the additional bone remodeling in pregnant women and the ossification in the foetus were modelled based on published data. Measurements of Pb concentrations in urine of pregnant women showed no differences in concentration between the first and third trimesters of pregnancy (Fort et al., 2014b). This observation was consistent with mobilisation of this metal from the bone tissues during this period (Gulson et al., 2004). The placental transfers between the woman and the foetus and the parameters of additional bone remodeling in women were estimated by Bayesian inference based on blood lead levels at several timepoints during pregnancy (n=47). The p-PBK model was then evaluated using sensitivity analysis and by comparing the predicted ratio of cord blood lead level (BLLs) over maternal BLL with data from the literature.

2.4.1. Structure of the p-PBK model

The structure of the p-PBK model is illustrated in Figure 12, based on the O'Flaherty model (O'Flaherty, 1991a, 1991b, 1991c; O'Flaherty, 1998; O'Flaherty, 2000). This new model includes in total 9 compartments for the mother. The original PBK model for lead included blood, bones, kidneys, liver, richly and poorly perfused tissues. Several compartments were added either because they were particularly relevant regarding physiological changes related to pregnancy (adipose tissues, mammary glands, and placenta) or for consistency with the fetal submodel which included the target organ for toxicity, the brain. The fetal submodel therefore included all maternal compartments except the mammary glands (i.e., 8 compartments).

¹ Ali Daoud, Y., Tebby, C., Beaudouin, R., & Brochot, C. (2023). Pregnancy PBPK model for lead. Zenodo. <https://doi.org/10.5281/zenodo.8032484>

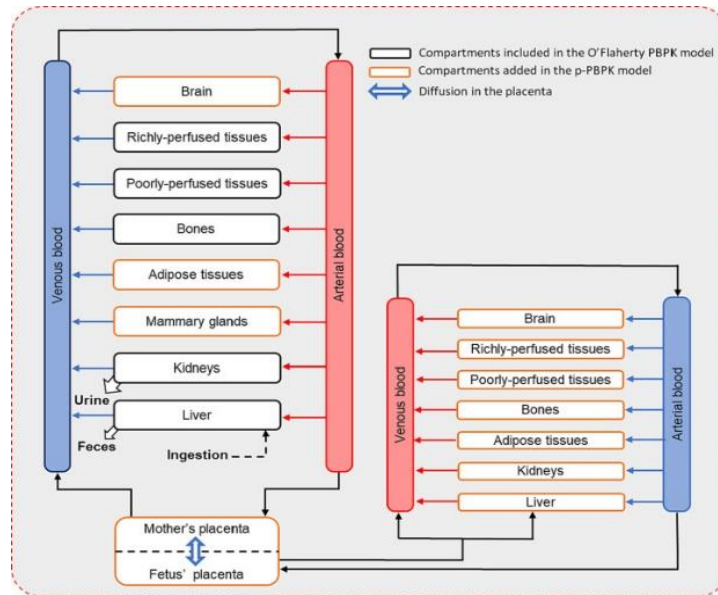


Figure 12. Structure of the p-PBK model for Pb developed by Daoud et al. (2023).

Maternal exposure by ingestion was modelled as an age-dependent fraction of ingested Pb entering the liver. Pb is distributed to the organs of the mother and the foetus by the plasma: the levels in the organs are driven by tissue:plasma partition coefficients and limited by blood flows. No metabolism is implemented in the model. Pb is eliminated through urine (70%) and bile (30%) in the mother depending on the bodyweight-dependent glomerular filtration rate (GFR). Fetal exposure is mediated by the diffusion of Pb across the placenta. A bidirectional transfer between the maternal and fetal placenta was assumed (Brochot et al., 2019a; Codaccioni & Brochot, 2020; Dallmann et al., 2019).

2.4.2. Model parametrisation

Compared to the original PBK model for lead by O'Flaherty (1991b) several parameters were updated to incorporate their evolution during pregnancy (**Erreur! Source du renvoi introuvable.** and **Erreur! Source du renvoi introuvable.** in Daoud et al. (2023)). Changes in hematocrit, glomerular filtration rate, cardiac output, blood flows and compartment volumes were modelled as functions of the gestational age, fetal age, or bodyweight (Abduljalil et al., 2021; Beaudouin et al., 2010; Brown et al., 1997; Dallmann et al., 2017; ICRP, 2002; Zhang et al., 2017). These changes were made in concordance with pregnancy-PBK models for PFAS (Brochot et al., 2019a; Ratier et al., 2024) whilst additionally ensuring coherence between the fetal bone growth model and the maternal bone compartment modeling. One of the main physiological novelties in this model is the modeling of additional maternal bone remodeling during pregnancy. The increase in bone remodeling during pregnancy was modelled by additional formation and resorption, assuming constant bone volume and weight (Shahtaheri et al., 1999).

Substance-specific parameters were set based on values used by O'Flaherty (O'Flaherty, 2000), and summarized in **Erreur! Source du renvoi introuvable.** of Daoud et al. (2023). The brain:plasma and placenta:plasma partition coefficients were set to that of well-perfused tissues. The fetal tissue:plasma partition coefficients were assumed to be equal to the maternal values. The fractional clearance of Pb from plasma into new bone in the foetus was set to that of the mother.

2.4.3. Model calibration

The parameters for additional bone remodeling and placental diffusion were estimated by Bayesian inference using, respectively, maternal BLLs over pregnancy and paired concentration

data in the mothers and newborns blood at delivery. Two datasets were used to calibrate the model parameters. The Rothenberg's study (Rothenberg et al., 1994) was used to estimate additional bone remodeling, measuring Pb in maternal blood in 105 women living in the valley of Mexico at four timepoints during pregnancy, from week 12 to week 36 of pregnancy. Data from the study of (Nashashibi et al., 1999) was included to calibrate the diffusion constant of Pb in the placenta (*KDpl*), which reports Pb levels in the mother's blood and cord blood at delivery in 47 mother-newborn pairs. The gestational age and the mother's age were not reported, thus, in the model, it was assumed that the women were on average 29 years old and at a gestational age of 39 weeks at delivery. Because the exposure of the women was not known, the daily intake (*DI*) of each woman was also estimated independently for each woman assuming a constant exposure per unit body weight of the women since birth.

2.4.4. Main Results

The mean *DI* of the mothers from the Rothenberg's study were estimated to $1.9 (\pm 0.034) \mu\text{g}\cdot\text{day}^{-1}\cdot\text{kg}^{-1}$ and $4.0 (\pm 1.2) \mu\text{g}\cdot\text{day}^{-1}\cdot\text{kg}^{-1}$ from the Nashashibi's study. The placental transfers were also estimated (*KDpl*). The estimated maternal BLLs and the 95% credibility interval (CI) during pregnancy with the data used for model calibration are presented in Figure 3 in Daoud et al. (2023). The median predicted maternal BLL decreased by 32% between the beginning of pregnancy and the start of additional bone remodeling, mainly due to the hemodilution and the increase of the maternal volume of distribution. Between the beginning of the additional bone remodeling (around 23 weeks of gestational age) and the end of pregnancy, the predicted median BLL is increased by 19% due to Pb bone release into maternal blood. Most concentrations in the mother and foetus were predicted within a 1.1-fold error range (84%), and all BLLs were predicted within a 2-fold error range, indicating a good agreement with the observations. All predicted cord blood:mother BLL ratios were at 98% predicted in the 2-fold error. The median predicted cord blood:mother BLL ratio was 0.88. The main parameters influencing the model outputs (the venous concentrations in the mother and foetus, the cord blood:mother blood ratio, and the concentration in the foetus' brain at the end of each trimester of pregnancy) are maternal bone accumulation, additional bone remodeling, maternal Pb binding red blood cells, fetal Pb binding red blood cells, fetal bone parameters, brain partition coefficient and placental transfer of Pb.

The p-PBK model for Pb was evaluated using observed ratios between Pb levels in the umbilical cord and maternal blood in five studies (Alemam et al., 2022; Gulson et al., 2016; Ladele et al., 2019; Ong et al., 1985; Yazbeck et al., 2007). Blood samples were collected at delivery or within hours. Mean gestational age at delivery was reported in one study (Ladele et al., 2019), otherwise, it was set to 39 weeks. Figure 13 shows the median of the cord blood:mother blood ratio throughout pregnancy with the 95% of CI (panel A), as well as the distribution of the observed ratios reported in five studies and the ratio predicted at delivery (panel B). The p-PBK model was used to predict the kinetics of Pb in fetal bone, blood and organs such as brain, which are different but characterized by three phases, hence the importance of modeling them (Figure 7 in Daoud et al. (2023)).

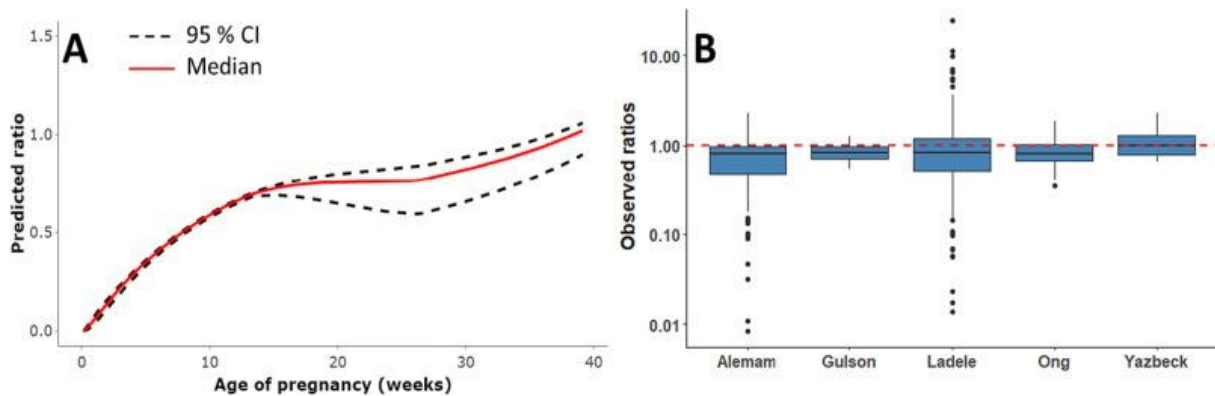


Figure 13. Predicted cord blood:mother blood ratios during pregnancy and observed ratios at delivery. A) The solid red curve represents the median of predicted ratios, and the black dashed curves represent the 95% CI of predicted ratios by the p-PBK model for 3000 MC simulations. B) The boxplots represent the distribution of ratios computed with measured concentrations reported in five studies (Gulson et al., 2016a; Ong et al., 1985; Yazbeck et al., 2007; Ladele et al., 2019; Alemam et al., 2022) and the dashed line the predicted ratio at delivery by our p-PBK model.

2.4.5. Conclusions and perspectives

The previous PARC review highlighted a gap in PBK models accounting for pregnancy and young children. For lead, PBK models were available for children (US EPA, 1994; White et al., 1998) or adults (Leggett, 1993), of lifetime from birth (O'Flaherty (1993), US EPA (2019)) in the literature. To better understand the effect of lead on neurodevelopment, it is important to be able to predict the prenatal and neonatal brain lead levels. Thus, in this PARC project, we have developed for the first time a PBK model that accounts for pregnancy and allows to predict fetal brain Pb levels, with the most recent information available. In the PARC case studies, the developed p-PBK model is ready to be used to assess prenatal lead exposure. This approach could be relevant when toxicologists aim to estimate lead exposures (external or internal) for the sensitive population.

One of the main results is the importance of considering the bone remodeling during pregnancy, which increase the maternal blood lead levels in the 3rd trimester. Fetal bone ossification was predicted to decrease the exposure of the other fetal organs. These results are important for users of the Pb p-PBK model, as this process directly impacts the blood levels and helps interpret HBM data for this sensitive population. Furthermore, placental transfer rates were estimated with a high inter-individual variability and uncertainty due in particular to variable maternal:cord blood ratios at delivery, absence of data on fetal levels during pregnancy, and unknown dietary exposure scenarios. This output suggests collecting additional HBM data at the end of pregnancy from epidemiological studies or *in vitro* data corresponding to critical time points during pregnancy.

This p-PBK model predicts Pb kinetics in blood or various tissues for pregnant women and their fetuses, including the fetal brain. Further developments could involve connecting the p-PBK model with the model developed for exposure starting at birth (O'Flaherty, 1993; Teby et al., 2022) and refining the blood-brain barrier (BBB) model for the fetus. The BBB module developed by WP5 (see section 2.7) could be used to reduce uncertainty in translation of neurological risk from *in vitro* data, and to have a better realistic description of internal kinetics, enabling a more precise assessment of the effects. These developments will benefit toxicologists who aim to relate Pb internal kinetics at different life stages of the critical window of exposure with the neurodevelopmental effects, such as in the case study in the mixture 6.2.3 PARC project.

2.5. PFAS PBK modeling refinement

2.5.1. PFAS PBK models developed during the first years of PARC

Different models for PFOA and PFOS have been developed and published during the first years of PARC by 6.2.2 partners (Husøy et al., 2023; Ratier et al., 2024; Westerhout et al., 2024). Each model is unique in a way to make it useful for a specific application. The model of Husøy describes the kinetics of PFOA from oral (from food and drinking water) and dermal (from personal care products) exposure, using data from the EuroMix biomonitoring study for model validation. The model of Westerhout describes the kinetics of PFOA and PFOS from oral, dermal and inhalation exposure in an occupational setting and uses the local organ concentrations to predict effects on cholesterol homeostasis based on *in vitro* transcriptomics data. Finally, the model of Ratier describes the kinetics of PFOA and PFOS for pregnant women, fetuses and children from their birth to teenage years through oral exposure (breast milk, drinking water and food). The model output was compared to the biomonitoring data from the HELIX cohort study. Several PARC project partners indicated to be working on the refinement of PBK models for PFOA, PFOS and other PFAS. IISPV is collaborating with other partners in WP 5.3.4 for developing open source generic PBK model of all 4 PFAS chemicals (PFOS, PFOA, PFNA, and PFHxS). The manuscript will be submitted by April 2025 and the model will be available in systems biology markup language (SBML) format utilizing PBK ontology.

2.5.2. PFAS PBK model working group

To harmonize these developments, a working group was initiated by RIVM so that all partners could jointly work on the same models. A GitHub repository was set up to facilitate this collaboration and different subgroups were formed to split the work between partners. The first goal is to combine parts of the different published models for PFOA to make it applicable to a wider range of exposure scenarios (oral, dermal and inhalation) and subpopulations (using the lifetime equations). Issues with the Loccisano et al., (2011) model code that is often used as a basis for these chemicals, were solved. Additionally, mechanistic information (e.g. *in vitro* transporter data) in the model were included rather than fitting specific model parameters based on epidemiological data. This was done to make the model applicable to other PFAS for which data gaps exists in the epidemiological data. Initially, the focus was on PFNA and PFHxS. The PFOA model is being finalized, making use of *in vitro* data on kidney transport processes, plasma protein binding and human tissue partitioning. Model predictions will be compared to data from the EuroMix HBM study. In parallel, the PFOS model is under development using the same approach as the PFOA model.

2.5.3. OECD evaluation template GD 331 and PFAS PBK models

In addition, joint work has been performed by multiple partners and led by IISPV to carry out a PBK model evaluation for PFAS compounds using OECD GD331. Relevant PFAS PBK models were selected for the case study by setting the inclusion criterion. We have excluded review, semi review, reports and PBK models published for species other than human. Also, in case of multiple models by same author, recently published model has been considered for the evaluation. A questionnaire was developed using the OECD evaluation template, with modifications to enable quantitative rather than qualitative assessment. A questionnaire was distributed among the PBK expert community to evaluate the existing models considering different aspects like documentation (context/implementation, software, model code, verification, peer engagement)

and assessment of model validity (input parameters, uncertainty, sensitivity analysis, goodness-of-fit and predictivity). Data obtained from experts were analysed and further points to improve the existing PFAS models were identified. This task has been converted into a draft publication “Evaluation of PBK models using the OECD assessment framework taking PFAS as a case study”. Currently, the draft has been submitted in “computational toxicology” and is under review.. To facilitate a broader adoption of the OECD PBK evaluation criterion, a template has been created and hosted on IISPV web server (https://app.shiny.insilicohub.org/Evaluation_PBK/). A similar task can be conducted with multiple groups of chemicals to identify a good model fitting that best fit the intended purpose and to assess the limitations of existing models.

2.5.4. PFAS PBK modeling and uncertainty analysis

A case study led by MU in the 7.3.2 activity, and in collaboration with several 6.2.2 partners, aims to quantify and assess uncertainty in PFAS exposure through a workflow that integrates HBM data, exposure assessment models, and PBK models. This workflow is structured around two main pathways: HBM exposure (internal) and external dietary exposure. In close collaboration with T8.3, it is currently being developed for potential implementation within the PARC model network.

We used both PBK models to derive individual daily intake estimates (EDIs) via reverse dosimetry based on internal exposure (blood PFAS concentrations) and exposure models to estimate individual EDIs using dietary patterns and data on the occurrence of PFAS in food and drinks. A critical aspect of this workflow is the uncertainty propagation in both the PBK model and exposure model, which aims to reflect real-world variability in both data and model parameters. An updated PBK model developed by the 6.2.2 PFAS PBK model working group was initially used for the Czech population. This model was applied in combination with the Bayesian Metropolis-Hastings Markov Chain Monte Carlo (MH-MCMC) algorithm for parameter calibration, which refines the parameter distribution based on likelihood estimates. Although this approach is well-established, it is computationally demanding and requires optimization of key elements like the acceptance rule, step sizes, and starting points to improve efficiency. The global sensitivity analysis (eFAST & Morris methods) is used as the first step to identify the most influential input parameters for the PBK model.

For estimating external exposure to PFAS, we used an exposure model with either a Monte Carlo (MC) simulation or an analytical Fenton-Wilkinson approximation. The MC method, though computationally intensive, is more robust in assessing uncertainty compared to the analytical approach, especially when dealing with zero-inflated data. Both methods provide a distribution of the estimated EDIs for individuals, with the MC simulation being preferred for its accuracy. The final comparison of modelled EDI from internal (PBK model) and external (dietary exposure model) sources is a key part of the uncertainty analysis.

The uncertainty assessment covers the entire workflow. Within the dietary exposure model, it starts from the input data: first the uncertainty in PFAS occurrence in food and drinks is estimated, based on our developed database of all available exposure studies. This provides one probability distribution for each combination of a compound \times food/drink item \times European country / region. On either individual or population level, probability distributions for dietary habits / food frequencies are defined, based on questionnaire data. While the PFAS occurrence tends to log-normal distributions, the Tweedie distribution is the suitable for describing the food/drink frequencies. In further steps, the uncertainty propagates through the model by compiling these distributions (multiplying frequencies \times occurrence and summing over all food items). This is done either by empirical way using simple Monte Carlo approach (generating eg. 1,000 values for each food item PFAS occurrence and frequency, multiply and sum the values getting an empirical distribution) or using analytical approximation for parametric combination of the probabilistic

distributions (eg. Fenton-Wilkinson). The final EDIs from external exposure model will be compared with EDIs from the reverse PBK modelling.

The uncertainty in PBK model parameters has not been fully assessed yet due to incomplete distributions of some model parameters, but preliminary results show that internal EDIs (based on blood concentrations) were generally higher than external EDIs for PFOS and in most cases also for PFOA. This difference may be assigned to non-dietary exposure such as dermal or inhalation intake of PFASs. The currently developed PBK model for PFAS by 6.2.2 working group is being adapted for all life stages, with a comprehensive set of physiological and chemical parameters. This model will be applied to HBM4EU adolescent data from nine European countries to estimate EDIs of PFOA, PFOS, PFNA and PFHxS based on blood concentration data. The model parameters were collected during year 3 (Y3) of PARC (including kinetic parameters and partitioning coefficients) and will be finalized in Y4; the distribution of each input parameter will be estimated based on literature research. A library of lifetime physiological equations for the PBK model developed in 6.2.2 will be used for the distribution of physiological parameters. Once the PBK model and parameter distributions are completed, various global sensitivity analysis and calibration methods will be tested to optimize the model predictions and refine the uncertainty estimates. For example, using MH-MCMC method, the intake distribution of selected PFAS compounds will be estimated for each participant. MH-MCMC simulations will be run repeatedly across a range of input parameter distributions to comprehensively explore the parameter space and capture the variability and uncertainty associated with the model parameters. A document will be developed recommending the use of different methods for quantifying uncertainties. This methodology will be applicable to other PBK models and compounds in the future, making the uncertainty assessment framework more versatile and expandable. This case study is important for advancing the uncertainty analysis methods for PBK models and exposure assessment, offering better insights into how variability in model parameters influences exposure estimates. These methods will be integrated into broader modeling frameworks (in collaboration with task 8.3), such as MCRA or PARC toolbox.

2.6. PBK models to aggregate exposure routes

HBM surveys are performed to monitor exposures related to the presence of substances in the body. However, HBM studies only provide a snapshot of the exposure at the sampling time. Ideally, information on the evolution of the substances over time (or between sampling times) in the biological matrices is needed to refine the risk assessment. Combined with HBM data based on exposure scenarios and exposure data, PBK modeling can link external to internal exposure (forward dosimetry) or internal to external exposure (reverse dosimetry) over time. Realistically, some environmental chemicals require multi-route PBK models, but, since the exposure from some routes is minor, it is often ignored (Deepika & Kumar, 2023). Considering the continuously growing interest in using PBK models in the risk assessment (RA) process, more precise implementation of the different routes of exposure in the PBK model could assist regulators, risk managers and decision-makers in establishing more effective strategies to manage and regulate general population exposure.

Absorption is the introduction of the compound into the body from the site of administration to the bloodstream. Absorption occurs through different routes: inhalation (pulmonary route), skin (or dermal) contact, ingestion (oral route) or intravenous injection. A set of complex mechanisms governs the passage of the substance between the site of administration and the bloodstream, with only a fraction reaching it. This step is one of the crucial pieces of information to have in hand to better characterize the internal exposure. The previous European project HBM4EU has already identified and reviewed available PBK models for about 30 compounds (Brochot et al., 2019b;

Sarigiannis et al., 2017), as well as the roadmap for action on new approach methodologies in risk assessment commissioned by EFSA (Escher et al., 2022). These reviews emphasised the lack or paucity of TK information for a high number of these prioritised compounds, particularly for the inhalation and dermal exposure routes for which absorption and metabolism data are lacking for most substances. In the PARC project on the refinement and development of PBK models for human risk assessment (project 6.2.2.a), the most recent PBK models of prioritized chemicals were inventoried, and a similar conclusion was established (PARC AD6.4).

This section aims to (i) summarise the physiology and the anatomy of the different exposure pathways as PBK models are based on the physiology, (ii) briefly review how absorption via inhalation, ingestion and dermal contact were modelled in PBK models inventoried in Y1 of PARC 6.2.2, gathering the parameters and data required to describe these exposure routes, and (iii) suggest a workflow to include different modules reflecting different levels of complexity in the three exposure pathways in PBK models, including some life stages differences to account for. In this report, we describe only briefly the different outcomes for each exposure route, while more details are planned to be applied in PARC 6.2 case studies by the end of the year and published in the beginning of 2026.

2.6.1. Oral Exposure

A. Physiology

Orally absorbed chemicals are primarily ingested through food and drinking water. This route involves a complex biological process where chemicals must traverse multiple organ barriers and the digestive system's chemical-eliminating organs before entering the bloodstream (Figure 14). The digestive system comprises the gastrointestinal (GI) tract (oral cavity, pharynx, esophagus, stomach, small intestine, large intestine, and anal canal) and accessory organs (teeth, tongue, salivary glands, liver, gallbladder, and pancreas) (Sensoy, 2021). The GI tract handles food movement and digestion, while accessory organs provide enzymes and bile to aid digestion.

After swallowing, food and water pass through the esophagus to the stomach, where chemicals are temporarily stored. The stomach's mucosal lining features an epithelial layer with gastric pits leading to glands that secrete gastric juice, creating a pH of 1.5 - 3.5 (Gaohua et al., 2021). This acidic environment, rich in digestive enzymes, facilitates the absorption of small, lipophilic, and non-ionized molecules into the portal vein, primarily via passive diffusion. However, the stomach absorbs much less chemicals than the small intestine due to its limited mucosal surface area (0.05 m²) (Helander & Fändriks, 2014). The stomach processes 2-3 liters of food per day, and gastric emptying depends on the food's physical properties and caloric density, with water exiting in about 10 minutes, and high-calorie liquids and solids taking up to 2 hours (Goyal et al., 2019).

From the stomach, contents move to the duodenum, the initial segment of the small intestine, followed by the jejunum and ileum. Over 90% of nutrients and chemicals are absorbed here due to several factors (Nunes et al., 2016). The small intestine, the longest GI tract section at around 300 cm, has an extensive surface area (~30 m²) due to plicae circulares, villi, and microvilli (Helander & Fändriks, 2014). Its optimal pH (4-7) supports digestion and absorption (Gaohua et al., 2021). A dense capillary network within the villi facilitates rapid transport to the hepatic portal vein, maintaining a concentration gradient for passive diffusion.

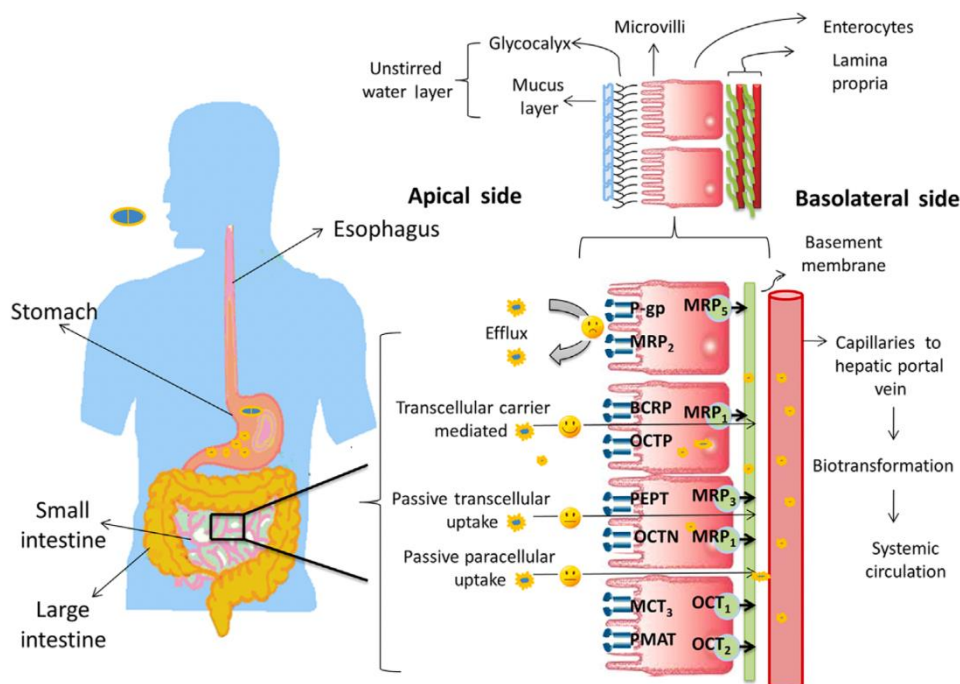


Figure 14. Schematic representation of the oral absorption pathway with focus of passive and active transportation in the gut. The figure was adapted from Gao et al. (2022).

Chemical absorption occurs through the epithelial barrier via passive paracellular and transcellular uptake, carrier-mediated transport, and active transport via uptake proteins like OATPs, OCTNs, and PEPTs on the enterocyte's apical surface, and OCT1 and OCT2 on the basolateral side (Estudante et al., 2013). The microvilli's glycoproteins create a protective unstirred water layer with a mucus about 100 μm thick. After passing through this layer, chemicals are absorbed into capillaries and transported to the liver via the hepatic portal vein. Efflux transporters, such as MDR1, BCRP, and MRP2, can actively return chemicals to the gut lumen, reducing systemic bioavailability and increasing the unabsorbed fraction (Estudante et al., 2013). The small intestine's pre-systemic metabolism involves diverse enzymes in enterocytes and gut microorganisms (Wang et al., 2024), with abundant P450 enzymes like CYP3A, CYP2C9, CYP3A5, and CYP1A2 (Drozdik et al., 2018; Paine et al., 2006). Other significant enzymes include UDP-Glucuronosyltransferases, carboxylesterases, and sulfotransferases (Gaohua et al., 2021; Goyal et al., 2019; Helander & Fändriks, 2014; Nunes et al., 2016).

The GI tract-liver axis, linked by the hepatic portal vein, is crucial for chemical absorption into systemic circulation. The liver connects to the bloodstream via the hepatic vein and artery, allowing bidirectional chemical movement. In hepatocytes, the cytochrome P450 enzyme system, with high protein abundance, facilitates chemical modification through phase I and II reactions (Drozdik et al., 2017). Some chemicals undergo enterohepatic circulation, where bile secretion recirculates chemicals between the liver and small intestine (Abbiati & Manca, 2017; Talevi & Bellera, 2021). Bile, produced in the liver, is stored and concentrated in the gallbladder until the small intestine signals its release for fat digestion. The bile, mixed with pancreatic juice, enters the duodenum, allowing chemicals to be reabsorbed and returned to the liver, potentially prolonging their half-life due to reduced elimination.

Overall, oral bioavailability (F) of a chemical is the product of the fraction absorbed from the GI tract (F_a), the fraction unaffected by first-pass extraction in the gut (F_g), and the liver (F_h). The unabsorbed fraction progresses through the large intestine and is excreted in feces. Chemical

absorption in the large intestine is limited due to its smaller surface area ($\sim 1.9 \text{ m}^2$) and tightly packed epithelial layer.

B. PBK compartment structures of oral absorption

We reviewed recently published PBK models for PFAS, bisphenols, pesticides, mycotoxins, and metals, focusing on their modeled oral absorption in humans (PARC Y 1). For this purpose, we analyzed each publication's compartmental diagrams and simplified the model structure (Figures not displayed in the report) to highlight only the oral absorption pathway, tracing the process from the absorbing compartment to entry into the bloodstream. For this purpose, similarities and dissimilarities are described within the same chemical groups

- **PFAS**

We reviewed the oral absorption pathways in 11 PBK models developed (Brochet et al., 2019a; Chou & Lin, 2019; Chou & Lin, 2021; Deepika et al., 2021; Fàbrega et al., 2014; Fàbrega et al., 2016; Husøy et al., 2023; Loccisano et al., 2011; Loccisano et al., 2013; Sweeney, 2022) only for PFOS, PFOA. PFAS was absorbed either in the gut, liver or stomach, and the GI tract was modelled with different complexities. All models accounted for binding to blood albumin to determine the free fraction in plasma. Biotransformation of the three PFAS was not incorporated due to nonexistence. Linear kinetics were assumed for all distribution steps, while dose intake was modeled as zero-order kinetics in the respective absorption compartment. Enterohepatic circulation and fecal excretion were implemented in three PBK models. The chemical-specific kinetic parameters and partition coefficients were primarily derived from studies conducted on rats and monkeys.

- **Bisphenols**

Ten PBK models (Deepika et al., 2022b; Hu et al., 2023; Karrer et al., 2018; Mielke & Gundert-Remy, 2009; Mielke et al., 2011; Sharma et al., 2018; Shin et al., 2004; Teeguarden et al., 2005; Wiśniowska et al., 2023; Yang et al., 2015) were identified for bisphenols, primarily focusing on bisphenol A, with two PBK models also covering other variants. The oral absorption in the PBK models differed in absorption compartments, gut/liver biotransformation, and excretion pathways. Bisphenols were mostly bound to albumin with low affinity. Linear kinetics were implemented for distributions, while absorption followed zero- or first-order kinetics. Biotransformation was modelled using clearance constants or Michaelis-Menten kinetics. In addition, it was assumed that only unconjugated bisphenol interacts with plasma proteins and endocrine receptors and that the metabolites were primarily renal excreted. Therefore, bisphenol metabolites were often modelled in a “volume of distribution” or “body volume” compartment. Also of importance is that some studies used rat studies to extrapolate to human. However, biliary excretion, enterohepatic circulation and fecal excretion influences bisphenol toxicokinetics in rats but are nearly neglectable in humans.

- **Pesticides**

Different PBK models were screened for the organophosphate pesticide chlorpyrifos and pyrethroid pesticides deltamethrin, permethrin and others. For chlorpyrifos, oral absorption was often modelled by means of a zero-order kinetic or single bolus dose in the gut and distributed directly into the liver compartment, where metabolic conversion takes place. Oral dose is thereby corrected for the fraction absorbed. The pyrethroid models were slightly more complex and included separate lumen compartments and separate compartments for the stomach and small and large intestine, taking into account faecal excretion and the enterohepatic circulation. In some PBK models, metabolic conversion has been implemented in both the GI tract and liver compartments. For other types of pesticides, i.e. epyrifenacil, haloxyfop, fipronil and chlordecone, oral absorption is modelled similarly to the pyrethroid models.

- **Mycotoxins**

The number of published PBK models for mycotoxins is limited, but we screened three models for zearalenone (Mendez-Catala et al., 2021; Mukherjee et al., 2014; Shin et al., 2009) and one model for deoxynivalinol (Notenboom et al., 2023) and aflatoxin B1 (Gilbert-Sandoval et al., 2020) each. In two PBK models, oral absorption was modelled across several small intestinal lumen compartments, where mycotoxins then further distributed to the liver. Enterohepatic circulation and faecal excretion were also implemented. Metabolic conversion occurred in compartments displaying the GI tract or/and the liver.

- **Metals**

Metals are a critical group of chemicals with significant health implications. In the models of Mann et al. (1996a) and Yu (1999b), the oral absorption of iAs is typically modeled as a first-order process, where arsenic is absorbed from the GI tract into the bloodstream at a constant rate. The model by El-Masri and Kenyon (2008) also adopts a similar approach. In the PBK models for mercury, such as those by Carrier et al. (2001), Gearhart et al. (1995), and Ou et al. (2018), the oral absorption of MeHg is modeled as nearly 100% efficient from the GI tract. These models assume rapid absorption into the bloodstream, where MeHg binds to red blood cells and is released into the bloodstream. In contrast, inorganic mercury (Hg^{2+}) exhibits lower absorption rates, though it is still considered within the GI compartment, with absorption rates varying depending on the model. In the models of Cd by Kjellström and Nordberg (1978) and Pouillot et al. (2022), oral absorption is described as a relatively efficient process, with Cd primarily absorbed through the GI tract after ingestion. In the PBK models of Pb by O'Flaherty (2000) and Tebby et al. (2022), ingestion input is directed in liver and then is released into the blood stream.

C. Complex oral absorption model

Other research has been also conducted to model oral absorption more physiological realistic. For instance, Abuhelwa et al. (2017) suggested the Advanced Compartmental Absorption and Transit Model for environmental exposures on the basis of drug models. This model mimics physiology correctly the passage of a chemical from absorption to entrance into the bloodstream, often simplified in the oral absorption pathways from the inventoried PBK models. Alone the gut tract consists of 26 compartments. This detailed model is however in need of many parameter values, which are often missing and difficult to parameterize. GastroPlus has implemented a similar complex structure as described by Abuhelwa et al. (2017)

2.6.2. Inhalation Exposure

A. Physiology

The respiratory system is the main route of exposure to inhaled chemicals, although a fraction can also be ingested through mucociliary clearance. The respiratory tract (RT) functionally consists of two areas (Figure 15): (i) the conducting airways (nose to bronchioles), which filter, warm, and humidify the inhaled air, and (ii) the respiratory area (respiratory bronchioles, alveolar ducts and alveoli), where a complex and efficient gas exchange system operates and xenobiotics absorption occurs (Hastedt et al., 2016) between the external environment at the epithelial surface of the alveoli and the internal pulmonary capillaries (Maina, 2002). This exchange is characterized by the vast alveolar surface area of 143 m² (Gehr et al., 1978), the ultra-thin epithelial barrier (0.5 to 1 μm), and a high perfusion (Ehrhardt & Kim, 2007). The epithelial lining of the RT is the principal barrier for chemical absorption, with a dynamic composition that changes from the conducting airways to the alveoli (Enlo-Scott et al., 2021). In the alveolar region, major cell types include Type I & Type II pneumocytes, endothelial cells, and macrophages. Type I pneumocytes cover 90% of the alveolar surface area, facilitating gas exchange. Type II pneumocytes (10% of the surface) are secretory cells that coat the alveolar surface with pulmonary surfactant and are also capable of

differentiation into Type I cells. Alveolar macrophages provide immunological defence against inhaled chemicals and other intruders, and contribute to phagocytosed particles transport from the alveoli to the mucociliary escalator in the airway or across the alveolar epithelium into the bloodstream (Chambers et al., 2019; Geiser, 2010). The lung-lining fluid (LLF) is a thin film that varies in composition and structure along the respiratory tract. In the conducting region, the Airway Surface Liquid (ASL), a mucus gel-aqueous layer (5–100 μm), interacts with epithelial cilia to form mucociliary escalator for rapid clearance of inhaled substances, facilitate the rapid clearance of inhaled chemicals to the oropharynx with a half-life of approximately 1 to 1.5 hours. In contrast, the alveolar regions are lined with a thin layer of Alveolar Subphase Fluid (0.1–0.2 μm) and pulmonary surfactant reduces surface tension (Hastedt et al., 2016; Ng et al., 2004).

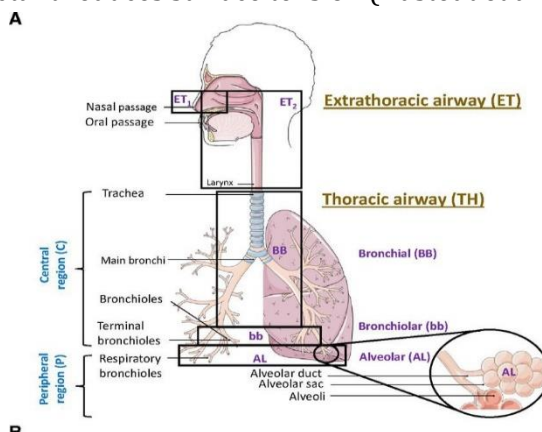


Figure 15. Illustration of the anatomical regions of the respiratory tract (source: Ladumor et al. (2019)).

B. PBK compartment structures of inhalation

We reviewed the recently inventoried PBK models in PARC for PFAS, bisphenols, pesticides, mycotoxins, and metals, focusing on their modelled inhalation absorption in humans. A total of 17 specific PBK models inventoried in Y1 of [PARC AD6.4](#) have included the inhalation exposure route in the model structure, often with the aim of modeling aggregated exposure including other absorption routes. In all these studies, inhalation appears to be a minor route of exposure to the substances compared to other exposure routes. In general, different levels of inhalation complexity have been implemented: the inhaled compound is absorbed (i) directly into the plasma or blood, (ii) into the lungs (or other respiratory compartments), which are considered as a single compartment (most PBK models, as a simplification of known physiology), and (iii) into the lungs, which are subdivided into sub-compartments, such as alveoli.

- **PFAS**

Among the 12 PFAS PBK models inventoried in Y1 of [PARC AD6.4](#), only one study (Rovira et al., 2019) assessed prenatal exposure to PFOS and PFOA including inhalation exposure as indoor dust ingestion and through air inhalation. In the absence of specific information, we assumed that inhaled PFAS were directly absorbed into arterial plasma.

- **Metals**

Among the 20 metals PBK models (As, Cd, Cr, Hg, and Pb) inventoried in Y1 of [PARC AD6.4](#), only Pb and Cd studies include an exposure by inhalation, supposing that inhaled chemicals are directly absorbed into the plasma (O'Flaherty, 1991a, 1991b, 1991c; O'Flaherty, 1998; O'Flaherty, 2000; Sweeney, 2021; Tebby et al., 2022) and/or via a respiratory compartment (e.g., lungs or respiratory tract) (Béchaux et al., 2014; Kjellström & Nordberg, 1978; Ruiz et al., 2010). Fractional absorption from the lungs to the blood has been implemented for lead (O'Flaherty, 1991a, 1991b, 1991c; O'Flaherty, 1998; O'Flaherty, 2000; Sweeney, 2021; Tebby et al., 2022). For cadmium,

inhalation is a major route of exposure, with deposition depending on particle size and respiratory characteristics. Models account for uptake in different regions of the respiratory tract but may not fully integrate physiological parameters such as inhalation rates or blood flow, instead using coefficients to estimate lung kinetics and daily uptake (Béchaux et al., 2014; Kjellström & Nordberg, 1978; Ruiz et al., 2010).

- **Bisphenols**

Among the 13 bisphenols PBK models inventoried in Y1 of PARC AD6.4, only one study (Sarigiannis et al., 2016a) provided a comprehensive risk characterization of bisphenol A (BPA), with the inhalation exposure route taking into account the absorption of gases and depending on the particle size distribution. The deposition fractions of particles across the different human respiratory tracts were also included. In the absence of specific information, we assumed that inhaled BPA is absorbed directly into the arterial plasma.

- **Pesticides**

Pesticides are the chemical family with the highest number of inventoried PBK models including the inhalation exposure route (n = 13 among the 24 pesticide PBK models inventoried in Y1 of PARC AD6.4). For pyrethroids and other pesticides, the inhalation models differed in their assumptions about lung absorption and exhalation, such as for chlorpyrifos, where exhalation was generally not considered due to its low volatility. A rapid equilibrium between lung air and blood is often assumed. Inhalation exposure was quantified by using either alveolar ventilation rates or total inhalation rates.

Some models simplified inhalation kinetics by directly integrating inhalation exposure into the blood, considering exhalation (Beamer et al., 2012; Mallick et al., 2020) or not (Bouchard et al. (2005); Knaak et al. (2004)). Some models describe inhalation absorption as inhalation exposure in the lung blood, considering exhalation (Emond and Multigner (2022) or not (Cooper et al., 2019; Darney et al., 2018; Lu et al., 2010; Poet et al., 2014; Wei et al., 2013; Zurlinden & Reisfeld, 2018a)), and then distributing to the bloodstream using lung tissue volume and partition coefficients to simulate lung-to-blood transfer. More complex models incorporate the alveolar compartment in addition to the lung compartment and assume exhalation (Quindroit et al., 2019b; Tornero-Velez et al., 2012).

C. Complex inhalation absorption model

More complex structures of the inhalation absorption pathway are implemented in PBK models available elsewhere in the scientific literature, such as performed in GastroPlus (Miller et al., 2022). The model includes a lung divided into five sub-compartments: an optional nose, extrathoracic, thoracic, bronchiolar and alveolar interstitial. Depending on the deposition, the mucociliary transit dictates the disposition of the substance in the lung, including for unbound fractions in the mucus, surfactant layers and the cells.

2.6.3. Dermal Exposure

A. Physiology

Skin is the largest human organ, shielding the body from the external environment to maintain the function and integrity of internal organs. This heterogeneous organ is composed of a multilayered barrier that is impenetrable to microorganisms, while semi-permeable to chemical substances. The structure of the skin is continuous with the membranes that line the surface of the body, consisting of specialized layers and associated appendages such as glands, hair, and nails (Hostýnek et al., 2001; Kolarsick et al., 2011; Venus et al., 2010). Anatomically, it is divided into three primary layers, as given here from outer to inner: the epidermis, dermis, and hypodermis (subcutaneous tissue) (Figure 16). The epidermis is the top layer and contains a diverse array of cells (viable and non-viable) including keratinocytes, melanocytes, dendritic cells, Langerhans

cells, and Merkel cells. Keratinocytes dominate this layer, connected by intercellular bridges, and are essential for the synthesis of keratin, a structural protein. The epidermis itself consists of four sublayers (Stratum Corneum, Stratum Germinativum, Stratum Spinosum, Stratum Granulosum), each defined by the positioning and morphology of the keratinocytes. In the Stratum Corneum, the outermost sublayer, keratinocytes transform into corneocytes (horny cells), flat, hard cells, which are high in protein and low in lipids. Moreover, this non-viable sublayer provides mechanical protection and acts as a barrier to environmental factors such as water loss and xenobiotics (Kolarsick et al., 2011; Murphrey et al., 2018; Schaefer & Redelmeier, 1997; WHO, 2006).

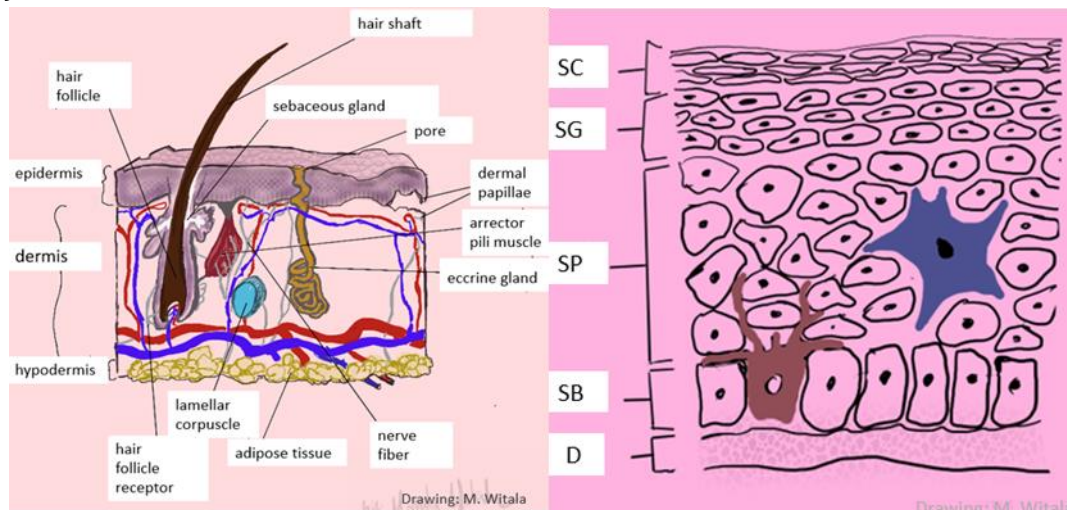


Figure 16. Left - Skin layers, cross section through the structure. Right - cross section showing (from the top) Stratum Corneum (SC), Stratum Granulosum (SG), Stratum Spinosum (SP), Stratum Basale (SB - also called Stratum Germinativum) and Dermis (D). Moreover, the Langerhans and Melanocyte cells are depicted (purple and brown, respective). The illustration is inspired and based on (Brito, Baek and Bin, 2024).

The Stratum Corneum (SC) is the skin's main barrier against foreign substances. Chemical absorption occurs through passive diffusion, following two primary pathways: The intercellular pathway, where substances move between corneocytes, and the transcellular pathway, where substances pass through corneocytes and the lipid matrix. A third, minor pathway involves absorption through hair follicles and glands. Once a chemical passes the SC, it can be metabolized in the epidermis or, if it reaches the dermis, enter the bloodstream for systemic distribution.

B. PBK compartment structures of dermal absorption

We reviewed previous inventoried PBK models to inspect the modeling approaches for dermal absorption. Dermal exposure was implemented in three PBK models for PFAS, in three PBK models for bisphenols, in 11 PBK models for pesticides, but was not considered for mycotoxins and metals. Diffusion models are generally based on the Fick's law of diffusion, where the skin chemical absorption is function of time and distance. The rate of penetration depends on the concentration gradient, the diffusion coefficient, and the thickness of the skin barrier. Most PBK models modelled dermal penetration by assuming that the epidermis being the rate limiting barrier, often with approach where skin is treated as single compartment, with bidirectional blood flow perfusing a portion of chemicals exposed skin. Therefore, we highlighted only PBK models for bisphenols that had a more complex physiology implemented to model dermal absorption.

Bisphenols

Noteworthy, the INTEGRA model for BPA incorporated two-layer skin structure, encompassing the stratum corneum and viable epidermis (Sarigiannis et al., 2016a). This approach is particularly noteworthy as it accounts for metabolic processes, thereby enhancing the model's

relevance to skin physiology. A similar two-skin compartment approach added a parallel sub-compartment designated as "follicle" in addition to SC and viable epidermis to represent a potential pathway for chemicals to traverse through skin appendages (Hu et al., 2023). The model further postulates the formation of a skin-surface depot for chemicals prior to their entry into the body via the follicle or SC and subsequent diffusion to the blood circulation.

2.6.4. QSAR models

A literature search was conducted to identify QSAR models for the prediction of ADME parameters for inhalation, dermal, and dietary exposure routes using PubMed and Google. Key information like sample size, set of employed descriptors/fingerprints, applicability domain, source of experimental data and their availability, modelling algorithm and software, were collected. New and original sources of experimental data were also noted, if available. The goal was to reconstruct which experimental data was used across different models using cross-referencing to any previous model or data source.

A. Inhalation exposure route

A limited number of QSAR models have been developed since 2015 related to the inhalation pathway but typically applied to only a few dozen chemicals. These models mainly focused on two parameters, namely the pulmonary permeability and the steady-state Epithelial Lining Fluid-to-plasma Ratio (EPR). Pulmonary permeability may roughly be estimated by the *in vitro* assays which determine the permeability of Caco-2 and CaLu-3 cells. CaLu-3 cells are recently being used more e to obtain more accurate predictions (Selo et al., 2021; Sibinovska et al., 2020). Ssteady state EPR, QSAR models were built and further developed for antibiotics, mainly by one research consortium. For all models, modeling activity employed elastic net regression in R based on *rcdk* descriptors, and similar workflows for data retrieval were used. The alveolar Macrophages – Epithelial lining fluid Ratio endpoint (MER) was included in the latest study [\(Aulin et al., 2022; Vålitalo et al., 2016\)](#) Publications reporting ADME parameters of QSAR models for inhalation exposure route are summarized in Annex 3, Table S1.

B. Dermal exposure route

Published QSAR models were mostly targeting permeation coefficient (k_p) and maximum flux (J_{max}) as identified in relevant papers published since 2015 (Annex 35 Table S2). These QSAR models complement traditional models for these endpoints based on a few simple descriptors like molecular weight and octanol/water partition coefficient. Publications reporting experimental data are summarized in Annex 3, Table S3.

C. Oral exposure route

QSAR models are available for oral absorption focusing on parameters like intestinal transporters, uptake, efflux, Caco-2 permeability, and absorption rate constant. Currently, most of available QSAR models are developed using advanced machine learning algorithms like support vector machine, random forest, k nearest neighbour with Dragon and MOE chemical descriptors. With 5-fold external validation, mostly these models provide good prediction accuracy ranging from 71-100%. Further details about some of the existing QSAR models has been provided in Annex 3, Table S4.

2.6.5. Limitations and Outlook

We identified multiple limitations in our inventory of absorption pathways via inhalation, dermal absorption, and oral ingestion. The following main limitations were identified:

1) More general challenges were related to code reporting and inconsistent descriptions between schematic representation of the PBK model, the verbal description of the absorption processes, and the mathematical descriptions if available.

2) Another general limitation was that the abbreviations used and the applied terms differ between studies, hampering the comparison of model structures. Different terminology used to address similar biological or chemical processes often leads to an error while reproducing the model and also makes it machine unreadable, a major bottleneck for automation. To overcome this challenge, a PBK model ontology is currently established that can be used for harmonizing future PBK model descriptions (2.8).

3) Different input types are needed for the exposure pathways (i.e., data from environmental media, food items, consumer products, or intake data). Here, future collaboration with other projects in PARC, such as the 6.2.1 activity, will help to overcome this limitation.

4) There is significant variability in modelled absorption pathways within and across chemical groups. Noteworthy, oral absorption routes have been modelled in a much broader complexity than inhalation and dermal absorption pathways. In addition, different parameters are needed to model absorption via the three pathways. For the oral absorption pathway, parameters such as absorption rate constant, fraction absorbed, intestinal permeability (P_{eff} , often from *in vitro* or *in silico* models), metabolism in gut/liver, partition coefficients (gut-to-blood, liver-to-blood, etc.). Key parameters for inhalation exposure include for instance respiratory volumes, lung function, pulmonary absorption and blood:air partitioning, while dermal absorption requires parameters such as diffusion coefficient in the stratum corneum thickness of the skin layers, partition coefficients (skin-to-water, skin-to-blood). In the future, QSAR models might help overcome the challenge of parameterization.

5) Absorption routes were modelled using different complexities (i.e., number of compartments, kinetic rates incorporation, chemical-specific process, life-stage dependent enzymatic activities, etc.) and being not always correct according to human physiology. Different reasons might underly these discrepancies. The complexity of absorption pathways might have been adapted on the scope and purpose of the PBK model in relation to its use for risk assessment. Generically speaking, the scientific purpose of the model, availability of the existing data, acceptable uncertainty, and usage of model for risk assessment are some of the factors determining complexity of model. OECD PBK modeling guidance (OECD, 2021) states that '*model should be only as complex as necessary to address the assessment in a fit-for-purpose manner*'. In some cases, a one-compartment model may determine the systemic exposure while other requires multi-compartment model with new approach methodology like *in vitro* to *in vivo* extrapolations (IVIVE) by utilizing Caco-2 or other cell line data for absorption. In general, increased complexity of absorption pathways correlates with increased knowledge and data availability. The comparison of absorption pathways of same chemical groups highlighted this correlation and showed an increased adaptation of the usage of *in vitro* bioassays for *in vitro* to *in vivo* extrapolation purposes. However, this approach is still at its beginning and the application of QSAR models might be helpful for implementing read-across extrapolations of *in vitro* endpoints for many different chemicals in PBK models.

6) The implementation of active transportation and biotransformation with multiple potential proteins is still limited and future implementation of *in vitro* to *in vivo* extrapolation is needed.

7) We also noted that the interaction between chemical exposure and microbiome has not yet been implemented according to the inventoried PBK models. Whether this interaction has an influence on the chemicals' toxicokinetics might be a novel research area.

In the next steps, we want first to solve the question of whether different complexities of absorption impact different accumulated amounts, depending on different inputs (e.g., exposure scenario, chemicals, life-stages, etc.). We therefore aim to harmonize equations for absorption using the currently developed PBK ontology database. Then, we will be able to model chemical accumulation in a harmonized set of equations and parameters. We will define the same

parameter sets for the respective chemical group and the outputs will be compared. If the differences will not be significant, we will suggest a simpler absorption pathway that needs less parameters (parsimony principle). In contrast, if the accumulation differences will be significant, we will explore the importance of parameter sensitivity, giving us a guidance for which parameter values are needed to be well measured or estimated by *in vitro* bioassays, QSAR models, read across approaches or other *in silico* approaches. If the current inventoried QSAR models allow, we can explore the adaptation of QSAR models in modeling absorption in PBK models. In addition, the time-course and contribution of accumulation from all three major absorption routes can be explored and might help to improve modeling aggregated exposure via dermal, inhalation, and oral absorption for refined risk assessment.

To illustrate our next steps, we have established a case study where we compared simulated oral ingestion of PFOA based on absorption pathways from two PBK models (Husøy et al., 2023; Loccisano et al., 2011; Loccisano et al., 2013), illustrated in Figure 17.

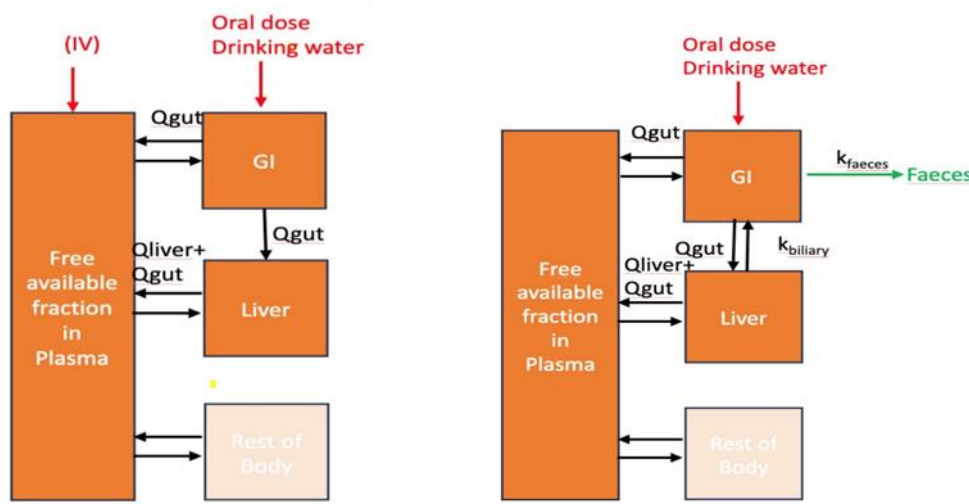


Figure 17. The absorption structures adopted from the PBK models originally published by Loccisano et al. (2011) (Left) and Husøy et al. (2024) (Right) that were used to compare PFOA accumulation via oral ingestion.

Loccisano et al. (2011, 2013) and following applications (Fabrega et al. 2014, 2016, Deepika et al. 2021) employed an absorption model where oral dosing was introduced into the GI compartment. According to the original compartment scheme PFOA was distributed either to the plasma or the liver via gastrointestinal blood flow (Q_g). Please note that in the differential equations, PFOA in the gut was only distributed to the blood via the liver ($((Q_{liver} + Q_{gut}) \times Free \times C_{liver} / P_{liver})$). Bidirectional chemical movement between the liver and blood was modelled through arterial and venous blood flow. We harmonized the differential equations to calculate amounts in gut, liver, and plasma as following (Eqs 1 - 3.):

$$\frac{dA_{gut}(t)}{dt} = (Q_{gut} \times Free \times C_{plasma}) - (Q_{gut} \times Free \times \frac{C_{gut}(t)}{P_{gut}}) + DOSE \quad (1)$$

$$\frac{dA_{Liver}(t)}{dt} = (Q_{liver} \times Free \times C_{plasma}) + (Q_{gut} \times Free \times \frac{C_{gut}(t)}{P_{gut}}) - ((Q_{liver} + Q_{gut}) \times Free \times \frac{C_{liver}(t)}{P_{liver}}) \quad (2)$$

$$\frac{dA_{plasma}(t)}{dt} = ((Q_{liver} + Q_{gut}) \times Free \times \frac{C_{liver}(t)}{P_{liver}}) - (Q_{plasma} \times Free \times C_{plasma}) \quad (3)$$

The abbreviations were defined as concentrations in gut (C_{gut}), liver (C_{liver}), and plasma (C_{plasma}), blood flows to the gut (Q_{gut}), liver (Q_{liver}), the partition coefficients gut:plasma (P_{gut}) and liver:plasma (P_{liver}), and the free fraction of PFOA in plasma (Free). The parameter DOSE was the aggregated daily intake based on the EFSA risk assessment. The equation of the plasma compartment was slightly modified to account only outflow to gut and liver, while the original differential equation accounts outflow to all organs using the cardiac output adjusted to haematocrit (Q_{plasma}).

Slightly similar to the first absorption structure was the PBK model from Husøy et al. (2023), who incorporated enterohepatic circulation, linking the liver to the GI tract via the biliary rate constant ($k_{biliary}$). Additionally, PFOA was eliminated through feces directly from the GI tract, bypassing the plasma compartment. The harmonized equations were the following (Eqs. 4 to 6):

$$\frac{dA_{gut}(t)}{dt} = (Q_{gut} \times \text{Free} \times C_{plasma}) + (k_{biliary} \times \text{Free} \times \frac{C_{liver}(t)}{P_{liver}}) - (Q_{gut} \times \text{Free} \times \frac{C_{gut}(t)}{P_{gut}}) - (k_{faeces} \times \text{Free} \times \frac{C_{gut}(t)}{P_{gut}}) + DOSE \quad (4)$$

$$\frac{dA_{liver}(t)}{dt} = (Q_{liver} \times \text{Free} \times C_{plasma}) + (Q_{gut} \times \text{Free} \times \frac{C_{gut}(t)}{P_{gut}}) - ((Q_{liver} + Q_{gut}) \times \text{Free} \times \frac{C_{liver}(t)}{P_{liver}}) - (k_{biliary} \times \text{Free} \times \frac{C_{liver}(t)}{P_{liver}}) \quad (5)$$

$$\frac{dA_{plasma}(t)}{dt} = ((Q_{liver} + Q_{gut}) \times \text{Free} \times \frac{C_{liver}(t)}{P_{liver}}) - (Q_{plasma} \times \text{Free} \times C_{plasma}) \quad (6)$$

Additional parameters to the first model were the biliary excretion rate ($k_{biliary}$) and the faecal excretion rate (k_{faeces}).

We simulated PFOA in the accumulating compartments gut, liver, and plasma and estimated identical PFOA concentrations in the respective compartments for both PBK models (Figure 18) using same parameter values. We applied 0.187 ng/kg and day as dose. The reason of this result is that faecal extraction implemented by Husøy et al. (2024) is an insensitive parameter according to global sensitivity analysis conducted in the PARC 6.2.2 working group 'PFAS PBK modeling refinement' (see 2.5), meaning the faecal extraction might be excluded for PFAS PBK models. However, this hypothesis needs to be explored for other PFAS as well before excluding faecal excretion. In addition, parameterization of faecal excretion based on animal studies, while PFAS measurements in human faecal is poorly studied. Enterohepatic circulation seemed to be also non-influential to the model simulations. The problem with the parameterization of the enterohepatic circulation is that it is difficult to calibrate based on experimental or human data because of missing direct experimental or human data.

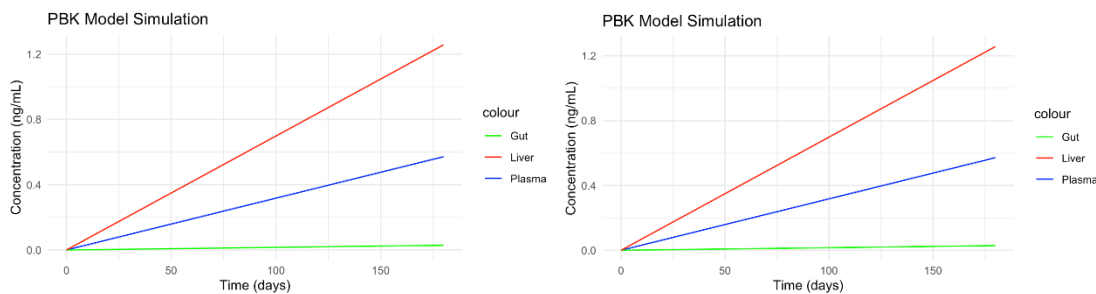


Figure 18. The accumulated PFOA concentrations in gut, liver, and plasma simulated based on the oral absorption pathways from Loccisano et al. (2011) (Left) and Husøy et al. (2024) (Right).

2.7. Blood-Brain Barrier in inventoried PARC PBK models

The blood-brain barrier (BBB) is a vascularized structure that creates a physical barrier between the bloodstream and the brain microenvironment, regulating the passage of substances (Ballabh et al., 2004; Engelhardt & Sorokin, 2009). However, some chemicals can cross this barrier and reach the brain tissue. Implementing this barrier into PBK models is relevant to understanding the kinetics of neurotoxic chemicals in the brain, such as pesticides or some heavy metals. It will also help to better link the internal concentrations of chemicals in the brain to the associated effects of prenatal exposure during childhood. In this section, we first present the anatomy and physiology of the BBB, then describe how this is implemented in the PBK models to identify the key parameters required and then explore the use of *in vitro* data collected in collaboration with WP5.

2.7.1. Overview of the blood-brain barrier

Anatomically, the BBB comprises a monolayer of endothelial cells tightly bound by tight junctions, reinforced by pericytes, astrocytes, and a basement membrane (Redzic, 2011). Figure 19 (Wu et al., 2023) summarizes the transport routes of the chemical across the BBB that occur via the pathways including paracellular and transcellular diffusion, receptor-mediated transcytosis, cell-mediated transcytosis, transporter-mediated transcytosis, adsorptive mediated transcytosis (panel a) and the structure and different cells contributing to the integrity of BBB (panel b).

Tight junctions are established around the 14th week of pregnancy and the maturation of the BBB occurs progressively. One aspect of BBB maturation involves mature astrocytes that only appear at birth.

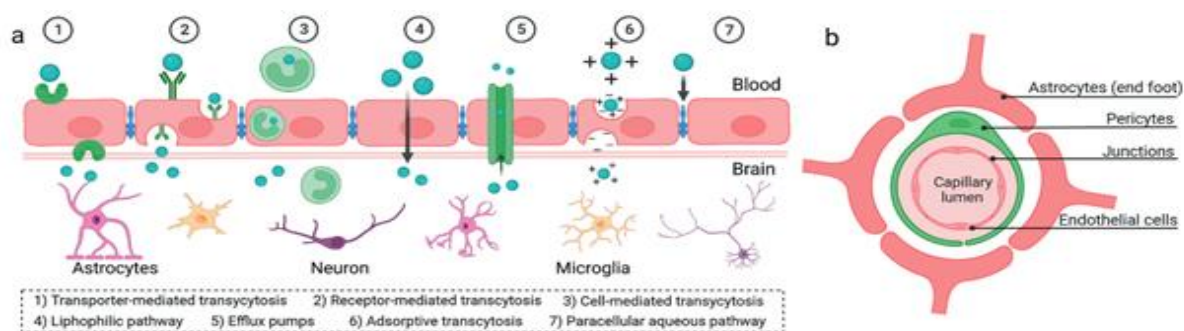


Figure 19. Longitudinal and transverse illustration of the BBB composition (Wu et al. (2023)).

2.7.2. BBB implementation in the inventoried PBK models in PARC

During the first year of PARC, more than half of inventoried PBK models considered a brain compartment in their general structure ($n = 48$ of 87 inventoried existing models, Annex 6). The brain is implemented in different ways, depending on the number of sub-compartments. The brain is often implemented as a unique compartment (43%, $n = 37$), suggesting a perfusion-limited distribution of the chemical, and to a lesser extent, in two (14%, $n = 12$) or four ($n = 2$) compartments, involving diffusion-limited processes.

Models with a brain composed of two sub-compartments assume diffusion-limited kinetics between brain blood and brain tissue (Carrier et al., 2001; Clewell et al., 1999; Darney et al., 2018; Emond & Multigner, 2022; Gearhart et al., 1995; Godin et al., 2010; Maass et al., 2023; Mallick et al., 2020; Pendse et al., 2020; Quindroit et al., 2019a; Tornero-Velez et al., 2012; Wei et al., 2013). Models with a brain composed of four sub-compartments (Sarigiannis et al. (2016b) and Sarigiannis et al. (2020)) represent the most complex structure for the brain among the existing PBK models inventoried in the first year of PARC, available for bisphenol-A. These models include

differences in permeability between four different brain regions, namely, the main brain, globus palidus, cerebellum and pituitary. However, to our knowledge, the parameter values and equations related to this structure were not detailed in these studies or elsewhere.

The various brain structures implemented in the inventoried PBK models (including structures in one, two and four sub-compartments) are presented below with their associated equations and parameters when available.

One compartment model

- *Structure*

The brain is implemented as a single homogenous compartment with the hypothesis of limited perfusion (Figure 20).

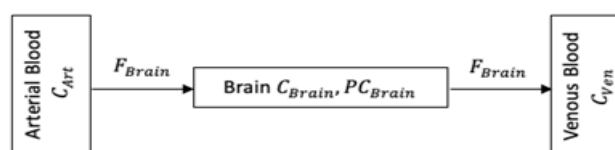


Figure 20. Schematic structure of the one-compartment model for the brain.

For **PFAS** (n = 12), if the model considers a brain in its structure (n = 6), it is always implemented as a unique compartment (Brochot et al., 2019a; Deepika et al., 2021; Fàbrega et al., 2015; Fàbrega et al., 2014; Fàbrega et al., 2016; Rovira et al., 2019). For **bisphenol**, the PBK models inventoried (n = 13) show similarities with models for PFAS where the brain is implemented as a unique compartment in the model structure (Deepika et al., 2022a; Edginton & Ritter, 2009; Hu et al., 2023; Karrer et al., 2018; Mielke & Gundert-Remy, 2009; Mielke et al., 2011; Sharma et al., 2018; Shin et al., 2004; Yang et al., 2015), except one model describing 4 sub-compartments. Similarly, for pesticides, and in particular for the **chlorpyrifos**, the brain is usually described as a single compartment (n = 13 of the 16 models inventoried for this substance; (Beamer et al., 2012; Foxenberg et al., 2011; Hinderliter et al., 2011; Knaak et al., 2004; Lowe et al., 2009; Lu et al., 2010; Mosquin et al., 2009; Poet et al., 2017; Poet et al., 2014; Smith et al., 2014; Timchalk et al., 2002a; Timchalk et al., 2002b; Zurlinden & Reisfeld, 2018b), or as for **epyrifenacil** (Hirasawa et al., 2022). For some **metals**, such as for arsenic (El-Masri & Kenyon, 2008) and mercury (Ou et al., 2018), a one-compartment model structure was also implemented. For **lifetime** generic models (n = 12), five models include a single compartment for the brain (Beaudouin et al., 2010; Brochot & Quindroit, 2018; Clewell et al., 2004; El-Masri et al., 2016; Verner et al., 2010).

- *Equations*

Equation (2) is used to describe the one-compartment of the brain:

$$\frac{dQ_{Brain}(t)}{dt} = F_{Brain} \times \left(C_{Art}(t) - \frac{C_{Brain}(t)}{PC_{Brain}} \right) \quad (2)$$

With Q_{Brain} the amount of the chemical in the brain tissue (in mmol), F_{Brain} the blood flow to the brain (L/h), C_{Art} is the arterial concentration of the chemical (mmol/L), C_{Brain} is the concentration of the chemical in the brain tissue (mmol/L), and PC_{Brain} the brain: blood partition coefficient.

- *Parameters*

Physiological information is required on brain volume and its associated blood flow, which depend on the age of the studied individual. For chemical parameterisation, the brain: blood partition coefficient is required.

Two-compartments model

- Structure

The two-compartment assumptions used to implement the brain in a PBK model supposed a diffusion-limited distribution to the brain tissue compartment. The two-compartment models consider a compartment outside the BBB, which is the circulating blood, and an internal compartment, which is the tissue part of the brain as illustrated in Figure 21.

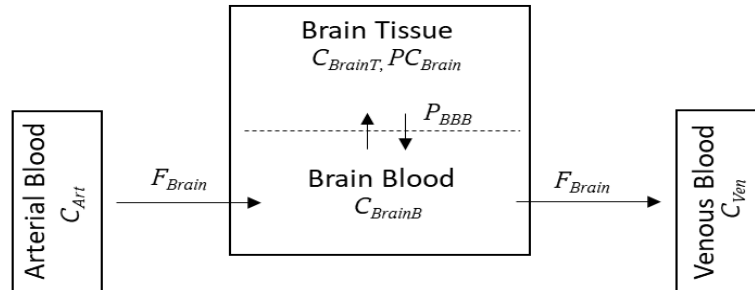


Figure 21. Schematic structure of the two compartments model for the brain.

- Equations

Equation **Erreur ! Source du renvoi introuvable.**, representing the amount of the chemical in the brain blood, and Equation **Erreur ! Source du renvoi introuvable.**, representing the amount of the chemical in the brain tissue, can be used to describe the brain compartment:

$$\frac{dQ_{BrainB}(t)}{dt} = F_{Brain} \times (C_{Art}(t) - C_{BrainB}(t)) - P_{BBB} \times \left(C_{BrainB}(t) - \frac{C_{BrainT}(t)}{PC_{Brain}} \right) \quad (3)$$

$$\frac{dQ_{BrainT}(t)}{dt} = P_{BBB} \times \left(C_{BrainB}(t) - \frac{C_{BrainT}(t)}{PC_{Brain}} \right) \quad (4)$$

With Q_{BrainB} the amount of the chemical in the brain blood (in mmol), Q_{BrainT} the amount of the chemical in the brain tissue (in mmol), F_{Brain} the blood flow to the brain (in L/h), C_{Art} the arterial concentration of the chemical (in mmol/L), C_{BrainT} the concentration of the chemical in the brain tissue (in mmol/L), C_{BrainB} the concentration of the chemical in the brain blood (in mmol/L), PC_{Brain} the brain: blood partition coefficient, and P_{BBB} the BBB permeability coefficient (in L/h).

- Parameters

As for the one-compartment structure, similar physiological information is required. The volume of cerebral blood relative to the brain tissue is also needed.

For the chemical parameters, the brain: blood partition coefficient ($PC_{brain: blood}$) and the BBB permeability coefficient (P_{BBB}) are required (Annex 7, Table S6).

Four- and six-compartment models

Apart from the studies of Sarigiannis et al. (2016b) and Sarigiannis et al. (2020) in which the brain is divided into four compartments (the main brain, globus palidus, cerebellum and pituitary), no inventoried PBK models were found at this level of complexity.

2.7.3. In vitro data in support of the implementation of BBB in PBK models, link with WP5

To develop a brain PBK model, *in vitro* data can be highly helpful especially to calculate permeation coefficients for different brain compartments. We conducted *in vitro* study using HCMEC/D3 cell lines for evaluating brain toxicokinetics for PFAS and insecticides. Data related to cell viability, bidirectional permeability, genetic expression was generated for five chemicals (PFOS, PFOA, Chlorpyrifos, permethrin and cyfluthrin). Bidirectional permeability was quantified using LC-MS technique, this analysis was conducted by CSIC. Statistical analysis was done with GraphPad prisma 9.3.1 software using one-way analysis of variance (ANOVA) followed by Dunnett

post-hoc test for comparison with control and Turkey test for comparison among different doses. In PARC 6.2.2 activity, the generated data is being used to develop a generalized brain PBK model which can be extended for multiple chemicals. Schema utilized for *in vitro* to *in vivo* extrapolation (IVIVE) and brain PBK development is shown on Figure 22 Figure 22.

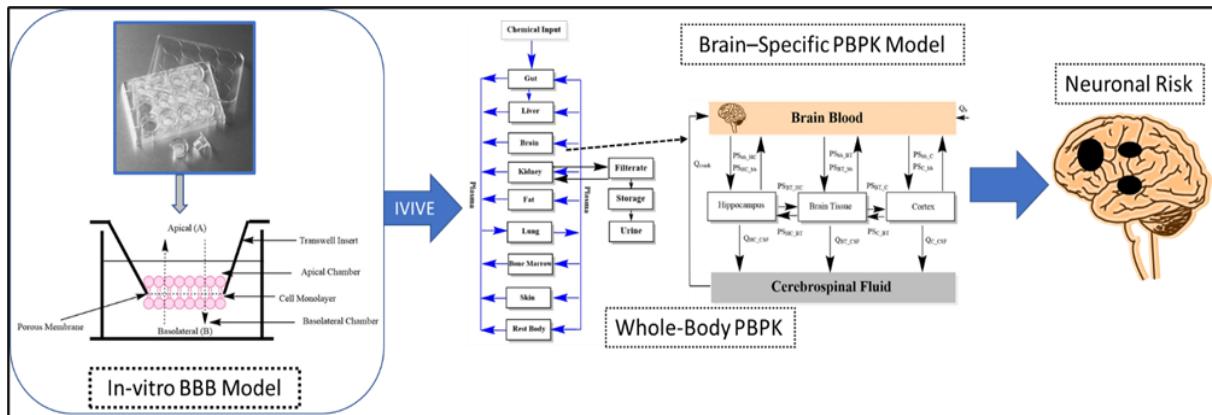


Figure 22. Integration of *in vitro* transwell permeability data with a brain specific PBK Model using mechanistic PBK-IVIVE for evaluating neurotoxic risk assessment.

First, IVIVE approach was used to calculate the PS (permeability surface area product) for *in vivo* from *in vitro* permeability coefficient using the equation below:

$$PS_{Bbb} = P_{appa} - b \cdot \text{Brain weight} \cdot \text{Surface area}$$

PS_{Bbb} refers to permeability for blood to brain, $P_{appa_{A-B}}$ refers to apical to basolateral permeability, brain weight is $150 \text{ cm}^2 \cdot \text{g} \cdot \text{brain}^{-1}$ (rats), $157 \text{ cm}^2 \cdot \text{g} \cdot \text{brain}^{-1}$ (human). Similar equation can be applied for PS_{bb_B} (permeability from brain to blood) where $P_{appa_{A-B}}$ is replaced by $P_{appa_{B-A}}$. Value generated from here has been used as input for parameterization of PBK model.

Then, the brain PBK model developed in PARC 5.3.4 activity has been taken and it is further extended to multiple groups of chemicals, different PFASs, insecticides and metals. Overall brain PBK structure is illustrated in Figure 23 Figure 23.

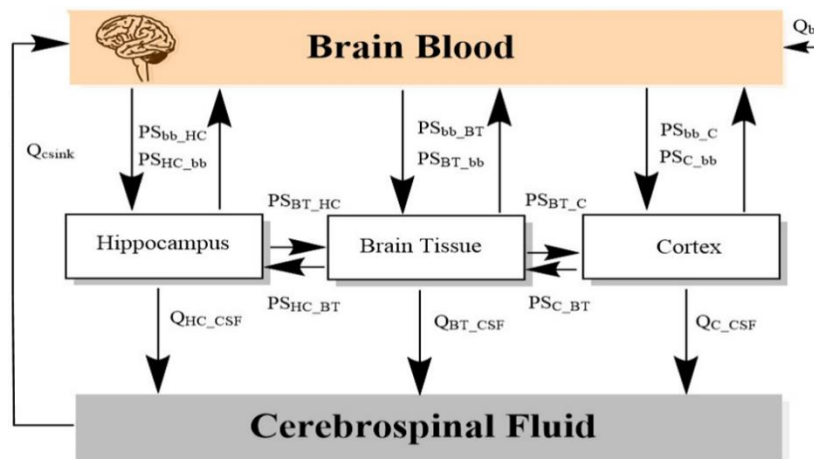


Figure 23. Framework for the brain-specific PBK model for PFOS and PFOA. The brain is divided in 5 compartments: brain blood (BB), hippocampus (HC), cortex (CR), rest brain tissue (BT) and cerebrospinal fluid (csf). CSF acts as a reservoir for all compartments and the compound move back to brain blood. PS: permeability surface area, BB: blood brain, HC: hippocampus, BT: rest of brain tissue, CR: cortex, Q represents blood flow in L/hr. Q_b represent blood flow in bb.

It has been divided into five compartments which include hippocampus, cortex, brain tissue, brain blood and cerebrospinal fluid. The model has been parameterized using some in-house *in vitro* data and data from other literature sources. Currently model is being validated for rats and then

further it will be extrapolated to humans. For PFOS, the hippocampus and cortex concentration in brain compartment of rat at the dose of 1,000 and 10,000 $\mu\text{g}/\text{Kg BW}/\text{day}$ has been shown in Figure 24. The concentration in hippocampus is almost 2 times higher than the cortex at similar doses for rat.

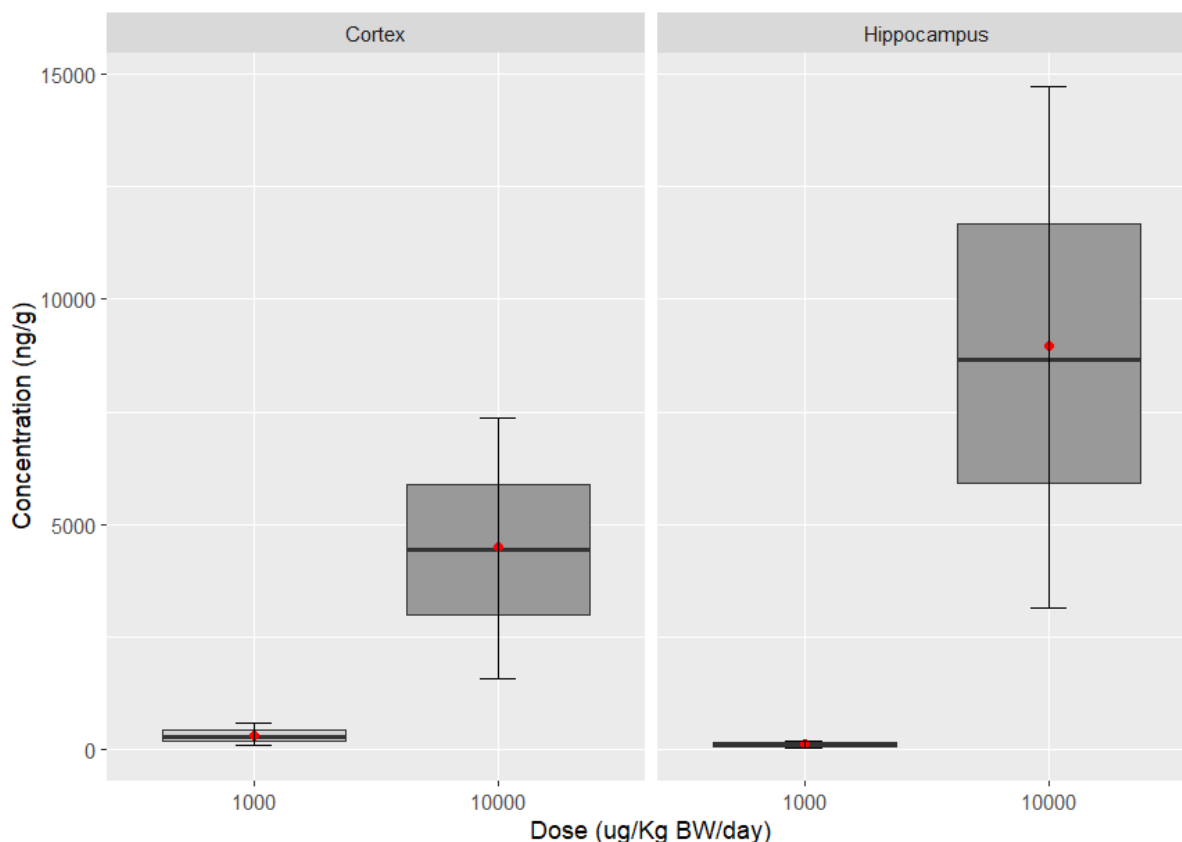


Figure 24. Observed and simulated hippocampus and cortex concentration in rat brain at two oral doses of 1000 and 10000 $\mu\text{g}/\text{Kg BW}/\text{day}$ at 14th day (Austin et al. 2003). The percentiles 97.5 and 2.5 are represented by the upper and lower whiskers, respectively.

2.7.4. QSAR models in support of the implementation of BBB in PBK models

In these last decades, the QSAR modeling approach could be used to estimate the potential range of ratios between plasma and brain tissue levels as a proxy for BBB integrity and to address the uncertainty of the concentration ratio in humans (Maass et al., 2023). For example, five QSAR models were selected based on those available (Bujak et al., 2015) to estimate the brain-plasma concentration ratio for deltamethrin in the study of Maass et al. (2023): Kaliszan and Markuszewski (1996), van de Waterbeemd and Gifford (2003), Takaku et al. (2015), Pan et al. (2004), Clark (1999), Mallick et al. (2020). At steady-state, the brain-plasma concentration ratio is used in PBK models to obtain the partition coefficient for the brain, which is a crucial parameter.

2.7.5. Summary and perspectives

To implement the BBB in PBK models, different structures can be selected depending on the level of complexity of the model structure and the data available for parameterisation. The main parameters required to implement the BBB are the permeability coefficient, as well as data on active efflux and uptake between the brain blood and the brain tissue when it is considered. As for exposure routes (2.6), we observed a lack of harmonization in the parameter names, data or

parameters are available only for some chemical classes (mainly for pesticides or some metals for the BBB).

In vitro data or QSAR models could be used to determine the apparent permeability of the compound. However, the reliability of extrapolating these data to *in vivo* could be investigated in the coming years. In addition, as a first link has been established with PARC 5.3.4 activity to link *in vitro* to *in vivo* approaches for BBB implementation, further efforts could be made to integrate more complex structures of the brain into the future development of PBK models. This implementation of the BBB in PBK models could lead to linking projects across Task 6.2, e.g. a case study on neurodevelopmental risk assessment of a chemical (or mixture) from external exposure (6.2.1 activity), internal exposure over time in the brain tissue through PBK modeling (6.2.2 activity) to 6.2.3 and 6.2.4 activities to perform risk assessment. Additionally, developing a successful brain PBK model will help in reducing uncertainty in translation of neurological risk from in-vitro data especially in cases where hippocampal cell lines has been utilized. It can be highly helpful for toxicologist and integrating this with systems biology model can help in predicting neurotoxicological risks from environmental chemicals.

2.8. FAIR PBK model standard and ontology

The essential role of PBK models in chemical risk assessment has already been clearly demonstrated, as evidenced by initiatives such as EFSA's strategic roadmap, ExpoAdvance. PBK models (generic or chemical specific) are therefore expected to be used more and more to address several questions in chemical risk assessment, reflecting a trend that is already well underway. However, their reuse in different contexts is currently challenging. Despite the recommendations provided in the OECD (2021) guidance document, there are no common standards for developing and publishing PBK models. Additionally, model codes are often unavailable, and even if available, to reuse them in another context than for which they were developed is cumbersome. For instance, PBK model developers commonly use their own modeling software, adopt their own terminology for naming terms, and units of measurement (for instance for dosing and parameters) used in the model need to be carefully checked.

To support a future where multiple PBK models can be seamlessly integrated in workflows to address various chemical risk assessment questions, we propose a harmonised (exchange) standard for PBK models. This standard would enable easy reuse of developed PBK models without requiring model reimplementations, thus streamlining their application in diverse chemical risk assessment scenarios, and improving transparency of model codes. Since such a standard is currently lacking, a FAIR PBK modeling standard is being proposed and developed as a joint effort of T8.3, WP7, and 6.2.2 activity.

2.8.1. PBK Ontology (PBKO)

Within Task 7.3, the PBKO was developed with the intent of improving the reporting of PBK models to become machine-readable as described in Figure 25. Although more than 1,000 models have been published, their reproducibility and reuse are still limited due to lack of harmonization. Harmonization as such is a broad term covering different aspects in PBK such as structure, coding, mechanism, terminology etc. but here we are using this term specifically in the context of terminology. Inconsistent terminology and ambiguous abbreviations used in PBK models can be improved by developing PBKO which can help in uniform parameters and coding and enabling structured, machine interpretable model representation. Similarly, several biological domain ontologies are already available on the BioPortal platform (<https://www.bioontology.org/>), one related to PBK modeling did not exist up to now. For the first time, the PARC community has attempted to close this gap with an ontological representation in the interest of the broader kinetic community, supportive of FAIR PBK modeling. In order to cover this need, PBKO has been developed, initially including more than 500 terms representing the different components of a complete PBK model. Several model types, compartments, physiological and biochemical parameters, output variables, routes of exposure, evaluation metrics, and many other items have been included in the ontology. PBKO has been developed by IISPV in collaboration with WR and JSI.

PBKO is publicly available on GitHub². Besides the above-mentioned source code, this repository also contains extensive documentation that provides a general introduction, overview, detailed description, and cross-references for object properties, classes, data properties, and acknowledgements. The current version of PBKO has been submitted to OBO (Open biological and biomedical ontologies) Foundry pending final review. OBO foundry is a community of biologists from all over the globe with the aim to create and use ontologies for life sciences. Currently it has more than 100 ontologies following OBO principles. In addition, IISPV continues working on the

² <https://github.com/InSilicoVida-Research-Lab/PBKo>

ontology development by collaborating with experts from 6.2.2 activity on the inclusion of commonly used terms and abbreviations. WR and SLU have contributed with suggestions for additional terms for future updates. Version 2 of PBKO will represent an even larger community of kinetic modeling experts and further harmonize the generalization of PBK models in order to make them even more reproducible and interoperable.

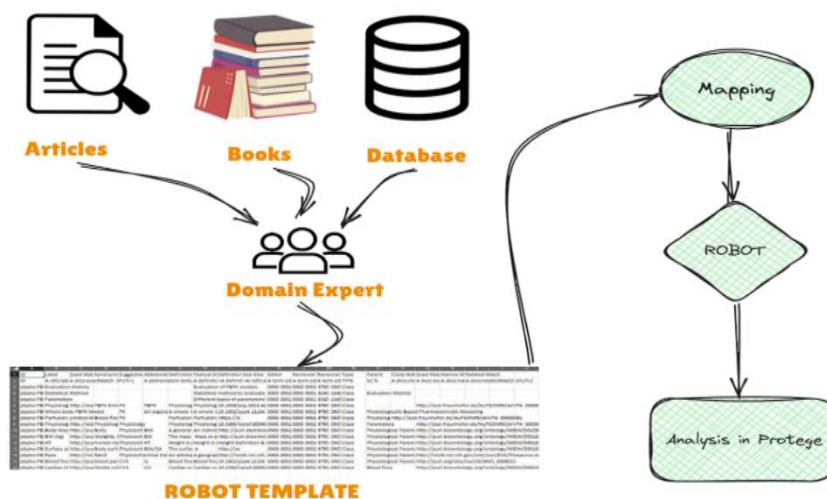


Figure 25. Workflow for PBKO from creation of robot template, adding the terms, abbreviations etc. and analysis in protégé.

2.8.2. FAIR PBK model

In addition to the development of the PBK ontology, a FAIR PBK modeling standard is being developed as a harmonised exchange format for PBK models. The standard combines the use of the SBML as a technical exchange format with specific rules and guidance for the annotation of PBK models using the PBK ontology (WP7). This standard is iteratively developed and tested in practice in a trilateral collaboration of T8.3 (standard development), WP7 (ontology development), and 6.2.2 activity (use, validation, and community uptake). Part of the activities on developing the FAIR PBK standard is to develop tooling that support/assist model developers in creating harmonised and FAIR PBK models, and for model-users to implement support for this FAIR standard in tools and software. WR has implemented support for SBML PBK models annotated using the current version of the FAIR PBK standard in the MCRA software, envisioned to be used in several case studies of T6.2. A proof-of-principle on using a FAIR PBK model in MCRA for aggregate exposure assessment is described in D8.6. Besides this, the FAIR PBK standard also enables tools that further facilitate automation and enable text mining of PBK model parameters and outputs, a range of example PBK models are being translated into SBML and linked to PBKO. To this end, IISPV has translated the PFAS model developed here into SBML and has used the ontology PBKO to annotate it. RIVM and WR have done similar exercises on translating the generic PBK model by Tebby et al. (2020) developed in the EuroMix project³ to SBML of which the model code is publicly available on GitHub⁴ and also converted some other models to SBML, including a

³ <https://cordis.europa.eu/project/id/633172>

⁴ <https://github.com/rivm-syso/euromix-to-sbml>

simple PFAS PBK model and some simple demonstration PBK models. WR has developed a FAIR PBK Inspector tool to facilitate annotation of PBK models with PBKO, showing its adoption by the wider community.

2.8.3. Combining FAIR PBK and PBK ontology

At present, the FAIR PBK modeling standard is available in the form of a proof-of-principle. Within 6.2.2 activity, some first examples of SBML PBK model (re-)implementations were developed, for example the EuroMix generic PBK model and the PFAS PBK model of Westerhout et. al. (2024). In a dedicated PARC 6.2.2 activity workshop held at RIVM on 7-8 October 2024, the main concepts were presented and discussed and T6.2.2 partners were trained to adopt the standard.

2.8.4. Next steps

It is planned to further develop the FAIR PBK standard, the PBK ontology and the FAIR PBK model (re-)implementations in an iterative way and slowly building up the necessary community uptake - both at the side of PBK model developers and PBK model consumers - initially within T6.2.2, then within PARC as a whole, and beyond PARC. On a short term, it is planned to create FAIR PBK model implementations for the PBK models required in the other WP6.2 tasks (T6.2.1 and T6.2.3). Over the long term, this initiative is anticipated to result in, or contribute to, the establishment of a broadly accepted standard for PBK models in chemical risk assessment — a critical development in light of the increasing demand for such models. This standard would enhance interoperability, reusability, and transparency across both scientific and regulatory domains, for instance within the framework of EFSA's strategic roadmap, ExpoAdvance. More details on the development of the FAIR PBK standard and tooling can be found in D8.6. More information on the ontology development can be found in D7.4.

3. Perspectives and Conclusions

This deliverable highlights the growing significance of PBK models in toxicology, particularly in the context of next-generation risk assessment (NGRA). These models offer regulatory scientists, toxicologists, and industry researchers a powerful tool to reduce reliance on animal testing, improve dose-response extrapolations, and enable more human-relevant chemical safety evaluations. Their ability to account for inter-individual variability, including age, sex, and physiological differences, enhances their applicability in diverse exposure scenarios.

A key contribution of this work is the advancement of PBK modeling methodologies to address contemporary challenges in PBK modeling and risk assessment. Specifically, it tackles a major current challenge: the lack of harmonization across PBK models, where the use of different terms for similar concepts makes models extremely difficult to reproduce and hinders their development as machine-readable resources. The case studies underscore the necessity of refining PBK models to better simulate complex exposure patterns and improve the risk characterization of chemicals. Specifically, advancements in modeling age-specific physiological changes, dietary exposure to contaminants, and lifetime-based risk assessment methodologies contribute to a more comprehensive understanding of chemical kinetics in human populations.

The application of PBK modeling to CH₃Hg, iHg, arsenic, lead, and PFAS demonstrates the versatility and adaptability of these models across different contaminants and exposure routes. These models provided state-of-the-art methodologies regarding the progression of PBK modeling in risk assessment. The development of pregnancy-specific PBK (p-PBK) models to simulate fetal exposure to neurotoxicants further strengthens the applicability of these tools in vulnerable populations. Additionally, the incorporation of blood-brain barrier dynamics into PBK models also enhances the understanding of neurotoxic chemical distribution, particularly during development. Key conclusions, such as e.g., the dominant role of passive diffusion for lipophilic neurotoxicants in early gestation and active efflux maturation reducing exposure postnatally, can provide a mechanistic framework to extrapolate adult data to developmental stages. This capability is critical for DT assessment, as it allows quantitative estimation of fetal/neonatal brain concentrations of neurotoxicants, informing risk characterization for developmental neurotoxicity, and informs reliably the decision-making arena.

Beyond these advancements, the deliverable contributes to the FAIRification of PBK models by developing a FAIR PBK framework, including an ontology, aimed at improving their Findability, Accessibility, Interoperability, and Reusability. The methodological framework for enhancing FAIR properties ensures greater transparency, reusability, and integration of PBK models into regulatory frameworks and the PARC PBK applications and model network of T8.3. Furthermore, implementing uncertainty analysis in PBK models, particularly for PFAS, provides a structured approach for quantifying variability and improving confidence in model predictions.

In summary, this deliverable strengthens the role of PBK models in risk assessment by addressing key methodological challenges such as e.g., detailed PFAS, As, Mercury, and lead PBK models, expanding their applicability to diverse exposure scenarios, and promoting FAIR data practices. The advancements presented here contribute to the broader objective of integrating PBK models into regulatory science decision-making, ultimately enhancing their utility in human health risk assessment of environmental contaminants.

4. Appendices

Annex 1 - Library of lifetime physiological equations for PBK models

<https://doi.org/10.1016/j.envres.2024.120393>

Annex 2 - Development of a pregnancy PBK model for Pb (Daoud et al. (2023) article)

<https://doi.org/10.1016/j.taap.2023.116651>

Annex 3 – List of Publications

Husoy, T., Caspersen, I. H., Thepaut, E., Knutsen, H., Haug, L. S., Andreassen, M., . . . Wojewodzcic, M. W. (2023). Comparison of aggregated exposure to perfluorooctanoic acid (PFOA) from diet and personal care products with concentrations in blood using a PBK model - Results from the Norwegian biomonitoring study in EuroMix. *Environ Res*, 239(Pt 2), 117341. doi:10.1016/j.envres.2023.117341

Ali Daoud, Y., Tebby, C., Beaudouin, R., Brochot, C. (2023). Development of a physiologically based toxicokinetic model for lead in pregnant women: The role of bone tissue in the maternal and fetal internal exposure. *Toxicology and Applied Pharmacology*, 476, DOI: <https://doi.org/10.1016/j.taap.2023.116651>

Ratier, A., Casas, M., Grazuleviciene, R., Slama, R., Småstuen Haug, L., Thomsen, C., Vafeiadi, M., Wright, J., Zeman, F., Vrijheid, M., Brochot, C. Estimating the dynamic early life exposure to PFOA and PFOS of the HELIX children: Emerging profiles via prenatal exposure, breastfeeding, and diet, *Environment International*, 108621_ (2024). <https://doi.org/10.1016/j.envint.2024.108621>

Gastellu, T., Mondou, A., Bellouard, M., Alvarez, J.-C., Le Bizec, B., & Rivière, G. (2024). Characterizing the risk related to the exposure to methylmercury over a lifetime: A global approach using population internal exposure. *Food and Chemical Toxicology*, 187, 114598. doi:<https://doi.org/10.1016/j.fct.2024.114598>

Westerhout, J., den Heijer-Jordaan, A., Princen, H. M. G., & Stierum, R. (2024). A systems toxicology approach for identification of disruptions in cholesterol homeostasis after aggregated exposure to mixtures of perfluorinated compounds in humans. *Toxicological Sciences*, 198(2), 191-209. doi:10.1093/toxsci/kfae006

Gastellu T, Karakoltzidis, A., Ratier, A., Bellouard, M., Alvarez, J.C., Le Bizec, B., Rivière, G., Karakitsios, S., Sarigiannis, D., Vogs, C. (2025) A Comprehensive Library of Lifetime Physiological Equations for PBK Models: Enhancing Dietary Exposure Modeling with Mercury as a Case Study *Environmental Research*.

Gastellu T, Le Bizec B, Rivière G (2025). Integrating the lifelong exposure dimension of a chemical mixture into the risk assessment process. Application to trace elements. *Food and Chemical Toxicology*. 195, 115111, <https://doi.org/10.1016/j.fct.2024.115111>.

Annex 4 – List of congress (oral communications and posters)

Zwartsen A, Minnema J, Ratier A, Engel J, Deepika D, Van Klaveren J, Kruisselbrink J. (2024). Workshop on Implementation of FAIR PBK models in SBML using Antimony. RIVM Bilthoven, The Netherlands. 7-8 October 2024.

<https://www.eu-parc.eu/index.php/events/trainings/risk-assessment/workshop-implementation-fair-pbk-models-sbml-using-antimony?color=%23008475>

Ratier A., Gestin O., Vrijheid M., Brochot C., Zeman F. A. (2024). Estimating the early life exposure to PFAS using PBK modelling and Human biomarker data. ISES Montréal, Canada, 20-24 October (Poster). DOI: 10.14293/P2199-8442.1.SOP-.PHUNH2.v1

Crépet A., Engel J., Ratier A., Buekers J., Karakitsios S., Purece A., Vernez D., De Brouwere K., Van Klaveren J. (2024). An integrated risk assessment to consider multiple exposures: application to European cohorts. ISEE Conference, August 25-28, Santiago, Chile.

Westerhout J., Ratier A. (2024). 20th RECETOX Summer School and PARC Training (2024). Introduction to toxicokinetics and modelling, how to build and use a PBBK Physiologically Based Toxicokinetic (PBTk) model? (Joost Westerhout); Considering variability and uncertainty in PBTk models (Aude Ratier). 10 – 12 June 2024, RECETOX, Masaryk University, Brno, Czech Republic

Gestin O., Ratier A., Brochot C., Casas M., Vrijheid M., and Zeman F. A. (2024). Exposure assessment to PFAS of pregnant women and children of the HELIX cohort using Physiologically Based Pharmacokinetic (PBK) modelling. 3rd International congress of PFAS: Environmental and health risk management, 4-6 June, Paris, France (Oral communication)

Ratier A., Beaudouin R., Billat P-A., Bodin C., Mombelli E., Zeman F. A. (2024) In silico tools for risk assessment in PARC. PARC Consortium meeting, 13-16 May, Hall in Tirol, Austria. *ScienceOpen Posters*. 2024. DOI: 10.14293/P2199-8442.1.SOP-.PHUNH2.v1

Ratier, A et al. (2023) Estimating the early-life exposure to two perfluorinated compounds (PFOS and PFOA) using PBK modelling and biomarker measurements. *ScienceOpen Posters*. DOI: 10.14293/P2199-8442.1.SOP-.PQDEVT.v1. DOHAD Canada May 2023, Montréal.

Ratier, A., et al. (2023). Estimating the early-life exposure to two perfluorinated compounds (PFOS and PFOA). 2nd International congress of PFAS: Environmental and health risk management, June 2023, Paris, France (Oral communication)

Annex 5 – QSAR models for exposure routes

Table S1. QSAR models for inhalation route ADME parameters. OPLS Orthogonal partial least squares, EN Elastic Net, RF Random Forest, VR Voting Regression, LR Linear Regression, MLR Multiple Linear Regression, * Data available as supplementary material to the publication

Reference	Endpoint	Sample size (# training set/ # test set)	Set of predictors	Relevant predictors	Algorithm (software)	Data source	Data availability
Gaohua et al. (2015)	CaLu-3 <i>in vitro</i> Permeability	28 compounds	Caco-2 <i>in vitro</i> Permeability (Model 1) Physicochemical properties (Model 2)	Model 2 (final Model): LogD, HDC	Model 2: MLR	Five publications (2000-2012)	
Lin et al. (2022)	CaLu-3 <i>in vitro</i> Permeability	57 chemicals, mostly drugs (46/11 + 4 additional)	1D, 2D PaDEL descriptors	AATS7i, ATSC5v, AATSC4m, AATSC0v, CrippenLogP, minHBint3, minHBint8, maxaasC, ZMIC4, MDEO-11, VE3_D	LR, VR, RF	Nine publications (2001-2020)	*
Välitalo et al. (2016)	EPR at steady state	56 compounds: (antibiotics, antifungals and associated agents such as β -lactamase inhibitors).	145 <i>rdck</i> descriptors / 919 PaDEL descriptors	MDEC24, MDEC12, MDEC34, khs.ssssC, C3SP3, khs.ssS, MLogP, XLogP, nAcid	EN	Systematic reviews of clinical studies. Complete overview of available literature up to 2011	*

Aulin et al. (2018)	EPR at steady state	56 compounds	145 <i>rcdk</i> descriptors	<i>Not Available</i>	EN	PubMed database and microbiology conference abstracts	*
Aulin et al. (2022)	EPR & MER at steady state	Clinical data for 40 anti-infective agents on systemic and pulmonary exposure	<i>rcdk</i> descriptors	<i>Not Available</i>	EN	Mainly Valitalo et al., 2016	*
Edwards et al. (2016)	IPRLu model-based lung absorption half-life (Endpoint 1) IPRLu model-based Log% solubilised dose in perfusate (%SDiP ; Endpoint 2) IPRLu model-based Log% total dose in perfusate (endpoint 3)	108 (82 drug discovery compounds + 14 drugs specifically designed for inhaled delivery + 3 marketed drugs)/7	Initially, 39 2D descriptors + Abraham + predicted set of ADME properties as Vd, P-gp substrate. The %SDiP endpoint was analyzed further since showing the best fitting. After feature selection: 20 QSAR descriptors + 6 predicted ADME properties	%SDiP endpoint: variables positively and negatively correlated with endpoint were established. Positively correlated: predictors related to permeability and hydrophobicity. Negatively correlated: relatable to charge, size, ionization.	OPLS (SIMCA-P+)	In-house measurement	Data available only for the 17 marketed drugs in the training set. See manuscript.

Table S2. QSAR models for dermal route ADME parameters MLR Multiple Linear Regression, ANN Artificial Neural Networks, SVM Support Vector Machine, GP Gaussian Process, RF Random Forest, PLS Partial Least Squares, * Data available as supplementary material to the publication

Reference	Endpoint	Sample size (# training set/ # test set)	Set of predictors	Relevant predictors	Algorithm (software)	Data source	Data availability
Abdallah et al. (2024)	k_p	441 records for 140 molecules with diverse Log k_p	145 1D/2D CDK descriptors	K_{ow} , HBD, HBA, TPSA, hydrophobicity, polarity, adherence to Lipinski rules	MLR, bagging, RF, ANN (Python)	Cheruvu et al. for training/testing + DrugBank for testing	Zenodo
Zeng et al. (2021)	k_p	274 compounds (drugs and industrial chemicals or solvents)	Three descriptors selected for actual modelling: A log P, X3v, and Neoplastic-80	Relevant predictors identified before modelling based on 4885 Dragon 6.0 descriptors	SVM (MATLAB)	Dataset from Khajeh and Modarress (2014)	*
(Wu et al., 2022)	k_p	96 compounds	Computed through Discovery Studio, SwissADME and E-Dragon	LogP, molecular volume, molecular connectivity index of order zero, neutrality, partial positive surface area. Molecular weight not relevant	Hierarchical SVM, PLS (Python)	20+ papers	*
Rezaei et al. (2019)	k_p	211 pharmaceuticals, chemicals, industrial compounds	GRIND descriptors (3D)	HBD, HBA	SVM (MATLAB)	Baba et al. (2017)	*
Baba et al., 2017	k_p (focus on ionization effects on permeability)	Experimental data gathered at several pH. 203 different permeants measured in <i>in vitro</i>	Predictors encoding the ionization effects of permeants.	logD	GP, SVM	Zhang et al. (2012)	*

		diffusion studies on human skin from the literature. Mostly drugs.	Employed software: ADMET Predictor, MOPAC 2012, Dragon 7.0				
--	--	--	--	--	--	--	--

Table S3. Experimental data sources for dermal route ADME parameters IVPT *In vitro* human skin Permeation Test, * Data available as supplementary material to the publication

Reference	Endpoint	Sample size	Applicability domain	Data availability
Brown et al. (2016)	k_p	392 values for 245 organic chemicals	Disparate types of chemicals, mostly drugs. Retrieved from published papers	*
Cheruvu et al. (2022)	k_p, J_{max}	476 records of 145 drugs, chemicals, and xenobiotics applied to <i>in vitro</i> human epidermal membranes from aqueous solutions either diluted or saturated in infinite dose amounts (constant concentration)	IVPT reports. Diverse range of molecules, including drugs, xenobiotics, and other chemical compounds.	Mendeley
Chedik, 2024	steady-state flux, k_p, J_{max}, t_{lag} (time to cross the skin barrier)	202 datapoints (SkinPiX dataset)		Institutional repository

Table S4. QSAR models for oral route ADME parameters k-NN k-Nearest Neighbor, RF Random Forest, PLS Partial Least Squares, SVM Support Vector Machine, MLP Multilayer Perceptron, NLLS Non-Linear Least Square, NB Naïve Bayes, DTI Decision Tree Induction, LAZAR fragment-based lazy-learning, , * Data available as supplementary material to the publication

Reference	Endpoint	Sample size (# training set/ # test set)	Set of predictors	Relevant predictors	Algorithm (software)	Data source	Data availability
(Sedykh et al., 2013)	Intestinal transporters	373 compounds with 742 binary data entry	2D 2030 Dragon descriptors and 185 2D MOE descriptors	Km, kd, IC50, ki, % inhibition at given concentration	RF, k-NN, SVM (WinSVM)	Public source	*
Linnankoski et al. (2006)	Ka (oral drug absorption kinetics)	Dataset 1 with 23 compounds and dataset 2 with 23 and additional 147 compounds	Multiple descriptors using software package	Log p (octanol water partition coefficient) at ph 7.4, 6.5, 6.0 and 5.5, log D at ph 7.4, PSA, HBD, HBA, Clog P	PLS	Literature and data from old paper	In the main file
Sedykh et al. (2013)	Intestinal drug absorption	458 small drug like molecules, FDA approved	1-, to 3-D molecular descriptors	Log P, hydrogen bonding	DTI, LAZAR, SVM, MLP, RF, k-NN, NB	Literature source	*
Suenderhauf et al. (2011)	Ccao 2 permeability coefficient (Pe)	768 diverse drugs and similar compounds	Physicochemical descriptors	H-bonding, molecular size	NLLS (R)	Public source	*

Annex 6 – Overview of brain compartment(s) in PBK models inventoried in the first year of PARC

Table S5. Overview of the PBK models inventoried in the first year of PARC associated with the number of compartments to describe the brain.

Chemical family	Substance	References	Number of compartment(s) for the brain	
PFAS	PFOA	Loccisano et al., 2011	0	
	PFOA	Loccisano et al., 2013	0	
	PFOA	Brochot et al., 2019	1	
	PFOA	Fabrega et al., 2014; 2015; 2016	1	
	PFOA	Rovira et al., 2019	1	
	PFOA	Husøy et al., 2023	0	
	PFOS	Loccisano et al., 2011	0	
	PFOS	Fabrega et al., 2014; 2015; 2016	1	
	PFOS	Brochot et al., 2019	1	
	PFOS	Chou and Lin, 2019	0	
	PFOS	Deepika et al., 2021	1	
	PFOS	Chou and Lin, 2021	0	
	PFHxs	Sweeney, 2022	0	
	PFHxs	Fabrega et al., 2015	1	
	PFBS, PFDS, PFNA, PFHxA, PFHpA, PFDA, PFUnDA, PFTeDA	Fabrega et al., 2015	1	
	Bisphenols	BPA	Shin et al., 2004	1
		BPA	Teeguarden et al., 2005	0
BPA		Edginton and Ritter, 2009	1	
BPA		Mielke and Gundert-Remy, 2009	1	
BPA		Mielke et al., 2011	1	
BPA		Yang et al., 2015	1	
BPA		Sarigiannis et al., 2016	5	
BPA		Sharma et al., 2018	1	
BPA		Karrer et al., 2018	1	
BPA		Gingrich et al., 2021	0	
BPA		Deepika et al., 2022; sex specific	1	
BPA		Hu et al., 2023	1	
BPA		Wisniowska et al., 2023	0	
BPS		Karrer et al., 2018	1	
BPS		Gingrich et al., 2021	0	
BPS		Hu et al., 2023	1	
BPAF		Karrer et al., 2018	1	
BPAF		Hu et al., 2023	1	
BPF		Karrer et al., 2018	1	

	BPF	Hu et al., 2023	1
Metals	Lead	O'Flaherty, 1993	0
	Lead	O'Flaherty, 1995	0
	Lead	Sharma et al., 2012	0
	Lead	Tebby et al., 2022	0
	Lead	Sweeney, 2021	0
	Chromium	O'Flaherty et al., 2001	0
	Chromium	Kirman et al., 2013	0
	Chromium	Kirman et al., 2017	0
	Cadmium	Kjellström and Nordberg, 1978	0
	Cadmium	Choudhury et al., 2001	0
	Cadmium	Ruiz et al., 2010	0
	Cadmium	Bechaux et al., 2014	0
	Cadmium	Pouillot et al., 2022	0
	Arsenic	El-Masri and Kenyon., 2008	1
	Arsenic	Yu, 1999a, b	0
	Arsenic	Mann et al., 1996a,b	0
	Mercury	Gearhart et al., 1995	2
	Mercury	Ou et al., 2018	1
	Mercury	Clewell et al., 1999	2
	Mercury	Carrier et al., 2001	2
Pesticides - OP	Chlorpyrifos metabolites	+ Timchalk et al., 2022a	1
	Chlorpyrifos metabolites	+ Timchalk et al., 2022b	1
	Organophosphates	Knaak et al., 2004	1
	Chlorpyrifos metabolites	+ Bouchard et al., 2005	0
	Chlorpyrifos	Lowe et al., 2009	1
	Chlorpyrifos metabolites	+ Mosquin et al., 2009	1
	Chlorpyrifos metabolites	+ Lu et al., 2010	1
	Chlorpyrifos metabolites	+ Foxenberg et al., 2011	1
	Chlorpyrifos metabolites	+ Hinderliter et al., 2011	1
	Chlorpyrifos metabolites	+ Beamer et al., 2012	1
	Chlorpyrifos metabolites	+ Poet et al., 2014	1
	Chlorpyrifos metabolites	+ Smith et al., 2014	1
	Chlorpyrifos metabolites	+ Poet et al., 2017	1

	Chlorpyrifos metabolites	+ Zurlinden and Reinfeld, 2018	1
	Chlorpyrifos metabolites	+ Zhao et al., 2019	0
	Chlorpyrifos metabolites	+ Zhao et al., unpublished	0
	Triazophos	no human PBK model existing	Not applicable
	Dichlorvos	no human PBK model existing	Not applicable
	Omethoate	no human PBK model existing	Not applicable
	Formetanate	no human PBK model existing	Not applicable
	Carbofuran	no human PBK model existing	Not applicable
	Azinphos-methyl metabolites	+ Carrier and Brunet, 1999	0
	Primiphos-methyl	no human PBK model existing	Not applicable
	Methomyl	no human PBK model existing	Not applicable
Pesticides - pyrethroids	deltamethrin	Godin et al., 2010; brain concentrations with simulations	2
	permethrin (cis and trans) + DCCA	Tornero-Velez et al., 2012 (DLT, Cis- and trans-PM)	2
	permethrin + 3-PBA	Wei et al., 2013 (from Tornero-Velez et al., 2012)	2
	permethrin (cis and trans) + DCCA	Darney et al., 2018	2
	deltamethrin, permethrin, cypermethrin, cyfluthrin + DCCA + PBA + F-PBA + DBCA	Quindroit et al., 2019; generic model	2
	deltamethrin, permethrin, bifenthrin, esfenvalerate, cyalothrin, cyfluthrin, cyphenothrin	Mallick et al., 2020; generic model	2
	deltamethrin	Maass et al., 2023; from rat PBK model	2
Other pesticides	epyrifenacil metabolite	+ Hirasawa et al., 2022	1
	haloxyfop metabolite	+ Cooper et al., 2019, not validated <!>	0
	DEET	no human PBK model existing	Not applicable
	glyphosate	no human PBK model existing	Not applicable
	fipronil	Tonnelier et al., 2012; 4 compartments	0
	chlordecone	Emond et al., 2022; not validated <!>	2

	Deoxynivalenol (DON) + metabolites	Notenboom et al., unpublished. Not published, but other subgroups can be modeled (all subgroups available in ICF)	0
	Zearalenone (ZEN)	Shin et al., 2009	0
	Zearalenone (ZEN) + metabolites	Mukherjee et al., 2014; also feces as biomarker possible; expands upon Shin et al., 2009	0
Mycotoxins	Zearalenone (ZEN) + metabolites	Mendez-Catala et al., 2021	0
	Nivalenol (NIV)	no human PBK model existing	Not applicable
	T-2	no human PBK model existing	Not applicable
	HT-2	no human PBK model existing	Not applicable
	Aflatoxin B1 (AFB1)	Gilbert-Sandoval et al., 2020	0
	Ochratoxin A	no human PBK model existing	Not applicable
	Alternaria toxins	no human PBK model existing	Not applicable
	Fumonisin	no human PBK model existing	Not applicable
	Enniatins	no human PBK model existing	Not applicable
	1,3-butadiene, TCDD	Beaudouin et al., 2010	1
	TCDD, Pb, PFAS	Brochot and Quindroit 2018 (MERLIN Expo)	1
	various substances	Clewell 2002	Not applicable
	TCDD	Clewell 2004	1
	PFOS	Deepika et al., 2021	1
Lifetime models	Triclosan, PFOS	El-Masri et al., 2016	1
	PYR	Mallick et al., 2020	2
	generic	Pendse et al., 2020 (PLETHEM R package)	2
	CPF	Poet et al., 2017	1
	BPA, DEHP, Cd	Sarigiannis et al., 2020	5
	CPF	Smith et al., 2014	1
	PCB, HCB	Verner et al., 2008	1

Annex 7 – Parameterization for implementing the BBB in PBK models

Table S6. Physiological and chemical parameters are required to describe the two brain compartments for the models inventoried in the first year of PARC. CO stands for cardiac output, BW for body weight, CV for the coefficient of variation, UB is for the upper bound, and LB is for the lower bound.

Reference	Chemical	Brain volume (% of BW)	Brain blood volume (% of brain volume)	Blood flow in the brain (% of CO)	Brain:blood partition coefficient ($PC_{\text{brain:blood}}$)	P_{BBB} permeability coefficient
Carrier et al., 2001	Hg ⁰				0.43	0.0028 (transfert rate, days ⁻¹)
Clewell et al., 1999	MeHg	2% (CV = 0.30, UB: 3.8%; LB: 0.2%)	0.7% (CV = 0.30, UB: 1.3%, LB: 0.07%) of BW	11.4% (CV = 0.30, UB: 21.7%, LB: 1.1%) in plasma	3 (CV = 0.30, UB: 6.93, LB: 1.19) in plasma	0.01 (L/hr scaled by BW ^{3/4}) (CV:0.30, UB: 0.0231, LB: 0.00397)
Gearhart et al., 1995	MeHg	ICRP (1975), Hytten and Leitch (1971), and Gerlowski and Jain (1983) - not provided directly			2-3	Not provided
Tornero-Velez et al., 2012	cis- and trans-permethrin	2%	4%	12%	1.5 (Cis-PM) 0.4 (Trans-PM)	0.003 (L/h)
Wei et al., 2013	Permethrin	2%	4%	11.4%	5.50	0.003 (L/h)

Darney et al., 2018	cis- and trans-permethrin	2%	4%	12%	1.5 (Cis-PM) 0.4 (Trans-PM)	0.003 (L/h)
Quindroit et al., 2019	cis-/trans-CYF; cis-/trans-CYP; cis-/trans-PM; DLT	variable	3%		8.94 (CYF) 7.94(CYP) 1.60 (cis-PM) 0.57 (trans-PM) 0.14 (DLT)	0.001 (cis-CYF) 0.0012 (trans-CYF) 0.001 (cis-CYP) 0.0012 (trans-CYP) 0.001 (cis-PM) 0.0012 (trans-PM) 0.002 (DLT) (L/h)
Godin et al., 2010		2%	3%	11.4%	0.14	0.002 L/h/kg tissue
Tornero-Velez et al., 2012	Deltamethrin	2%	4%	12%	0.22	Not applicable
Maass et al., 2023		variable			0.44 (0.37–1.5) 0.2 (0.01-10)	10 (0.0000001-10) cm/min
Mallick et al., 2020		variable		11.6% (plasma)	0.44	0.095 (L/h/Kg ^{0.75} tissues weight)
Emond & Multigner, 2022	Chlordec one	variable (Luecke et al. 2007)	0.96	variable (Luecke et al. 2007)	11.13	0.0096 (permeability limited fraction between tissue blood and cellular matrix)

5. References

- Abass, K., Huusko, A., Knutsen, H. K., Nieminen, P., Myllynen, P., Meltzer, H. M., Vahakangas, K., & Rautio, A. (2018). Quantitative estimation of mercury intake by toxicokinetic modelling based on total mercury levels in humans. *Environment international*, *114*, 1-11. <https://doi.org/10.1016/j.envint.2018.02.028>
- Abbiati, R. A., & Manca, D. (2017). Enterohepatic circulation effect in physiologically based pharmacokinetic models: the sorafenib case. *Industrial & Engineering Chemistry Research*, *56*(12), 3156-3166. <https://doi.org/10.1021/acs.iecr.6b03686>
- Abdallah, R. M., Hasan, H. E., & Hammad, A. (2024). Predictive modeling of skin permeability for molecules: Investigating FDA-approved drug permeability with various AI algorithms. *PLOS digital health*, *3*(4), e0000483. <https://doi.org/10.1371/journal.pdig.0000483>
- Abduljalil, K., Pan, X., Clayton, R., Johnson, T. N., & Jamei, M. (2021). Fetal Physiologically Based Pharmacokinetic Models: Systems Information on Fetal Cardiac Output and Its Distribution to Different Organs during Development. *Clin Pharmacokinetics*, *60*(6), 741-757. <https://doi.org/10.1007/s40262-020-00973-0>
- Abuhelwa, A. Y., Williams, D. B., Upton, R. N., & Foster, D. J. (2017). Food, gastrointestinal pH, and models of oral drug absorption. *European journal of pharmaceuticals and biopharmaceutics*, *112*, 234-248. <https://doi.org/10.1016/j.ejpb.2016.11.034>
- Alam, M., Allinson, G., Stagnitti, F., Tanaka, A., & Westbrooke, M. (2002). Arsenic contamination in Bangladesh groundwater: a major environmental and social disaster. *International Journal of Environmental Health Research*, *12*(3), 235-253. <https://doi.org/10.1080/0960312021000000998>
- Alemam, H., Enattah, N., Fellah, A., Elftisi, E., Akarem, A., & Bashein, A. (2022). Correlation between maternal and fetal umbilical cord blood lead concentrations in Libya. *Eastern Mediterranean Health Journal*, *28*(5), 345-351.
- ANSES. (2011). Étude de l'alimentation totale française 2 (EAT 2) Tome 2. <https://www.anses.fr/fr/system/files/PASER2006sa0361.pdf>
- ATSDR. (2022). Toxicological profile for mercury. <https://www.atsdr.cdc.gov/toxprofiles/tp46.pdf>
- Aulin, L. B., Tandar, S. T., van Zijp, T., van Ballegooye, E., van der Graaf, P. H., Saleh, M. A., Väitalo, P., & van Hasselt, J. C. (2022). Physiologically based modelling framework for prediction of pulmonary pharmacokinetics of antimicrobial target site concentrations. *Clinical Pharmacokinetics*, *61*(12), 1735-1748. <https://doi.org/10.1007/s40262-022-01186-3>
- Aulin, L. B., Väitalo, P. A., Rizk, M. L., Visser, S. A., Rao, G., van der Graaf, P. H., & van Hasselt, J. C. (2018). Validation of a model predicting anti-infective lung penetration in the epithelial lining fluid of humans. *Pharmaceutical Research*, *35*, 1-4. <https://doi.org/10.1007/s11095-017-2336-7>
- Baba, H., Ueno, Y., Hashida, M., & Yamashita, F. (2017). Quantitative prediction of ionization effect on human skin permeability. *International Journal of Pharmaceutics*, *522*(1-2), 222-233. <https://doi.org/10.1016/j.ijpharm.2017.03.009>
- Ballabh, P., Braun, A., & Nedergaard, M. (2004). The blood–brain barrier: an overview: structure, regulation, and clinical implications. *Neurobiology of disease*, *16*(1), 1-13. <https://doi.org/10.1016/j.nbd.2003.12.016>
- Beamer, P. I., Canales, R. A., Ferguson, A. C., Leckie, J. O., & Bradman, A. (2012). Relative pesticide and exposure route contribution to aggregate and cumulative dose in young farmworker children. *Int J Environ Res Public Health*, *9*(1), 73-96. <https://doi.org/10.3390/ijerph9010073>
- Beaudouin, R., Micallef, S., & Brochot, C. (2010). A stochastic whole-body physiologically based pharmacokinetic model to assess the impact of inter-individual variability on tissue dosimetry over the human lifespan. *Regulatory Toxicology and Pharmacology*, *57*(1), 103-116. <https://doi.org/10.1016/j.yrtph.2010.01.005>

- Béchaux, C., Bodin, L., Cléménçon, S., & Crépet, A. (2014). PBPK and population modelling to interpret urine cadmium concentrations of the French population. *Toxicology and Applied Pharmacology*, 279(3), 364-372. <https://doi.org/https://doi.org/10.1016/j.taap.2014.06.026>
- Bellouard, M., de la GrandMaison, G. L., Cappy, J., Grimaldi, L., Lontsi-Djeagou, A., & Alvarez, J.-C. (2022). Trace elements repartition in body fluids, hair and organs in an autopsied population evaluated by ICP-MS high resolution. *Environmental toxicology and pharmacology*, 95, 103978. <https://doi.org/10.1016/j.etap.2022.103978>
- Bouchard, M., Carrier, G., Brunet, R. C., Bonvalot, Y., & Gosselin, N. H. (2005). Determination of biological reference values for chlorpyrifos metabolites in human urine using a toxicokinetic approach. *Journal of occupational and environmental hygiene*, 2(3), 155-168. <https://doi.org/10.1080/15459620590922407>
- Branco, V., Caito, S., Farina, M., Teixeira da Rocha, J., Aschner, M., & Carvalho, C. (2017). Biomarkers of mercury toxicity: Past, present, and future trends. *Journal of Toxicology and Environmental Health, Part B*, 20(3), 119-154. <https://doi.org/10.1080/10937404.2017.1289834>
- Brochot, C., Casas, M., Manzano-Salgado, C., Zeman, F. A., Schettgen, T., Vrijheid, M., & Bois, F. Y. (2019a). Prediction of maternal and foetal exposures to perfluoroalkyl compounds in a Spanish birth cohort using toxicokinetic modelling [Article]. *Toxicology and Applied Pharmacology*, 379, 14, Article 114640. <https://doi.org/10.1016/j.taap.2019.114640>
- Brochot, C., Karakitsios, S. P., Petridis, I., Santonen, T., Zeman, F. A., Sarigiannis, D., Huuskonen, P., Porras, S., Kumar, V., L'Hourre, G., Alvito, P., ASSUNÇÃO, R., HORVAT, M., RUNKEL, A., TRATNIK, J. S., STRUMYLAITE, L., OSÍTE, A., DOMÍNGUEZ-ROMERO, E., SCHERINGER, M., . . . Bessems, J. (2019b). *HBM4EU - Horizon 2020 programme - Deliverable Report AD 12.8. Review of available models for the 2nd set of prioritised substances*. <https://www.hbm4eu.eu/work-packages/deliverable-12-8-report-on-the-results-of-exposure-reconstruction-algorithms-on-available-hbm-data-in-the-eu-for-all-priority-compounds/>
- Brochot, C., & Quindroit, P. (2018). Modelling the Fate of Chemicals in Humans Using a Lifetime Physiologically Based Pharmacokinetic (PBPK) Model in MERLIN-Expo. In P. Ciffroy, A. Tediosi, & E. Capri (Eds.), *Modelling the Fate of Chemicals in the Environment and the Human Body* (pp. 215-257). Springer International Publishing. https://doi.org/10.1007/978-3-319-59502-3_10
- Brown, R. P., Delp, M. D., Lindstedt, S. L., Rhomberg, L. R., & Beliles, R. P. (1997). Physiological parameter values for physiologically based pharmacokinetic models. *Toxicol Ind Health*, 13(4), 407-484. <https://doi.org/10.1177/074823379701300401>
- Brown, T. N., Armitage, J. M., Egeghy, P., Kircanski, I., & Arnot, J. A. (2016). Dermal permeation data and models for the prioritization and screening-level exposure assessment of organic chemicals. *Environment international*, 94, 424-435. <https://doi.org/10.1016/j.envint.2016.05.025>
- Buchet, J.-P., Lauwerys, R., & Roels, H. (1981). Comparison of the urinary excretion of arsenic metabolites after a single oral dose of sodium arsenite, monomethylarsonate, or dimethylarsinate in man. *Int Arch Occup Environ Health*, 48, 71-79. <https://doi.org/10.1007/BF00405933>
- Bujak, R., Struck-Lewicka, W., Kaliszan, M., Kaliszan, R., & Markuszewski, M. J. (2015). Blood–brain barrier permeability mechanisms in view of quantitative structure–activity relationships (QSAR). *Journal of pharmaceutical and biomedical analysis*, 108, 29-37. <https://doi.org/https://doi.org/10.1016/j.jpba.2015.01.046>
- Carrier, G., Bouchard, M., Brunet, R. C., & Caza, M. (2001). A Toxicokinetic Model for Predicting the Tissue Distribution and Elimination of Organic and Inorganic Mercury Following Exposure to Methyl Mercury in Animals and Humans. II. Application and Validation of the Model in Humans. *Toxicology and Applied Pharmacology*, 171(1), 50-60. <https://doi.org/https://doi.org/10.1006/taap.2000.9113>

- Chambers, D., Huang, C., & Matthews, G. (2019). *Basic physiology for anaesthetists*. Cambridge University Press.
- Cheruvu, H. S., Liu, X., Grice, J. E., & Roberts, M. S. (2022). An updated database of human maximum skin fluxes and epidermal permeability coefficients for drugs, xenobiotics, and other solutes applied as aqueous solutions. *Data in brief*, *42*, 108242. <https://doi.org/10.1016/j.dib.2022.108242>
- Chou, W.-C., & Lin, Z. (2019). Bayesian evaluation of a physiologically based pharmacokinetic (PBPK) model for perfluorooctane sulfonate (PFOS) to characterize the interspecies uncertainty between mice, rats, monkeys, and humans: Development and performance verification. *Environment international*, *129*, 408-422. <https://doi.org/https://doi.org/10.1016/j.envint.2019.03.058>
- Chou, W. C., & Lin, Z. M. (2021). Development of a Gestational and Lactational Physiologically Based Pharmacokinetic (PBPK) Model for Perfluorooctane Sulfonate (PFOS) in Rats and Humans and Its Implications in the Derivation of Health-Based Toxicity Values. *Environmental Health Perspectives*, *129*(3). <https://doi.org/10.1289/EHP7671>
- Chowdhury, U. K., Zakharyan, R. A., Hernandez, A., Avram, M. D., Kopplin, M. J., & Aposhian, H. V. (2006). Glutathione-S-transferase-omega [MMA (V) reductase] knockout mice: enzyme and arsenic species concentrations in tissues after arsenate administration. *Toxicology and Applied Pharmacology*, *216*(3), 446-457. <https://doi.org/10.1016/j.taap.2006.06.014>
- Clark, D. E. (1999). Rapid calculation of polar molecular surface area and its application to the prediction of transport phenomena. 2. Prediction of blood–brain barrier penetration. *Journal of pharmaceutical sciences*, *88*(8), 815-821. <https://doi.org/10.1021/js980402t>
- Clewell, H. J., Gearhart, J. M., Gentry, P. R., Covington, T. R., VanLandingham, C. B., Crump, K. S., & Shipp, A. M. (1999). Evaluation of the Uncertainty in an Oral Reference Dose for Methylmercury Due to Interindividual Variability in Pharmacokinetics. *Risk Analysis*, *19*(4), 547-558. <https://doi.org/https://doi.org/10.1111/j.1539-6924.1999.tb00427.x>
- Clewell, H. J., Gentry, P. R., Covington, T. R., Sarangapani, R., & Teeguarden, J. G. (2004). Evaluation of the Potential Impact of Age- and Gender-Specific Pharmacokinetic Differences on Tissue Dosimetry 2Current address: Novartis Pharmaceuticals, East Hanover, NJ 07936. *Toxicological Sciences*, *79*(2), 381-393. <https://doi.org/10.1093/toxsci/kfh109>
- Codaccioni, M., & Brochot, C. (2020). Assessing the impacts on fetal dosimetry of the modelling of the placental transfers of xenobiotics in a pregnancy physiologically based pharmacokinetic model. *Toxicology and Applied Pharmacology*, *409*, 115318. <https://doi.org/10.1016/j.taap.2020.115318>
- Cohen, S. M., Arnold, L. L., Eldan, M., Lewis, A. S., & Beck, B. D. (2006). Methylated arsenicals: the implications of metabolism and carcinogenicity studies in rodents to human risk assessment. *Critical Reviews in Toxicology*, *36*(2), 99-133. <https://doi.org/10.1080/10408440500534230>
- Cooper, A. B., Aggarwal, M., Bartels, M. J., Morriss, A., Terry, C., Lord, G. A., & Gant, T. W. (2019). PBTK model for assessment of operator exposure to haloxyfop using human biomonitoring and toxicokinetic data. *Regulatory Toxicology and Pharmacology*, *102*, 1-12. <https://doi.org/10.1016/j.yrtph.2018.12.004>
- Dallmann, A., Ince, I., Solodenko, J., Meyer, M., Willmann, S., Eissing, T., & Hempel, G. (2017). Physiologically Based Pharmacokinetic Modeling of Renally Cleared Drugs in Pregnant Women. *Clin Pharmacokinet*, *56*(12), 1525-1541. <https://doi.org/10.1007/s40262-017-0538-0>
- Dallmann, A., Liu, X. I., Burckart, G. J., & van den Anker, J. (2019). Drug Transporters Expressed in the Human Placenta and Models for Studying Maternal-Fetal Drug Transfer. *The Journal of Clinical Pharmacology*, *59*(S1), S70-S81. <https://doi.org/https://doi.org/10.1002/jcph.1491>
- Daoud, Y. A., Tebby, C., Beaudouin, R., & Brochot, C. (2023). Development of a physiologically based toxicokinetic model for lead in pregnant women: The role of bone tissue in the maternal and fetal internal exposure. *Toxicology and Applied Pharmacology*, *476*, 116651. <https://doi.org/10.1016/j.taap.2023.116651>

- Darney, K., Bodin, L., Bouchard, M., Côté, J., Volatier, J.-L., & Desvignes, V. (2018). Aggregate exposure of the adult French population to pyrethroids. *Toxicology and Applied Pharmacology*, 351, 21-31. <https://doi.org/10.1016/j.taap.2018.05.007>
- Deepika, D., Kumar, S., Bravo, N., Esplugas, R., Capodiferro, M., Sharma, R. P., Schuhmacher, M., Grimalt, J. O., Blanco, J., & Kumar, V. (2022a). Chlorpyrifos, permethrin and cyfluthrin effect on cell survival, permeability, and tight junction in an in-vitro model of the human blood-brain barrier (BBB). *Neurotoxicology*, 93, 152-162. <https://doi.org/10.1016/j.neuro.2022.09.010>
- Deepika, D., & Kumar, V. (2023). The role of “physiologically based pharmacokinetic model (PBPK)” new approach methodology (NAM) in pharmaceuticals and environmental chemical risk assessment. *International Journal of Environmental Research and Public Health*, 20(4), 3473. <https://doi.org/10.3390/ijerph20043473>
- Deepika, D., Sharma, R. P., Schuhmacher, M., & Kumar, V. (2021). Risk assessment of perfluorooctane sulfonate (PFOS) using dynamic age dependent physiologically based pharmacokinetic model (PBPK) across human lifetime. *Environ Res*, 199, 111287. <https://doi.org/10.1016/j.envres.2021.111287>
- Deepika, D., Sharma, R. P., Schuhmacher, M., Sakhi, A. K., Thomsen, C., Chatzi, L., Vafeiadi, M., Quentin, J., Slama, R., Grazuleviciene, R., Andrusaitytė, S., Waiblinger, D., Wright, J., Yang, T. C., Urquiza, J., Vrijheid, M., Casas, M., Domingo, J. L., & Kumar, V. (2022b). Unravelling sex-specific BPA toxicokinetics in children using a pediatric PBPK model. *Environ Res*, 114074. <https://doi.org/10.1016/j.envres.2022.114074>
- Desalegn, A., Bopp, S., Asturiol, D., Lamon, L., Worth, A., & Paini, A. (2019). Role of Physiologically Based Kinetic modelling in addressing environmental chemical mixtures—A review. *Computational Toxicology*, 10, 158-168. <https://doi.org/10.1016/j.comtox.2018.09.001>
- Drozdik, M., Busch, D., Lapczuk, J., Müller, J., Ostrowski, M., Kurzawski, M., & Oswald, S. (2018). Protein abundance of clinically relevant drug-metabolizing enzymes in the human liver and intestine: a comparative analysis in paired tissue specimens. *Clinical pharmacology & therapeutics*, 104(3), 515-524. <https://doi.org/10.1002/cpt.967>
- Edginton, A. N., & Ritter, L. (2009). Predicting plasma concentrations of bisphenol A in children younger than 2 years of age after typical feeding schedules, using a physiologically based toxicokinetic model. *Environmental Health Perspectives*, 117(4), 645-652. <https://doi.org/10.1289/ehp.0800073>
- Edwards, C. D., Luscombe, C., Eddershaw, P., & Hessel, E. M. (2016). Development of a novel quantitative structure-activity relationship model to accurately predict pulmonary absorption and replace routine use of the isolated perfused respiring rat lung model. *Pharmaceutical Research*, 33, 2604-2616. <https://doi.org/10.1007/s11095-016-1983-4>
- Ehrhardt, C., & Kim, K.-J. (2007). *Drug absorption studies: in situ, in vitro and in silico models*. Springer Science & Business Media.
- El-Masri, H., Kleinstreuer, N., Hines, R. N., Adams, L., Tal, T., Isaacs, K., Wetmore, B. A., & Tan, Y.-M. (2016). Integration of Life-Stage Physiologically Based Pharmacokinetic Models with Adverse Outcome Pathways and Environmental Exposure Models to Screen for Environmental Hazards. *Toxicological Sciences*, 152(1), 230-243. <https://doi.org/10.1093/toxsci/kfw082>
- El-Masri, H. A., & Kenyon, E. M. (2008). Development of a human physiologically based pharmacokinetic (PBPK) model for inorganic arsenic and its mono- and di-methylated metabolites. *Journal of Pharmacokinetics and Pharmacodynamics*, 35(1), 31-68. <https://doi.org/10.1007/s10928-007-9075-z>
- Emond, C., & Multigner, L. (2022). Chlordecone: development of a physiologically based pharmacokinetic tool to support human health risks assessments. *Archives of Toxicology*, 96(4), 1009-1019. <https://doi.org/10.1007/s00204-022-03231-3>
- Engelhardt, B., & Sorokin, L. (2009). The blood-brain and the blood-cerebrospinal fluid barriers: function and dysfunction. *Semin Immunopathol*, 31(4), 497-511. <https://doi.org/10.1007/s00281-009-0177-0>

- Enlo-Scott, Z., Swedrowska, M., & Forbes, B. (2021). Epithelial permeability and drug absorption in the lungs. In *Inhaled medicines* (pp. 267-299). Elsevier. <https://doi.org/10.1016/B978-0-12-814974-4.00004-3>
- Escher, S. E., Partosch, F., Konzok, S., Jennings, P., Luijten, M., Kienhuis, A., de Leeuw, V., Reuss, R., Lindemann, K.-M., & Bennekou, S. H. (2022). Development of a Roadmap for Action on New Approach Methodologies in Risk Assessment. *EFSA Supporting Publications*, 19(6), 7341E. <https://doi.org/10.2903/sp.efsa.2022.EN-7341>
- Estudante, M., Morais, J. G., Soveral, G., & Benet, L. Z. (2013). Intestinal drug transporters: an overview. *Advanced drug delivery reviews*, 65(10), 1340-1356. <https://doi.org/10.1016/j.addr.2012.09.042>
- Fàbrega, F., Kumar, V., Benfenati, E., Schuhmacher, M., Domingo, J. L., & Nadal, M. (2015). Physiologically based pharmacokinetic modeling of perfluoroalkyl substances in the human body. *Toxicological & Environmental Chemistry*, 97(6), 814-827. <https://doi.org/10.1080/02772248.2015.1060976>
- Fàbrega, F., Kumar, V., Schuhmacher, M., Domingo, J. L., & Nadal, M. (2014). PBPK modeling for PFOS and PFOA: validation with human experimental data. *Toxicol Lett*, 230(2), 244-251. <https://doi.org/10.1016/j.toxlet.2014.01.007>
- Fàbrega, F., Nadal, M., Schuhmacher, M., Domingo, J. L., & Kumar, V. (2016). Influence of the uncertainty in the validation of PBPK models: A case-study for PFOS and PFOA. *Regulatory Toxicology and Pharmacology*, 77, 230-239. <https://doi.org/https://doi.org/10.1016/j.yrtph.2016.03.009>
- Farris, F., Dedrick, R., Allen, P., & Smith, J. C. (1993). Physiological model for the pharmacokinetics of methyl mercury in the growing rat. *Toxicology and Applied Pharmacology*, 119(1), 74-90. <https://doi.org/10.1006/taap.1993.1046>
- Farris, F. F., Kaushal, A., & Strom, J. G. (2008). Inorganic mercury pharmacokinetics in man: a two-compartment model. *Toxicological & Environmental Chemistry*, 90(3), 519-533. <https://doi.org/10.1080/02772240701602736>
- Foxenberg, R. J., Ellison, C. A., Knaak, J. B., Ma, C., & Olson, J. R. (2011). Cytochrome P450-specific human PBPK/PD models for the organophosphorus pesticides: Chlorpyrifos and parathion. *Toxicology*, 285(1), 57-66. <https://doi.org/https://doi.org/10.1016/j.tox.2011.04.002>
- Gao, P., Shen, X., Zhang, X., Jiang, C., Zhang, S., Zhou, X., Rose, S. M. S.-F., & Snyder, M. (2022). Precision environmental health monitoring by longitudinal exposome and multi-omics profiling. *Genome research*, 32(6), 1199-1214. <https://doi.org/10.1016/j.apsb.2016.09.005>
- Gaohua, L., Miao, X., & Dou, L. (2021). Crosstalk of physiological pH and chemical pKa under the umbrella of physiologically based pharmacokinetic modeling of drug absorption, distribution, metabolism, excretion, and toxicity. *Expert opinion on drug metabolism & toxicology*, 17(9), 1103-1124. <https://doi.org/10.1080/17425255.2021.1951223>
- Gaohua, L., Wedagedera, J., Small, B., Almond, L., Romero, K., Hermann, D., Hanna, D., Jamei, M., & Gardner, I. (2015). Development of a multicompartment permeability-limited lung PBPK model and its application in predicting pulmonary pharmacokinetics of antituberculosis drugs. *CPT: pharmacometrics & systems pharmacology*, 4(10), 605-613. <https://doi.org/10.1002/psp4.12034>
- Gastellu, T., Karakoltzidis, A., Ratier, A., Bellouard, M., Alvarez, J.-C., Le Bizec, B., Rivière, G., Karakitsios, S., Sarigiannis, D. A., & Vogs, C. (2025a). A comprehensive library of lifetime physiological equations for PBK models: Enhancing dietary exposure modeling with mercury as a case study. *Environ Res*, 265, 120393. <https://doi.org/10.1016/j.envres.2024.120393>
- Gastellu, T., Le Bizec, B., & Rivière, G. (2025b). Integrating the lifelong exposure dimension of a chemical mixture into the risk assessment process. Application to trace elements. *Food and Chemical Toxicology*, 195, 115111. <https://doi.org/10.1016/j.fct.2024.115111>
- Gastellu, T., Mondou, A., Bellouard, M., Alvarez, J.-C., Le Bizec, B., & Rivière, G. (2024). Characterizing the risk related to the exposure to methylmercury over a lifetime: A global approach using

- population internal exposure. *Food and Chemical Toxicology*, 114598. <https://doi.org/10.1016/j.fct.2024.114598>
- Gearhart, J. M., Clewell, H. J., Crump, K. S., Shipp, A. M., & Silvers, A. (1995). Pharmacokinetic dose estimates of mercury in children and dose-response curves of performance tests in a large epidemiological study [journal article]. *Water, Air, and Soil Pollution*, 80(1), 49-58. <https://doi.org/10.1007/bf01189652>
- Gehr, P., Bachofen, M., & Weibel, E. R. (1978). The normal human lung: ultrastructure and morphometric estimation of diffusion capacity. *Respiration physiology*, 32(2), 121-140. [https://doi.org/10.1016/0034-5687\(78\)90104-4](https://doi.org/10.1016/0034-5687(78)90104-4)
- Geiser, M. (2010). Update on macrophage clearance of inhaled micro-and nanoparticles. *Journal of aerosol medicine and pulmonary drug delivery*, 23(4), 207-217. <https://doi.org/10.1089/jamp.2009.0797>
- Georgopoulos, P. G., Sasso, A. F., Isukapalli, S. S., Liroy, P. J., Vallero, D. A., Okino, M., & Reiter, L. (2009). Reconstructing population exposures to environmental chemicals from biomarkers: Challenges and opportunities. *Journal of Exposure Science and Environmental Epidemiology*, 19(2), 149-171. <https://doi.org/10.1038/jes.2008.9>
- Gilbert-Sandoval, I., Wesseling, S., & Rietjens, I. M. C. M. (2020). Predicting the Acute Liver Toxicity of Aflatoxin B1 in Rats and Humans by an In Vitro–In Silico Testing Strategy. *Mol Nutr Food Res*, 64(13), 2000063. <https://doi.org/10.1002/mnfr.202000063>
- Godin, S. J., DeVito, M. J., Hughes, M. F., Ross, D. G., Scollon, E. J., Starr, J. M., Setzer, R. W., Conolly, R. B., & Tornero-Velez, R. (2010). Physiologically Based Pharmacokinetic Modeling of Deltamethrin: Development of a Rat and Human Diffusion-Limited Model. *Toxicological Sciences*, 115(2), 330-343. <https://doi.org/10.1093/toxsci/kfq051>
- Goullé, J.-P., Mahieu, L., Anagnostides, J.-G., Bouige, D., Sausseureau, E., Guerbet, M., & Lacroix, C. (2010). Profil métallique tissulaire par ICP-MS chez des sujets décédés. *Annales de Toxicologie Analytique*,
- Goyal, R. K., Guo, Y., & Mashimo, H. (2019). Advances in the physiology of gastric emptying. *Neurogastroenterology & Motility*, 31(4), e13546. <https://doi.org/10.1111/nmo.13546>
- Gulson, B., Mizon, K., Korsch, M., & Taylor, A. (2016). Revisiting mobilisation of skeletal lead during pregnancy based on monthly sampling and cord/maternal blood lead relationships confirm placental transfer of lead. *Archives of Toxicology*, 90(4), 805-816. <https://doi.org/10.1007/s00204-015-1515-8>
- Haddad, S., Restieri, C., & Krishnan, K. (2001). Characterization of age-related changes in body weight and organ weights from birth to adolescence in humans. *Journal of Toxicology and Environmental Health Part A*, 64(6), 453-464. <https://doi.org/10.1080/152873901753215911>
- Haddad, S., Tardif, G.-C., & Tardif, R. (2006). Development of physiologically based toxicokinetic models for improving the human indoor exposure assessment to water contaminants: trichloroethylene and trihalomethanes. *Journal of Toxicology and Environmental Health, Part A*, 69(23), 2095-2136. <https://doi.org/10.1080/15287390600631789>
- Hastedt, J. E., Bäckman, P., Clark, A. R., Doub, W., Hickey, A., Hochhaus, G., Kuehl, P. J., Lehr, C.-M., Mauser, P., & McConville, J. (2016). Scope and relevance of a pulmonary biopharmaceutical classification system AAPS/FDA/USP Workshop March 16-17th, 2015 in Baltimore, MD. In: Springer.
- Helander, H. F., & Fändriks, L. (2014). Surface area of the digestive tract—revisited. *Scandinavian journal of gastroenterology*, 49(6), 681-689. <https://doi.org/10.3109/00365521.2014.898326>
- Hinderliter, P. M., Price, P. S., Bartels, M. J., Timchalk, C., & Poet, T. S. (2011). Development of a source-to-outcome model for dietary exposures to insecticide residues: An example using chlorpyrifos. *Regulatory Toxicology and Pharmacology*, 61(1), 82-92. <https://doi.org/https://doi.org/10.1016/j.yrtph.2011.06.004>
- Hirasawa, K., Abe, J., Nagahori, H., & Kitamoto, S. (2022). Prediction of the human pharmacokinetics of epyrifenacil and its major metabolite, S-3100-CA, by a physiologically based

- pharmacokinetic modeling using chimeric mice with humanized liver. *Toxicology and Applied Pharmacology*, 439, 115912. <https://doi.org/https://doi.org/10.1016/j.taap.2022.115912>
- Hostýnek, J. J., Dreher, F., Nakada, T., Schwindt, D., Anigbogu, A., & Maibach, H. I. (2001). Human Stratum Corneum Adsorption of Nickel Salts. *Acta Dermato-Venereologica*, 81. <https://doi.org/10.1080/000155501753279587>
- Hu, M., Zhang, Z., Zhang, Y., Zhan, M., Qu, W., He, G., & Zhou, Y. (2023). Development of human dermal PBPK models for the bisphenols BPA, BPS, BPF, and BPAF with parallel-layered skin compartment: Basing on dermal administration studies in humans. *Science of the Total Environment*, 868, 161639. <https://doi.org/https://doi.org/10.1016/j.scitotenv.2023.161639>
- Husøy, T., Caspersen, I. H., Thépaut, E., Knutsen, H., Haug, L. S., Andreassen, M., Gkrillas, A., Lindeman, B., Thomsen, C., & Herzke, D. (2023). Comparison of aggregated exposure to perfluorooctanoic acid (PFOA) from diet and personal care products with concentrations in blood using a PBPK model—Results from the Norwegian biomonitoring study in EuroMix. *Environ Res*, 239, 117341. <https://doi.org/10.1016/j.envres.2023.117341>
- ICRP. (2002). Basic Anatomical and Physiological Data for Use in Radiological Protection Reference Values *ICRP Publication*, 89(32(3-4)), 1-282.
- IPCS. (2001). Arsenic and arsenic compounds. *World Health Organisation, Geneva*.
- Johnson, T. N., Small, B. G., & Rowland Yeo, K. (2022). Increasing application of pediatric physiologically based pharmacokinetic models across academic and industry organizations. *CPT: pharmacometrics & systems pharmacology*, 11(3), 373-383. <https://doi.org/10.1002/psp4.12764>
- Kaliszan, R., & Markuszewski, M. (1996). Brain/blood distribution described by a combination of partition coefficient and molecular mass. *International Journal of Pharmaceutics*, 145(1), 9-16. [https://doi.org/https://doi.org/10.1016/S0378-5173\(96\)04712-6](https://doi.org/https://doi.org/10.1016/S0378-5173(96)04712-6)
- Karrer, C., Roiss, T., von Goetz, N., Gramec Skledar, D., Peterlin Mašič, L., & Hungerbühler, K. (2018). Physiologically Based Pharmacokinetic (PBPK) Modeling of the Bisphenols BPA, BPS, BPF, and BPAF with New Experimental Metabolic Parameters: Comparing the Pharmacokinetic Behavior of BPA with Its Substitutes. *Environmental Health Perspectives*, 126(7), 077002. <https://doi.org/10.1289/EHP2739>
- Kenyon, E., Del Razo, L., & Hughes, M. (2005a). Tissue distribution and urinary excretion of inorganic arsenic and its methylated metabolites in mice following acute oral administration of arsenate. *Toxicological Sciences*, 85(1), 468-475. <https://doi.org/10.1093/toxsci/kfi107>
- Kenyon, E. M., Del Razo, L. M., Hughes, M. F., & Kitchin, K. T. (2005b). An integrated pharmacokinetic and pharmacodynamic study of arsenite action: 2. Heme oxygenase induction in mice. *Toxicology*, 206(3), 389-401. <https://doi.org/10.1016/j.tox.2004.08.003>
- Khajeh, A., & Modarress, H. (2014). Linear and nonlinear quantitative structure-property relationship modelling of skin permeability. *SAR and QSAR in Environmental Research*, 25(1), 35-50. <https://doi.org/10.1080/1062936X.2013.826275>
- Khan, M., Sakauchi, F., Sonoda, T., Washio, M., & Mori, M. (2003). Magnitude of arsenic toxicity in tube-well drinking water in Bangladesh and its adverse effects on human health including cancer: evidence from a review of the literature. *Asian Pacific Journal of Cancer Prevention*, 4(1), 7-14. https://journal.waocp.org/article_24154_93223914addbb8e557e533c5e19741e8.pdf
- Kjellström, T., & Nordberg, G. F. (1978). A kinetic model of cadmium metabolism in the human being. *Environ Res*, 16(1-3), 248-269. [https://doi.org/10.1016/0013-9351\(78\)90160-3](https://doi.org/10.1016/0013-9351(78)90160-3)
- Knaak, J. B., Dary, C. C., Power, F., Thompson, C. B., & Blancato, J. N. (2004). Physicochemical and Biological Data for the Development of Predictive Organophosphorus Pesticide QSARs and PBPK/PD Models for Human Risk Assessment. *Critical Reviews in Toxicology*, 34(2), 143-207. <https://doi.org/10.1080/10408440490432250>
- Kolarsick, P. A., Kolarsick, M. A., & Goodwin, C. (2011). Anatomy and physiology of the skin. *Journal of the Dermatology Nurses' Association*, 3(4), 203-213. <https://doi.org/10.1097/JDN.0b013e3182274a98>

- Kuepfer, L., Niederal, C., Wendl, T., Schlender, J. F., Willmann, S., Lippert, J., Block, M., Eissing, T., & Teutonico, D. (2016). Applied concepts in PBPK modeling: how to build a PBPK/PD model. *CPT: pharmacometrics & systems pharmacology*, 5(10), 516-531. <https://doi.org/10.1002/psp4.12134>
- Ladele, J. I., Fajolu, I. B., & Ezeaka, V. C. (2019). Determination of lead levels in maternal and umbilical cord blood at birth at the Lagos University Teaching Hospital, Lagos. *PLoS One*, 14(2), e0211535. <https://doi.org/10.1371/journal.pone.0211535>
- Ladumor, M. K., Thakur, A., Sharma, S., Rachapally, A., Mishra, S., Bobe, P., Rao, V. K., Pammi, P., Kangne, H., & Levi, D. (2019). A repository of protein abundance data of drug metabolizing enzymes and transporters for applications in physiologically based pharmacokinetic (PBPK) modelling and simulation. *Scientific reports*, 9(1), 9709. <https://doi.org/10.1038/s41598-019-45778-9>
- Lamon, L., Doyle, J., Paini, A., Moeller, R., Viegas, S., Cubadda, F., Hoet, P., van Nieuwenhuysse, A., Louro, H., Dusinska, M., Galea, K. S., Canham, R., Martins, C., Gama, A., Teófilo, V., Diniz-da-Costa, M., João Silva, M., Ventura, C., Alvito, P., . . . Price, P. (2024). Roadmap for action for advancing aggregate exposure to chemicals in the EU. *EFSA Supporting Publications*, 21(7), 8971E. <https://doi.org/10.2903/sp.efsa.2024.EN-8971>
- Leggett, R. W. (1993). An age-specific kinetic model of lead metabolism in humans. *Environmental Health Perspectives*, 101(7), 598-616. <https://doi.org/10.1289/ehp.93101598>
- Lin, H.-L., Chiu, Y.-W., Wang, C.-C., & Tung, C.-W. (2022). Computational prediction of Calu-3-based in vitro pulmonary permeability of chemicals. *Regulatory Toxicology and Pharmacology*, 135, 105265. <https://doi.org/10.1016/j.yrtph.2022.105265>
- Linnankoski, J., Mäkelä, J. M., Ranta, V.-P., Urtti, A., & Yliperttula, M. (2006). Computational prediction of oral drug absorption based on absorption rate constants in humans. *Journal of medicinal chemistry*, 49(12), 3674-3681. <https://doi.org/10.1021/jm051231p>
- Loccisano, A. E., Campbell Jr, J. L., Andersen, M. E., & Clewell III, H. J. (2011). Evaluation and prediction of pharmacokinetics of PFOA and PFOS in the monkey and human using a PBPK model. *Regulatory Toxicology and Pharmacology*, 59(1), 157-175. <https://doi.org/10.1016/j.yrtph.2010.12.004>
- Loccisano, A. E., Longnecker, M. P., Campbell, J. L., Jr., Andersen, M. E., & Clewell, H. J., 3rd. (2013). Development of PBPK models for PFOA and PFOS for human pregnancy and lactation life stages. *J Toxicol Environ Health A*, 76(1), 25-57. <https://doi.org/10.1080/15287394.2012.722523>
- Lowe, E. R., Poet, T. S., Rick, D. L., Marty, M. S., Mattsson, J. L., Timchalk, C., & Bartels, M. J. (2009). The effect of plasma lipids on the pharmacokinetics of chlorpyrifos and the impact on interpretation of blood biomonitoring data. *Toxicol Sci*, 108(2), 258-272. <https://doi.org/10.1093/toxsci/kfp034>
- Lu, C., Holbrook, C. M., & Andres, L. M. (2010). The implications of using a physiologically based pharmacokinetic (PBPK) model for pesticide risk assessment. *Environ Health Perspect*, 118(1), 125-130. <https://doi.org/10.1289/ehp.0901144>
- Maass, C., Schaller, S., Dallmann, A., Bothe, K., & Müller, D. (2023). Considering developmental neurotoxicity in vitro data for human health risk assessment using physiologically-based kinetic modeling: deltamethrin case study. *Toxicological Sciences*, kfad007. <https://doi.org/10.1093/toxsci/kfad007>
- Maina, J. N. (2002). Structure, function and evolution of the gas exchangers: comparative perspectives. *Journal of anatomy*, 201(4), 281-304. <https://doi.org/10.1046/j.1469-7580.2002.00099.x>
- Mallick, P., Moreau, M., Song, G., Efremenko, A. Y., Pendse, S. N., Creek, M. R., Osimitz, T. G., Hines, R. N., Hinderliter, P., Clewell, H. J., Lake, B. G., & Yoon, M. (2020). Development and Application of a Life-Stage Physiologically Based Pharmacokinetic (PBPK) Model to the Assessment of Internal Dose of Pyrethroids in Humans. *Toxicol Sci*, 173(1), 86-99. <https://doi.org/10.1093/toxsci/kfz211>

- Mann, S., Droz, P., & Vahter, M. (1996a). A physiologically based pharmacokinetic model for arsenic exposure: I. Development in hamsters and rabbits. *Toxicology and Applied Pharmacology*, *137*(1), 8-22. <https://doi.org/10.1006/taap.1996.0052>
- Mann, S., Droz, P., & Vahter, M. (1996b). A physiologically based pharmacokinetic model for arsenic exposure: II. Validation and application in humans. *Toxicology and Applied Pharmacology*, *140*(2), 471-486. <https://doi.org/10.1006/taap.1996.0244>
- Mendez-Catala, D. M., Wang, Q., & Rietjens, I. M. C. M. (2021). PBK Model-Based Prediction of Intestinal Microbial and Host Metabolism of Zearalenone and Consequences for its Estrogenicity. *Mol Nutr Food Res*, *65*(23), 2100443. <https://doi.org/10.1002/mnfr.202100443>
- Mielke, H., & Gundert-Remy, U. (2009). Bisphenol A levels in blood depend on age and exposure. *Toxicology letters*, *190*(1), 32-40. <https://doi.org/10.1016/j.toxlet.2009.06.861>
- Mielke, H., Partosch, F., & Gundert-Remy, U. (2011). The contribution of dermal exposure to the internal exposure of bisphenol A in man. *Toxicol Lett*, *204*(2-3), 190-198. <https://doi.org/10.1016/j.toxlet.2011.04.032>
- Miller, N. A., Graves, R. H., Edwards, C. D., Amour, A., Taylor, E., Robb, O., O'Brien, B., Patel, A., Harrell, A. W., & Hessel, E. M. (2022). Physiologically based pharmacokinetic modelling of inhaled nemiralisib: mechanistic components for pulmonary absorption, systemic distribution, and oral absorption. *Clinical Pharmacokinetics*, 1-13. <https://doi.org/10.1007/s40262-021-01066-2>
- Mosquin, P. L., Licata, A. C., Liu, B., Sumner, S. C., & Okino, M. S. (2009). Reconstructing exposures from small samples using physiologically based pharmacokinetic models and multiple biomarkers. *J Expo Sci Environ Epidemiol*, *19*(3), 284-297. <https://doi.org/10.1038/jes.2008.17>
- Mukherjee, D., Royce, S. G., Alexander, J. A., Buckley, B., Isukapalli, S. S., Bandera, E. V., Zarbl, H., & Georgopoulos, P. G. (2014). Physiologically-Based Toxicokinetic Modeling of Zearalenone and Its Metabolites: Application to the Jersey Girl Study. *PLoS One*, *9*(12), e113632. <https://doi.org/10.1371/journal.pone.0113632>
- Mukherjee, S. C., Saha, K. C., Pati, S., Dutta, R. N., Rahman, M. M., Sengupta, M. K., Ahamed, S., Lodh, D., Das, B., & Hossain, M. A. (2005). Murshidabad—one of the nine groundwater arsenic-affected districts of West Bengal, India. Part II: dermatological, neurological, and obstetric findings. *Clinical toxicology*, *43*(7), 835-848. <https://doi.org/10.1080/15563650500357495>
- Murphrey, M. B., Miao, J. H., & Zito, P. M. (2018). Histology, stratum corneum.
- Nashashibi, N., Cardamakis, E., Bolbos, G., & Tzingounis, V. (1999). Investigation of Kinetic of Lead during Pregnancy and Lactation. *Gynecologic and Obstetric Investigation*, *48*(3), 158-162. <https://doi.org/10.1159/000010164>
- Navas-Acien, A., Sharrett, A. R., Silbergeld, E. K., Schwartz, B. S., Nachman, K. E., Burke, T. A., & Guallar, E. (2005). Arsenic exposure and cardiovascular disease: a systematic review of the epidemiologic evidence. *American journal of epidemiology*, *162*(11), 1037-1049. <https://doi.org/10.1093/aje/kwi330>
- Ng, A. W., Bidani, A., & Heming, T. A. (2004). Innate host defense of the lung: effects of lung-lining fluid pH. *Lung*, *182*, 297-317. <https://doi.org/10.1007/s00408-004-2511-6>
- Notenboom, S., Hoogenveen, R. T., Zeilmaker, M. J., Van den Brand, A. D., Assunção, R., & Mengelers, M. J. B. (2023). Development of a Generic PBK Model for Human Biomonitoring with an Application to Deoxynivalenol. *Toxins*, *15*(9), 569. <https://doi.org/10.3390/toxins15090569>
- Nunes, R., Silva, C., & Chaves, L. (2016). Tissue-based in vitro and ex vivo models for intestinal permeability studies. *Concepts and Models for Drug Permeability Studies*, 203-236. <https://doi.org/10.1016/B978-0-08-100094-6.00013-4>
- O'Flaherty, E. J. (1991a). Physiologically based models for bone-seeking elements: I. Rat skeletal and bone growth. *Toxicology and Applied Pharmacology*, *111*(2), 299-312. [https://doi.org/https://doi.org/10.1016/0041-008X\(91\)90032-A](https://doi.org/https://doi.org/10.1016/0041-008X(91)90032-A)

- O'Flaherty, E. J. (1991b). Physiologically based models for bone-seeking elements: II. Kinetics of lead disposition in rats. *Toxicology and Applied Pharmacology*, *111*(2), 313-331. [https://doi.org/https://doi.org/10.1016/0041-008X\(91\)90033-B](https://doi.org/https://doi.org/10.1016/0041-008X(91)90033-B)
- O'Flaherty, E. J. (1991c). Physiologically based models for bone-seeking elements: III. Human skeletal and bone growth. *Toxicology and Applied Pharmacology*, *111*(2), 332-341. [https://doi.org/https://doi.org/10.1016/0041-008X\(91\)90034-C](https://doi.org/https://doi.org/10.1016/0041-008X(91)90034-C)
- O'Flaherty, E. J. (1993). Physiologically Based Models for Bone-Seeking Elements: IV. Kinetics of Lead Disposition in Humans. *Toxicology and Applied Pharmacology*, *118*(1), 16-29. <https://doi.org/https://doi.org/10.1006/taap.1993.1004>
- O'Flaherty, E. J. (1998). A physiologically based kinetic model for lead in children and adults. *Environmental Health Perspectives*, *106*(suppl 6), 1495-1503. <https://doi.org/doi:10.1289/ehp.98106s61495>
- O'Flaherty, E. J. (2000). Modeling normal aging bone loss, with consideration of bone loss in osteoporosis. *Toxicol Sci*, *55*(1), 171-188. <https://doi.org/10.1093/toxsci/55.1.171>
- OECD. (2021). Guidance document on the characterisation, validation and reporting of Physiologically Based Kinetic (PBK) models for regulatory purposes. *OECD Series on Testing and Assessment, No. 331, OECD Publishing, Paris*. <https://doi.org/10.1787/d0de241f-en>
- Oleko, A., Saudi, A., Zeghnoun, A., Pecheux, M., Cirimele, V., Cirtiu, C. M., Berail, G., Szego, E., Denys, S., & Fillol, C. (2024). Exposure of the general French population to metals and metalloids in 2014–2016: Results from the Esteban study. *Environ Res*, *252*, 118744. <https://doi.org/10.1016/j.envres.2024.118744>
- Ong, C. N., Phoon, W. O., Law, H. Y., Tye, C. Y., & Lim, H. H. (1985). Concentrations of lead in maternal blood, cord blood, and breast milk. *Archives of disease in childhood*, *60*(8), 756. <https://doi.org/10.1136/adc.60.8.756>
- Ou, L., Wang, H., Chen, C., Chen, L., Zhang, W., & Wang, X. (2018). Physiologically based pharmacokinetic (PBPK) modeling of human lactational transfer of methylmercury in China. *Environment international*, *115*, 180-187. <https://doi.org/10.1016/j.envint.2018.03.018>
- Paine, M. F., Hart, H. L., Ludington, S. S., Haining, R. L., Rettie, A. E., & Zeldin, D. C. (2006). The human intestinal cytochrome P450 “pie”. *Drug Metabolism and Disposition*, *34*(5), 880-886. <https://doi.org/10.1124/dmd.105.008672>
- Paini, A., Leonard, J. A., Joossens, E., Bessems, J. G. M., Desalegn, A., Dorne, J. L., Gosling, J. P., Heringa, M. B., Klaric, M., Kliment, T., Kramer, N. I., Loizou, G., Louise, J., Lumen, A., Madden, J. C., Patterson, E. A., Proença, S., Punt, A., Setzer, R. W., . . . Tan, Y. M. (2019). Next generation physiologically based kinetic (NG-PBK) models in support of regulatory decision making. *Computational Toxicology*, *9*, 61-72. <https://doi.org/https://doi.org/10.1016/j.comtox.2018.11.002>
- Pan, D., Iyer, M., Liu, J., Li, Y., & Hopfinger, A. J. (2004). Constructing Optimum Blood Brain Barrier QSAR Models Using a Combination of 4D-Molecular Similarity Measures and Cluster Analysis. *Journal of chemical information and computer sciences*, *44*(6), 2083-2098. <https://doi.org/10.1021/ci0498057>
- Pelletier, M., Bonvallot, N., & Glorennec, P. (2017). Aggregating exposures & cumulating risk for semivolatile organic compounds: A review. *Environ Res*, *158*, 649-659. <https://doi.org/10.1016/j.envres.2017.06.022>
- Pendse, S. N., Efremenko, A., Hack, C. E., Moreau, M., Mallick, P., Dzierlenga, M., Nicolas, C. I., Yoon, M., Clewell, H. J., & McMullen, P. D. (2020). Population Life-course exposure to health effects model (PLETHEM): An R package for PBPK modeling. *Computational Toxicology*, *13*, 100115. <https://doi.org/https://doi.org/10.1016/j.comtox.2019.100115>
- Poet, T. S., Timchalk, C., Bartels, M. J., Smith, J. N., McDougal, R., Juberg, D. R., & Price, P. S. (2017). Use of a probabilistic PBPK/PD model to calculate Data Derived Extrapolation Factors for chlorpyrifos. *Regulatory Toxicology and Pharmacology*, *86*, 59-73. <https://doi.org/https://doi.org/10.1016/j.vrtph.2017.02.014>

- Poet, T. S., Timchalk, C., Hotchkiss, J. A., & Bartels, M. J. (2014). Chlorpyrifos PBPK/PD model for multiple routes of exposure. *Xenobiotica*, *44*(10), 868-881. <https://doi.org/10.3109/00498254.2014.918295>
- Pope, Q., & Rand, M. D. (2021). Variation in methylmercury metabolism and elimination in humans: physiological pharmacokinetic modeling highlights the role of gut biotransformation, skeletal muscle, and hair. *Toxicological Sciences*, *180*(1), 26-37. <https://doi.org/10.1093/toxsci/kfaa192>
- Pouillot, R., Farakos, S. S., Spungen, J., Schaefer, H. R., Flannery, B. M., & Van Doren, J. M. (2022). Cadmium physiologically based pharmacokinetic (PBPK) models for forward and reverse dosimetry: Review, evaluation, and adaptation to the U.S. population. *Toxicology letters*, *367*, 67-75. <https://doi.org/https://doi.org/10.1016/j.toxlet.2022.07.812>
- Price, K., Haddad, S., & Krishnan, K. (2003). Physiological modeling of age-specific changes in the pharmacokinetics of organic chemicals in children. *Journal of Toxicology and Environmental Health Part A*, *66*(5), 417-433. <https://doi.org/10.1080/15287390306450>
- Pruvost-Couvreur, M., Le Bizec, B., Béchaux, C., & Rivière, G. (2020). Dietary risk assessment methodology: how to deal with changes through life. *Food Additives & Contaminants: Part A*, *37*(5), 705-722. <https://doi.org/10.1080/194440049.2020.1727964>
- Quindroit, P., Beaudouin, R., & Brochot, C. (2019a). Estimating the cumulative human exposures to pyrethroids by combined multi-route PBPK models: Application to the French population. *Toxicology Letters*, *312*, 125-138. <https://doi.org/https://doi.org/10.1016/j.toxlet.2019.05.007>
- Quindroit, P., Beaudouin, R., & Brochot, C. (2019b). Estimating the cumulative human exposures to pyrethroids by combined multi-route PBPK models: Application to the French population. *Toxicology letters*. <https://doi.org/10.1016/j.toxlet.2019.05.007>
- Ratier, A., Casas, M., Grazuleviciene, R., Slama, R., Haug, L. S., Thomsen, C., Vafeiadi, M., Wright, J., Zeman, F. A., & Vrijheid, M. (2024). Estimating the dynamic early life exposure to PFOA and PFOS of the HELIX children: Emerging profiles via prenatal exposure, breastfeeding, and diet. *Environment international*, *186*, 108621. <https://doi.org/10.1016/j.envint.2024.108621>
- Reale, E., Jeddi, M. Z., Paini, A., Connolly, A., Duca, R., Cubadda, F., Benfenati, E., Bessems, J., Galea, K. S., & Dirven, H. (2024). Human biomonitoring and toxicokinetics as key building blocks for next generation risk assessment. *Environment international*, *184*, 108474. <https://doi.org/10.1016/j.envint.2024.108474>
- Redzic, Z. (2011). Molecular biology of the blood-brain and the blood-cerebrospinal fluid barriers: similarities and differences. *Fluids Barriers CNS*, *8*(1), 3. <https://doi.org/10.1186/2045-8118-8-3>
- Rezaei, S., Behnejad, H., Shiri, F., & Ghasemi, J. B. (2019). Exploring 3D-QSPR models of human skin permeability for a diverse dataset of chemical compounds. *Journal of Receptors and Signal Transduction*, *39*(5-6), 442-450. <https://doi.org/10.1080/10799893.2019.1690512>
- Ring, C. L., Pearce, R. G., Setzer, R. W., Wetmore, B. A., & Wambaugh, J. F. (2017). Identifying populations sensitive to environmental chemicals by simulating toxicokinetic variability. *Environment international*, *106*, 105-118. <https://doi.org/10.1016/j.envint.2017.06.004>
- Rothenberg, S. J., Karchmer, S., Schnaas, L., Perroni, E., Zea, F., & Fernández Alba, J. (1994). Changes in serial blood lead levels during pregnancy. *Environmental Health Perspectives*, *102*(10), 876-880. <https://doi.org/10.1289/ehp.94102876>
- Rovira, J., Martínez, M., Sharma, R. P., Espuis, T., Nadal, M., Kumar, V., Costopoulou, D., Vassiliadou, I., Leondiadis, L., Domingo, J. L., & Schuhmacher, M. (2019). Prenatal exposure to PFOS and PFOA in a pregnant women cohort of Catalonia, Spain. *Environ Res*, *175*, 384-392. <https://doi.org/10.1016/j.envres.2019.05.040>
- Ruiz, P., Mumtaz, M., Osterloh, J., Fisher, J., & Fowler, B. A. (2010). Interpreting NHANES biomonitoring data, cadmium. *Toxicology letters*, *198*(1), 44-48. <https://doi.org/10.1016/j.toxlet.2010.04.022>

- Sarigiannis, D., Karakitsios, S. P., Dominguez-Romero, E., Papadaki, K., Brochot, C., Kumar, V., Schumacher, M., Sy, M., Mielke, H., Greiner, M., Mengelers, M., & Scheringer, M. (2017). *HBM4EU - Horizon 2020 programme - Deliverable Report D 12.1. Review paper on PBTK/D models for the 1st set of priority compounds*. <https://www.hbm4eu.eu/work-packages/deliverable-12-1-review-paper-on-pbtkd-models-for-the-1st-set-of-priority-compounds/>
- Sarigiannis, D. A., Karakitsios, S. P., Handakas, E., Simou, K., Solomou, E., & Gotti, A. (2016a). Integrated exposure and risk characterization of bisphenol-A in Europe. *Food and Chemical Toxicology*, *98*, 134-147. <https://doi.org/10.1016/j.fct.2016.10.017>
- Sarigiannis, D. A., Karakitsios, S. P., Handakas, E., Simou, K., Solomou, E., & Gotti, A. (2016b). Integrated exposure and risk characterization of bisphenol-A in Europe. *Food Chem Toxicol*, *98*(Pt B), 134-147. <https://doi.org/10.1016/j.fct.2016.10.017>
- Sarigiannis, D. A., Tratnik, J. S., Mazej, D., Kosjek, T., Heath, E., Horvat, M., Anesti, O., & Karakitsios, S. P. (2019). Risk characterization of bisphenol-A in the Slovenian population starting from human biomonitoring data. *Environ Res*, *170*, 293-300. <https://doi.org/10.1016/j.envres.2018.12.056>
- Sarigiannis, D. A., Karakitsios, S. P., Handakas, E., & Gotti, A. (2020). Development of a generic lifelong physiologically based biokinetic model for exposome studies. *Environmental Research*, *185*, 109307. <https://doi.org/https://doi.org/10.1016/j.envres.2020.109307>
- Schaefer, H., & Redelmeier, T. E. (1997). Skin barrier: principles of percutaneous absorption. (*No Title*).
- Schwerdtle, T., Walter, I., Mackiw, I., & Hartwig, A. (2003). Induction of oxidative DNA damage by arsenite and its trivalent and pentavalent methylated metabolites in cultured human cells and isolated DNA. *Carcinogenesis*, *24*(5), 967-974. <https://doi.org/10.1093/carcin/bgg018>
- Sedykh, A., Fourches, D., Duan, J., Hucke, O., Garneau, M., Zhu, H., Bonneau, P., & Tropsha, A. (2013). Human intestinal transporter database: QSAR modeling and virtual profiling of drug uptake, efflux and interactions. *Pharmaceutical Research*, *30*, 996-1007. <https://doi.org/10.1007/s11095-012-0935-x>
- Selo, M. A., Sake, J. A., Kim, K.-J., & Ehrhardt, C. (2021). In vitro and ex vivo models in inhalation biopharmaceutical research — advances, challenges and future perspectives. *Advanced drug delivery reviews*, *177*, 113862. <https://doi.org/10.1016/j.addr.2021.113862>
- Sensoy, I. (2021). A review on the food digestion in the digestive tract and the used in vitro models. *Current research in food science*, *4*, 308-319. <https://doi.org/10.1016/j.crf.2021.04.004>
- Shahtaheri, S. M., Aaron, J. E., Johnson, D. R., & Purdie, D. W. (1999). Changes in trabecular bone architecture in women during pregnancy. *Br J Obstet Gynaecol*, *106*(5), 432-438. <https://doi.org/10.1111/j.1471-0528.1999.tb08296.x>
- Sharma, R. P., Schuhmacher, M., & Kumar, V. (2018). The development of a pregnancy PBPK Model for Bisphenol A and its evaluation with the available biomonitoring data. *Science of the Total Environment*, *624*, 55-68. <https://doi.org/10.1016/j.scitotenv.2017.12.023>
- Shin, B. S., Hyun, H. S., B., B. J., Bong, L. J., Wook, H. S., Jun, K. H., Du, Y. S., Hae-Seong, Y., Jung, K. D., Mu, L. B., & and Yoo, S. D. (2009). Physiologically Based Pharmacokinetics of Zearalenone. *Journal of Toxicology and Environmental Health, Part A*, *72*(21-22), 1395-1405. <https://doi.org/10.1080/15287390903212741>
- Shin, B. S., Kim, C. H., Jun, Y. S., Kim, D. H., Lee, B. M., Yoon, C. H., Park, E. H., Lee, K. C., Han, S. Y., Park, K. L., Kim, H. S., & Yoo, S. D. (2004). Physiologically based pharmacokinetics of bisphenol A. *J Toxicol Environ Health A*, *67*(23-24), 1971-1985. <https://doi.org/10.1080/15287390490514615>
- Sibinovska, N., Žakelj, S., Roškar, R., & Kristan, K. (2020). Suitability and functional characterization of two Calu-3 cell models for prediction of drug permeability across the airway epithelial barrier. *International Journal of Pharmaceutics*, *585*, 119484. <https://doi.org/10.1016/j.ijpharm.2020.119484>

- Sirof, V., Guérin, T., Mauras, Y., Garraud, H., Volatier, J.-L., & Leblanc, J.-C. (2008). Methylmercury exposure assessment using dietary and biomarker data among frequent seafood consumers in France: CALIPSO study. *Environ Res*, *107*(1), 30-38.
<https://doi.org/10.1016/j.envres.2007.12.005>
- Smith, J. N., Hinderliter, P. M., Timchalk, C., Bartels, M. J., & Poet, T. S. (2014). A human life-stage physiologically based pharmacokinetic and pharmacodynamic model for chlorpyrifos: Development and validation. *Regulatory Toxicology and Pharmacology*, *69*(3), 580-597.
<https://doi.org/https://doi.org/10.1016/j.yrtph.2013.10.005>
- Suenderhauf, C., Hammann, F., Maunz, A., Helma, C., & Huwyler, J. r. (2011). Combinatorial QSAR modeling of human intestinal absorption. *Molecular pharmaceuticals*, *8*(1), 213-224.
<https://doi.org/10.1021/mp100279d>
- Sweeney, L. M. (2021). Probabilistic pharmacokinetic modeling of airborne lead corresponding to toxicologically relevant blood lead levels in workers. *Regulatory Toxicology and Pharmacology*, *122*, 104894. <https://doi.org/https://doi.org/10.1016/j.yrtph.2021.104894>
- Sweeney, L. M. (2022). Physiologically based pharmacokinetic (PBPK) modeling of perfluorohexane sulfonate (PFHxS) in humans. *Regulatory Toxicology and Pharmacology*, *129*, 105099.
<https://doi.org/https://doi.org/10.1016/j.yrtph.2021.105099>
- Takaku, T., Nagahori, H., Sogame, Y., & Takagi, T. (2015). Quantitative Structure–Activity Relationship Model for the Fetal–Maternal Blood Concentration Ratio of Chemicals in Humans. *Biological and Pharmaceutical Bulletin*, *38*(6), 930-934. <https://doi.org/10.1248/bpb.b14-00883>
- Talevi, A., & Bellera, C. L. (2021). Enterohepatic recycling. *The ADME Encyclopedia: A Comprehensive Guide on Biopharmacy and Pharmacokinetics*, 1-9. https://doi.org/10.1007/978-3-030-51519-5_72-1
- Tebby, C., Caudeville, J., Fernandez, Y., & Brochot, C. (2022). Mapping blood lead levels in French children due to environmental contamination using a modeling approach. *Science of the Total Environment*, *808*, 152149. <https://doi.org/10.1016/j.scitotenv.2021.152149>
- Tebby, C., van der Voet, H., de Sousa, G., Rorije, E., Kumar, V., de Boer, W., Kruisselbrink, J. W., Bois, F. Y., Faniband, M., Moretto, A., & Brochot, C. (2020). A generic PBTK model implemented in the MCRA platform: Predictive performance and uses in risk assessment of chemicals. *Food and Chemical Toxicology*, *142*, 111440.
<https://doi.org/https://doi.org/10.1016/j.fct.2020.111440>
- Teeguarden, J. G., Waechter, J. M., Jr., Clewell, H. J., III, Covington, T. R., & Barton, H. A. (2005). Evaluation of Oral and Intravenous Route Pharmacokinetics, Plasma Protein Binding, and Uterine Tissue Dose Metrics of Bisphenol A: A Physiologically Based Pharmacokinetic Approach. *Toxicological Sciences*, *85*(2), 823-838. <https://doi.org/10.1093/toxsci/kfi135>
- Thomas, D. J., Li, J., Waters, S. B., Xing, W., Adair, B. M., Drobna, Z., Devesa, V., & Styblo, M. (2007). Arsenic (+ 3 oxidation state) methyltransferase and the methylation of arsenicals. *Experimental Biology and Medicine*, *232*(1), 3-13. <https://doi.org/10.3181/00379727-207-232000>
- Thomas, D. J., Waters, S. B., & Styblo, M. (2004). Elucidating the pathway for arsenic methylation. *Toxicology and Applied Pharmacology*, *198*(3), 319-326.
<https://doi.org/10.1016/j.taap.2003.10.020>
- Timchalk, C., Kousba, A., & Poet, T. S. (2002a). Monte Carlo analysis of the human chlorpyrifos-oxonase (PON1) polymorphism using a physiologically based pharmacokinetic and pharmacodynamic (PBPK/PD) model. *Toxicology letters*, *135*(1), 51-59.
[https://doi.org/https://doi.org/10.1016/S0378-4274\(02\)00233-3](https://doi.org/https://doi.org/10.1016/S0378-4274(02)00233-3)
- Timchalk, C., Nolan, R. J., Mendrala, A. L., Dittenber, D. A., Brzak, K. A., & Mattsson, J. L. (2002b). A Physiologically Based Pharmacokinetic and Pharmacodynamic (PBPK/PD) Model for the Organophosphate Insecticide Chlorpyrifos in Rats and Humans. *Toxicological Sciences*, *66*(1), 34-53. <https://doi.org/10.1093/toxsci/66.1.34>
- Tornero-Velez, R., Davis, J., Scollon, E. J., Starr, J. M., Setzer, R. W., Goldsmith, M.-R., Chang, D. T., Xue, J., Zartarian, V., De Vito, M. J., & Hughes, M. F. (2012). A Pharmacokinetic Model of cis-

- and trans-Permethrin Disposition in Rats and Humans With Aggregate Exposure Application. *Toxicological Sciences*, 130(1), 33-47. <https://doi.org/10.1093/toxsci/kfs236>
- Tsuji, J. S., Lennox, K. P., Watson, H. N., & Chang, E. T. (2021). Essential concepts for interpreting the dose-response of low-level arsenic exposure in epidemiological studies. *Toxicology*, 457, 152801. <https://doi.org/10.1016/j.tox.2021.152801>
- US EPA. (1994). Guidance manual for the integrated exposure uptake biokinetic model for lead in children. *US Environmental Protection Agency: Washington, DC, USA*.
- US EPA. (2001). National primary drinking water regulations; arsenic and clarifications to compliance and new source contaminants monitoring. *Federal Register*, 66(14), 69-76.
- US EPA. (2019). All-Ages Lead Model (AALM). *Version 2.0 (External Review Draft, 2019)*. *US Environmental Protection Agency, Washington, DC, EPA/600/R-19, 11, 2019*.
- Välitalo, P. A., Griffioen, K., Rizk, M. L., Visser, S. A., Danhof, M., Rao, G., van der Graaf, P. H., & van Hasselt, J. C. (2016). Structure-based prediction of anti-infective drug concentrations in the human lung epithelial lining fluid. *Pharmaceutical Research*, 33, 856-867. <https://doi.org/10.1007/s11095-015-1832-x>
- van de Waterbeemd, H., & Gifford, E. (2003). ADMET in silico modelling: towards prediction paradise? *Nature Reviews Drug Discovery*, 2(3), 192-204. <https://doi.org/10.1038/nrd1032>
- Venus, M., Waterman, J., & McNab, I. (2010). Basic physiology of the skin. *Surgery (Oxford)*, 28(10), 469-472. <https://doi.org/10.1016/j.mpsur.2010.07.011>
- Verner, M.-A., Charbonneau, M., López-Carrillo, L., & Haddad, S. (2008). Physiologically based pharmacokinetic modeling of persistent organic pollutants for lifetime exposure assessment: a new tool in breast cancer epidemiologic studies. *Environmental Health Perspectives*, 116(7), 886-892. <https://doi.org/10.1289/ehp.10917>
- Verner, M. A., Plusquellec, P., Muckle, G., Ayotte, P., Dewailly, É., Jacobson, S. W., Jacobson, J. L., Charbonneau, M., & Haddad, S. (2010). Alteration of infant attention and activity by polychlorinated biphenyls: Unravelling critical windows of susceptibility using physiologically based pharmacokinetic modeling. *Neurotoxicology*, 31(5), 424-431. <https://doi.org/https://doi.org/10.1016/j.neuro.2010.05.011>
- Wang, K., Jiang, K., Wei, X., Li, Y., Wang, T., & Song, Y. (2021). Physiologically based pharmacokinetic models are effective support for pediatric drug development. *AAPS PharmSciTech*, 22, 1-12. <https://doi.org/10.1208/s12249-021-02076-w>
- Wang, S., Zhang, Z., Saunders, L. J., Li, D., & Li, L. (2024). Understanding the Impacts of Presystemic Metabolism on the Human Oral Bioavailability of Chemicals. *Environmental science & technology*, 58(32), 14135-14145. <https://doi.org/10.1021/acs.est.4c03344>
- Waters, S. B., Devesa, V., Del Razo, L. M., Styblo, M., & Thomas, D. J. (2004a). Endogenous reductants support the catalytic function of recombinant rat cyt19, an arsenic methyltransferase. *Chem Res Toxicol*, 17(3), 404-409. <https://doi.org/10.1021/tx0342161>
- Waters, S. B., Devesa, V., Fricke, M. W., Creed, J. T., Styblo, M., & Thomas, D. J. (2004b). Glutathione modulates recombinant rat arsenic (+ 3 oxidation state) methyltransferase-catalyzed formation of trimethylarsine oxide and trimethylarsine. *Chem Res Toxicol*, 17(12), 1621-1629. <https://doi.org/10.1021/tx0497853>
- Wei, B., Isukapalli, S. S., & Weisel, C. P. (2013). Studying permethrin exposure in flight attendants using a physiologically based pharmacokinetic model. *J Expo Sci Environ Epidemiol*, 23(4), 416-427. <https://doi.org/10.1038/jes.2013.12>
- Westerhout, J., den Heijer-Jordaan, A., Princen, H. M., & Stierum, R. (2024). A systems toxicology approach for identification of disruptions in cholesterol homeostasis after aggregated exposure to mixtures of perfluorinated compounds in humans. *Toxicological Sciences*, 198(2), 191-209. <https://doi.org/10.1093/toxsci/kfae006>
- White, P. D., Van Leeuwen, P., Davis, B. D., Maddaloni, M., Hogan, K. A., Marcus, A. H., & Elias, R. W. (1998). The conceptual structure of the integrated exposure uptake biokinetic model for lead in children. *Environmental Health Perspectives*, 106(suppl 6), 1513-1530. <https://doi.org/10.1289/ehp.98106s61513>

- WHO. (2006). *WHO guidelines for the safe use of wastewater excreta and greywater* (Vol. 4). World Health Organization.
- Wiśniowska, B., Linke, S., Polak, S., Bielecka, Z., Luch, A., & Pirow, R. (2023). Physiologically based modelling of dermal absorption and kinetics of consumer-relevant chemicals: A case study with exposure to bisphenol A from thermal paper. *Toxicology and Applied Pharmacology*, 459, 116357. <https://doi.org/https://doi.org/10.1016/j.taap.2022.116357>
- Wu, D., Chen, Q., Chen, X., Han, F., Chen, Z., & Wang, Y. (2023). The blood–brain barrier: Structure, regulation and drug delivery. *Signal Transduction and Targeted Therapy*, 8(1), 217. <https://doi.org/10.1038/s41392-023-01481-w>
- Wu, H., Yoon, M., Verner, M.-A., Xue, J., Luo, M., Andersen, M. E., Longnecker, M. P., & Clewell, H. J. (2015). Can the observed association between serum perfluoroalkyl substances and delayed menarche be explained on the basis of puberty-related changes in physiology and pharmacokinetics? *Environment international*, 82, 61-68. <https://doi.org/https://doi.org/10.1016/j.envint.2015.05.006>
- Wu, Y.-W., Ta, G. H., Lung, Y.-C., Weng, C.-F., & Leong, M. K. (2022). In silico prediction of skin permeability using a two-QSAR approach. *Pharmaceutics*, 14(5), 961. <https://doi.org/10.3390/pharmaceutics14050961>
- Yang, X., Doerge, D. R., Teeguarden, J. G., & Fisher, J. W. (2015). Development of a physiologically based pharmacokinetic model for assessment of human exposure to bisphenol A. *Toxicol Appl Pharmacol*, 289(3), 442-456. <https://doi.org/10.1016/j.taap.2015.10.016>
- Yazbeck, C., Cheymol, J., Dandres, A. M., & Barbéry-Courcoux, A. L. (2007). Intoxication au plomb chez la femme enceinte et le nouveau-né: bilan d'une enquête de dépistage. *Archives de Pédiatrie*, 14(1), 15-19. <https://doi.org/https://doi.org/10.1016/j.arcped.2006.09.016>
- Yoshida, T., Yamauchi, H., & Sun, G. F. (2004). Chronic health effects in people exposed to arsenic via the drinking water: dose–response relationships in review. *Toxicology and Applied Pharmacology*, 198(3), 243-252. <https://doi.org/10.1016/j.taap.2003.10.022>
- Yu, D. H. (1999a). A pharmacokinetic modeling of inorganic arsenic: A short-term oral exposure model for humans [Article]. *Chemosphere*, 39(15), 2737-2747. [https://doi.org/10.1016/s0045-6535\(99\)00207-6](https://doi.org/10.1016/s0045-6535(99)00207-6)
- Yu, D. H. (1999b). A physiologically based pharmacokinetic model of inorganic arsenic [Article]. *Regulatory Toxicology and Pharmacology*, 29(2), 128-141. <https://doi.org/10.1006/rtph.1999.1282>
- Zakharyan, R. A., & Aposhian, H. V. (1999). Enzymatic reduction of arsenic compounds in mammalian systems: the rate-limiting enzyme of rabbit liver arsenic biotransformation is MMAV reductase. *Chem Res Toxicol*, 12(12), 1278-1283. <https://doi.org/10.1021/tx9901231>
- Zeng, R., Deng, J., Dang, L., & Yu, X. (2021). Correlation between the structure and skin permeability of compounds. *Scientific reports*, 11(1), 10076. <https://doi.org/10.1038/s41598-021-89587-5>
- Zhang, K., Chen, M., Scriba, G. K., Abraham, M. H., Fahr, A., & Liu, X. (2012). Human skin permeation of neutral species and ionic species: Extended linear free energy relationship analyses. *Journal of pharmaceutical sciences*, 101(6), 2034-2044. <https://doi.org/10.1002/jps.23086>
- Zhang, Z., Imperial, M. Z., Patilea-Vrana, G. I., Wedagedera, J., Gaohua, L., & Unadkat, J. D. (2017). Development of a Novel Maternal-Fetal Physiologically Based Pharmacokinetic Model I: Insights into Factors that Determine Fetal Drug Exposure through Simulations and Sensitivity Analyses. *Drug Metabolism and Disposition*, 45(8), 920-938. <https://doi.org/10.1124/dmd.117.075192>
- Zurlinden, T. J., & Reisfeld, B. (2018a). A novel method for the development of environmental public health indicators and benchmark dose estimation using a health-based end point for chlorpyrifos. *Environmental Health Perspectives*, 126(4), 047009. <https://doi.org/10.1289/EHP4279>
- Zurlinden, T. J., & Reisfeld, B. (2018b). A Novel Method for the Development of Environmental Public Health Indicators and Benchmark Dose Estimation Using a Health-Based End Point for Chlorpyrifos. *Environ Health Perspect*, 126(4), 047009. <https://doi.org/10.1289/ehp1743>